

University of Louisville

ThinkIR: The University of Louisville's Institutional Repository

Electronic Theses and Dissertations

8-2022

Statistical methods for personalized treatment selection and survival data analysis based on observational data with high-dimensional covariates.

Don Ramesh Dinendra Sudaraka Tholkage
University of Louisville

Follow this and additional works at: <https://ir.library.louisville.edu/etd>



Part of the [Applied Statistics Commons](#), [Biostatistics Commons](#), [Statistical Models Commons](#), and the [Survival Analysis Commons](#)

Recommended Citation

Tholkage, Don Ramesh Dinendra Sudaraka, "Statistical methods for personalized treatment selection and survival data analysis based on observational data with high-dimensional covariates." (2022). *Electronic Theses and Dissertations*. Paper 3945.

<https://doi.org/10.18297/etd/3945>

This Doctoral Dissertation is brought to you for free and open access by ThinkIR: The University of Louisville's Institutional Repository. It has been accepted for inclusion in Electronic Theses and Dissertations by an authorized administrator of ThinkIR: The University of Louisville's Institutional Repository. This title appears here courtesy of the author, who has retained all other copyrights. For more information, please contact thinkir@louisville.edu.

STATISTICAL METHODS FOR PERSONALIZED TREATMENT
SELECTION AND SURVIVAL DATA ANALYSIS BASED ON
OBSERVATIONAL DATA WITH HIGH-DIMENSIONAL
COVARIATES

By

Don Ramesh Dinendra Sudaraka Tholkage
B.S., University of Kelaniya, 2016
M.S., Sam Houston State University, 2018

A Dissertation
Submitted to the Faculty of the
School of Public Health and Information Sciences
of the University of Louisville
in Partial Fulfillment of the Requirements
for the Degree of

Doctor of Philosophy
in Biostatistics

Department of Bioinformatics and Biostatistics
University of Louisville
Louisville, Kentucky

August 2022

STATISTICAL METHODS FOR PERSONALIZED TREATMENT
SELECTION AND SURVIVAL DATA ANALYSIS BASED ON
OBSERVATIONAL DATA WITH HIGH-DIMENSIONAL
COVARIATES

By

Don Ramesh Dinendra Sudaraka Tholkage
B.S., University of Kelaniya, 2016
M.S., Sam Houston State University, 2018

A Dissertation Approved on

July 01, 2022

by the following Dissertation Committee:

Qi Zheng, Ph.D
Dissertation Director

KB Kulasekera, Ph.D
Dissertation Co-Director

Maiying Kong, Ph.D
Dissertation Co-Director

Riten Mitra, Ph.D

Nichola C Garbett, Ph.D

DEDICATION

To my family.

ACKNOWLEDGMENTS

I would like to express my sincere gratitude to my dissertation advisor Dr. Qi Zheng and co-advisors Drs. K.B Kulasekera and Maiying Kong for their excellent guidance towards the completion of my dissertation. I also thank my dissertation committee members Drs. Nichola Garbett and Riten Mitra for their continuous support and direction.

I am grateful to the Department of Bioinformatics and Biostatistics at the University of Louisville for providing financial support throughout my Ph.D. program. I would like to thank all of the faculty members in the Department of Biostatistics and Bioinformatics for enriching my biostatistics knowledge, the administrative staff for their assistance, guidance, and collaboration, and my colleagues who have helped me and made my life more enjoyable during my studies. Last but not least, I would not have made it through graduate school without my parents' selflessness, unconditional love, and my wife's unwavering support.

ABSTRACT

STATISTICAL METHODS FOR PERSONALIZED TREATMENT SELECTION AND SURVIVAL DATA ANALYSIS BASED ON OBSERVATIONAL DATA WITH HIGH-DIMENSIONAL COVARIATES

Don Ramesh Dinendra Sudaraka Tholkage

July 01, 2022

Due to the wide availability of functional data from multiple disciplines, the studies of functional data analysis have become popular in the recent literature. However, the related development in censored survival data has been relatively sparse. In Chapter 2, we consider the problem of analyzing time-to-event data in the presence of functional predictors. We develop a conditional generalized Kaplan Meier (KM) estimator that incorporates functional predictors using kernel weights and rigorously establishes its asymptotic properties. In addition, we propose to select the optimal bandwidth based on a time-dependent Brier score. We then carry out extensive numerical studies to examine the finite sample performance of the proposed functional KM estimator and bandwidth selector. We also illustrated the practical usage of our proposed method by using a data set from Alzheimer’s Disease Neuroimaging Initiative data.

Estimating the optimal treatment regime based on individual patient characteristics has been discussed in many forums. Advanced computational power has added momentum to this discussion over the last two decades, and practitioners have

advocated using new methods to determine the best treatment. Treatments geared towards the "best" outcome for a patient based on their genetic markers and characteristics are highly important. In Chapter 3, we develop an approach to predict the optimal personalized treatment based on observational data. We have used inverse probability of treatment weighted machine learning methods to obtain score functions to predict the optimal treatment. Extensive simulation studies showed that our proposed method has desirable performance in selecting the optimal treatment. We provided a case study to examine the statin use on cognitive function to illustrate the use of our proposed method.

Personalized treatment selection methods that assign individuals to treatments based on patients' characteristics have been widely recognized in modern medicine. Survivorship is considered the most representative of clinical effectiveness among many clinical outcomes. As a result, in personalized treatment selection, survival time is arguably a better choice for a patient's outcome. Many methods have been developed for randomized experimental data, which may not be suitable for observational data due to the confounding between treatment assignment and outcome variable. In Chapter 4, we propose a penalized semiparametric modeling approach to estimate the optimal treatment regime, which is suitable for both randomized experimental and observational data. The proposed method has a variable selection feature so that it can handle high-dimensional covariates as well as censored observations. The proposed method has been developed to identify the optimal treatment in multiple treatment settings. Extensive simulation studies showed that our proposed method has desirable performance in selecting the optimal treatment. We demonstrated the application of the proposed method using data obtained from the Kentucky Medicaid database on patients diagnosed with cirrhosis.

TABLE OF CONTENTS

	PAGE
DEDICATION	iii
ACKNOWLEDGMENTS	iv
ABSTRACT	v
LIST OF TABLES	ix
LIST OF FIGURES	xi
CHAPTER 1: INTRODUCTION	1
1.1 Conditional kaplan-meier estimator with functional covariates for time- to-event data	2
1.2 Personalized treatment selection using observational data	4
1.3 Identifying optimal treatment regimes using single index models for survival data	7
CHAPTER 2: CONDITIONAL KAPLAN-MEIER ESTIMATOR WITH FUNC- TIONAL COVARIATES FOR TIME-TO-EVENT DATA	10
2.1 Model setup and estimation method	11
2.1.1 The proposed method	11
2.1.2 Bandwidth selection	14
2.2 Theoretical properties	15
2.3 Simulation study	18
2.4 Case study	22

2.5	Discussion	24
2.6	Tables and Figures	25
CHAPTER 3: PERSONALIZED TREATMENT SELECTION USING OB-		
SERVATIONAL DATA		25
3.1	Treatment selection method	31
3.2	Simulation study	37
3.3	Case study	41
3.4	Discussion	43
3.5	Tables and Figures	45
CHAPTER 4: IDENTIFYING OPTIMAL TREATMENT REGIME USING		
SINGLE INDEX MODELS FOR SURVIVAL DATA		45
4.1	Treatment selection method	48
4.2	Simulation study	54
4.3	Case study	58
4.4	Discussion	61
4.5	Tables and Figures	63
REFERENCES		69
APPENDICES		81
A	First Appendix	81
B	Second Appendix	87
C	Third Appendix	91
CURRICULUM VITAE		93

LIST OF TABLES

TABLE	PAGE
2.1 The MSPEs of the survival probability in the test data using conditional functional KM, regular KM, and FLCRM under different scenarios.	25
3.1 Three different simulation scenarios which correspond to different complexities of outcome models.	38
3.2 The average prediction accuracy based on 500 test sets using different methods under different scenarios.	45
3.3 The composite average gain of responses to choose the optimal versus the second optimal treatment (Λ_{12}), and the optimal versus the worst treatment (Λ_{13}).	46
3.4 Summarized optimal treatment assignments compared with the original assignments based on one-fold testing data as well as based on 5-folds testing data.	46
4.1 Summarized simulation results for the settings with 10% censoring rate and a high signal-noise ratio (≈ 3.2).	63
4.2 Summarized simulation results for the settings with 30% censoring rate and a high signal-noise ratio (≈ 3.2).	64
4.3 Summarized simulation results for the settings with 10% censoring rate and a low signal-noise ratio (≈ 2.2).	65
4.4 Summarized simulation results for the settings with 30% censoring rate and a low signal-noise ratio (≈ 2.2).	66

4.5	Summarized optimal treatment assignments compared with the original assignments.	67
4.6	Comparison of optimal treatment assignment for two sets of patients with similar characteristics.	67
B.1	Parameters for the gbm model	87
B.2	The estimated patient scores $U(X) = (S(X), \delta(X))^T$ for the first 10 patients in the training data	89
B.3	The estimated patient scores $U(X_0) = (S(X_0), \delta(X_0))^T$ for the first 10 patients in the training data	89
B.4	Proposed treatment for the first 10 patients in the testing data	90

LIST OF FIGURES

FIGURE	PAGE
2.1 Simulation results of the average Brier score for sample size 100 over 100 replications plotted against the grid of bandwidth for different scenarios. The vertical lines indicate the optimal bandwidth based on Brier scores and MSE.	26
2.2 Simulation results of the average Brier score for sample size 400 over 100 replications plotted against the grid of bandwidth for different scenarios. The vertical lines indicate the optimal bandwidth based on Brier scores and MSE.	27
2.3 The boxplots represent the sampling distribution of the MSE based on the 100 simulation test sets using different methods: Cond.KM.Brier= Conditional Kaplan-Meier (Bandwidth selection based on Brier scores), Cond.KM.MSE= Conditional Kaplan-Meier (Bandwidth selection based on MSE), KM= Kaplan-Meier and FLCRM= Functional Linear Cox Regression Model	28
2.4 Hippocampus radial distance curves	29
(a) Hippocampus radial distance curve of 19 th patient	29
(b) Hippocampus radial distance curve of 207 th patient	29
(c) Hippocampus radial distance curves of all the patients	29
2.5 Brier scores on the ADNI data	30

3.1	The boxplots of the predicted accuracy based on the 500 simulation test sets using different methods under three different scenarios. GBM=GBM for variable selection; LASSO=LASSO for variable selection; LL= Local Linear Estimator; NW= Nadaraya-Watson type estimator; .W=Methods that used inverse probability of treatment weights . . .	47
4.1	Kaplan-Meier survival curves for the three treatment groups and the patients who received the estimated optimal treatment weighted by the respective propensity scores.	68
B.1	Relative influence of the covariates obtained from the GBM models of the three treatment groups.	88

CHAPTER 1

INTRODUCTION

High-quality observational studies play a significant role in biomedical research because they can investigate issues that would otherwise be difficult or impossible to investigate. Major technological advances have contributed significantly to obtaining high-quality data, especially in biomedical research. As a result, functional data analysis methods have become one of the most active and significant areas in the field of statistics, and most classical multivariate problems have a comparable functional component. In the first project, we focus on the related development of the survival data, which is relatively sparse in the literature.

Estimating the optimal treatment regime based on individual patient characteristics has been discussed in many forums. In the second project, we develop an approach to predict the optimal personalized treatment based on observational data. Survivorship is considered the most representative of clinical effectiveness among many clinical outcomes. Therefore the survival time is arguably a better choice for the outcome for a patient in personalized treatment selection. In the third project, we propose a penalized semiparametric modeling approach to estimate the optimal treatment regime with high-dimensional covariates in the presence of censored observations.

1.1 Conditional kaplan-meier estimator with functional covariates for time-to-event data

The development of technology has greatly improved the ability to record and store complex data. In many scientific fields such as biomedical, economic, and environmental studies, sampled data are functions of certain index variables, such as time, location, and temperature over a continuum. For example, in optical spectrometric data collected to analyze different compounds in food samples, the intensity of light is a function of continuous wavelength (e.g. Borggaard and Thodberg, 1992); in speech recognition, human voices of pronouncing certain word are digitized and recorded as a function of time (e.g. Ferraty and Vieu, 2003); In Febrero et al. (2008), the NOx level in the air is measured over the course of a day near an industrial area. For more examples of functional data, we refer readers to Ramsay and Silverman (2002).

Let $\{X(s), s \in \mathcal{S}\}$ denote a function variable, where s is some index variable on a continuum \mathcal{S} . However, due to the limitation of measurement and storage, $X(s)$ is usually collected only on a grid $G_{\mathcal{S}} = \{s_1, \dots, s_p\}$ over \mathcal{S} in practice. Therefore, the measured data are often in the form of discretized vectors $(X_1, X_2, \dots, X_p)^T$ with $X_k = X(s_k), k = 1, \dots, p$. When the grid $G_{\mathcal{S}}$ is fine, the covariate vector resembles a smooth variation of $X(s)$.

Although functional data is commonly represented by vectors, it is inherently different from ordinary multivariate vectors, due to the temporal/spatial intercorrelation between consecutive entries. As a result, direct use of traditional multivariate statistical methods inevitably faces the difficulty of multicollinearity, and therefore may not produce reliable results (see, e.g., Ramsay and Silverman, 2002). Motivated by this, enormous efforts have been devoted to developing statistical tools for functional data analysis. For instance, Müller and Stadtmüller (2005) considered the generalized functional linear models with functional covariates; James (2002) de-

veloped functional principal component analysis (FPCA); Marx and Eilers (1999), Cardot et al. (1999, 2003), and Cardot and Sarda (2005) investigated functional B-splines regression methods; Ferraty and Vieu (2006) and Ferraty et al. (2007) studied nonparametric kernel methods.

In biomedical applications, there are also tons of functional data available, such as the cornea images in ophthalmology (Locantore et al., 1999), the magnetic resonance imaging in the studies of Alzheimer’s Disease (Kong et al., 2018), the electroencephalography in psychiatry (Hasenstab et al., 2017), and the electrocardiograms in cardiology (Zhou and Sedransk, 2009). In many of those studies, the response variable of primary interest is the time-to-event time in the presence of censoring. For example, Fang et al. (2016) investigated multiple myeloma patient’s disease free survival against absolute lymphocyte cell counts, which were measured as a function of time. Gellar et al. (2015) examined the association between the post-hospital mortality of the patients who suffer from acute lung injury/respiratory distress syndrome and the sequential organ failure assessment score, as a function of ICU time.

However, the related development for the time-to-event time subject to censoring has been relatively sparse in functional data analysis. James (2002) proposed a functional censored regression model coupled with an EM algorithm introduced by Schmee and Hahn (1979) to assess the expected survival time. Müller and Zhang (2005) incorporated functional covariates as longitudinal covariates and developed time varying functional principal component scores for predicting age-at-death distributions. However, their method does not account for censoring. Gellar et al. (2015) developed a penalized signal regression for mixed effect proportional hazard models. Kong et al. (2018) utilized FPCA and introduced a functional linear cox regression Model (FLCRM).

Kaplan-Meier (KM) estimator proposed by Kaplan and Meier (1958) has been

a popular method in time-to-event data (see, e.g., Beran, 1981; Gentleman and Crowley, 1991; Gonzalez-Manteiga and Cadarso-Suarez, 1994), as it is a nonparametric approach without stringent model assumptions and describes the survival probabilities directly. KM estimator has also been used in functional data. For example, Rutikanga et al. (2021) employed it to estimate the extreme quantiles. However, to the best of our knowledge, the asymptotic properties of the functional KM estimator have not been thoroughly investigated and thus the procedures built upon it lack theoretical guarantees. In this paper, we raise to this challenge by developing a generalized conditional KM estimator with desirable asymptotic properties for functional data. We also develop a bandwidth selection approach based on time dependent Brier scores (Graf et al., 1999; Gerds and Schumacher, 2006) so that users can confidently apply our proposed estimator to study functional time-to-event data.

The chapter 2 is organized as follows. In Section 2.1 we discuss the model setup and develop the functional KM estimator. We provide theoretical properties including consistency and asymptotic normality of the proposed estimator in Section 2.2. In Section 2.3, we carry out extensive numerical studies to examine the finite sample performance of the proposed method. In Section 2.4, we illustrate the practical use of our proposed method by a case study on Alzheimer’s Disease Neuroimaging Initiative Data. Section 2.5 provides a discussion and some concluding remarks. All proofs are relegated to the Appendix A.

1.2 Personalized treatment selection using observational data

Estimating the optimal treatment regime based on individual patient characteristics has been a topic of discussion in many forums. Advanced computational power that is fairly inexpensive to handle vast amounts of data has added momentum to this discussion over the last two decades and practitioners have been advocating the use of new methods in determining the best treatment (Van’t Veer and Bernard, 2008; Vazquez,

2013). Treatments that are geared towards the “best” outcome (e.g., survival time) for a patient based on his/her genetic and genomic markers are of high importance. Literature on this topic largely deals with deciding between treatments based on a single outcome measure modeled against patient characteristics. Assuming without any loss of generality that a larger outcome is better, the methods developed in the literature essentially determine the best treatment as the one associated with the largest of a measure of dominance. Majority of the existing literature use either a conditional location parameter(Cai et al., 2011; Qian and Murphy, 2011; Zhao et al., 2012; Zhang et al., 2012; Zhao et al., 2015) or a measure based on a conditional probability of an outcome for one treatment exceeding the outcomes for others(Siriwardhana et al., 2019) given the set of markers for the patient. In recent literature, using covariate information to construct different treatment rules has attracted a lot of attention and discussion. Wang et al. (2019) and Li et al. (2021) considered a linear combination of covariate values to derive the treatment assignment using a two-stage multiple change point detection method. Jiang et al. (2019) proposed an entropy learning approach for estimating optimal treatment rules. Almost all existing optimal treatment selection procedures based on prior data from randomized clinical trials (RCTs) for comparing treatments are either using a classification algorithm or a reward maximization scheme. While the RCT framework generates high-quality data for treatment comparisons by removing the selection bias arising from treatment assignment, there are many situations where a RCT cannot be conducted. When such infeasibilities arise, one resorts to using observational studies to make comparisons. Observational studies can be riddled with bias due to confounding variables which are causally related to both treatment assignment and outcome variable. When one can measure all the confounding variables which are the source of treatment assignment bias, an observational study can provide valuable information for a comparative study. There is a modest amount of literature on optimal treatment selection using observational data.

Again, these methods are rooted either in single stage classification concepts or two-stage value optimization methods (see Tao and Wang, 2017; Huang et al., 2019, and Hreferences therein).

In this study, we propose a treatment selection procedure based on existing observational data. Our approach is similar to the method proposed by Cai et al. (2011), which was generalized by Siriwardhana et al. (2019), where we use a summarized covariate information called a score to generate smoothed versions of responses for each treatment and estimate the optimal treatment for a new covariate value based on those smoothed past responses. In contrast to the method in Siriwardhana et al. (2019), we use a weighted estimation where the weights are inverse probability of getting a treatment, to adjust for bias due to confounding. Related to this is work done by Ma et al. (2015), who discuss the possibility of using observational data for optimal treatment selection for the two treatment case using a regression based approach. In our exploration we introduce and combine several regression related procedures such as Generalized Boosting and Adaptive LASSO which have not been studied before in the context of a search for the optimal conditional reward. As shown in the sequel via a detailed simulation study, the method we propose appears to select the optimal treatment with high accuracy under a variety of conditions.

The chapter 3 is organized as follows. In Section 3.1, we describe response models under consideration and develop the estimation method. In Section 3.2, we provide extensive simulation studies which show that our proposed method has desirable performance in selecting the optimal treatment. In Section 3.3, we provide a case study to illustrate the use of our proposed method. Section 3.4 provides a discussion and a few concluding remarks.

1.3 Identifying optimal treatment regimes using single index models for survival data

Modern medicine has widely recognized that the reaction of patients in response to a certain treatment varies significantly. A treatment that is beneficial to a majority of individuals may fail to work for patients with specific characteristics (Sorensen, 1996). For instance, selective serotonin reuptake inhibitors (SSRIs) have been considered standard treatments for patients with panic disorder. However, Zamorski and Albucher (2002) discovered that 30% of patients are not able to tolerate these drugs or have an unfavorable response and proposed investigating the optimization of SSRI dosing based on patients' characteristics. As a result, personalized treatment selection methods that assign a patient to the optimal treatment to achieve the best clinical outcome based on the patient's characteristics have attracted increasing research interest.

There have been extensive studies on identifying optimal individualized treatment rules (ITR), using data from either randomized clinical trials (RCT) or observational studies. The RCT framework is favorable in personalized treatment selection since it generally does not involve any selection bias arising from the treatment assignment (Ma et al., 2015). However, there are many situations where an RCT cannot be conducted because they are either unethical or expensive. On the other hand, the advancement of modern technology has made the data from observational studies widely available. The major limitation in observational studies is that the association between the treatment and the outcome variable is distorted by the confounding variables. Under the assumption that there are no unmeasured confounding variables, the optimal treatment selection methods with appropriate control of confounding can still be developed. For example, Kulasekera et al. (2022) recently proposed a patient specific score based method to select the optimal treatment using observational

data, where the inverse probability of treatment weighting was used to remove the confounding effect.

In the literature, there are two main approaches to identifying the ITR: Q-learning (Murphy, 2003, 2005; Moodie et al., 2012) and A-learning (Robins, 2004; Lu et al., 2013; Schulte et al., 2014). In Q-learning, the optimal treatment regimes are decided using a posited parametric regression model between the outcome variable and covariates and treatments. In A-learning, a semiparametric approach is used to estimate the contrast function between treatment and control, and the optimal treatment regimes hence can be determined by the contrast function (Schulte et al., 2014). The other approaches include the outcome-weighted learning method proposed by Zhao et al. (2012), in which the estimation of the optimal treatment regimes was shown to be equivalent to a weighted classification problem. In this article, we focus on estimating the contrast function, since the contrast function not only helps identify the ITR but also gauges the individual treatment effect.

Among many clinical outcomes, survivorship can be considered the most representative of clinical effectiveness (Ma et al., 2015). Nonetheless, the majority of the aforementioned methods were restricted to complete data, and the development of survival data has been relatively sparse. There are two major aspects to consider for survival outcomes resulting from observational studies: the censoring observations and the other is the confounding variables. A Q-learning method that is adjusted for censored data uses inverse probability of censoring weights as was proposed by Goldberg and Kosorok (2012). A-learning approach implemented through additive hazard models (Kang et al., 2018) and semiparametric models (Geng et al., 2015; Jiang et al., 2017) on the estimation of the ITR with survival data have been proposed. Zhao et al. (2015) extended the outcome weighted learning method (Zhao et al., 2012) to accommodate censored data by incorporating the inverse probability of censoring weights. To handle the confounding variables, the propensity-score-based methods have been

developed in both Q-learning (Zhao et al., 2020) and A-learning (Geng et al., 2015; Jiang et al., 2017; Kang et al., 2018) approaches, censoring is present. However, there are several limitations in the aforementioned studies. In the Q-learning approaches, the simple linear models may be severely misspecified and may lead to inaccurate estimates of ITR. The A-learning approaches are more robust to model misspecification than Q-learning in estimating optimal ITR. However, in Geng et al. (2015); Jiang et al. (2017); Kang et al. (2018), the contrast function between treatment and control is assumed to be linear and fails to capture the underlying contrast function when the contrast function is nonlinear. All of the above methods discussed are not designed to work in the presence of high-dimensional covariates and also fail to work in multiple treatment settings.

This study proposes a novel method to identify the optimal treatment regime in a multiple treatment setting. The proposed loss function takes the form of A-learning, as it directly estimates the contrast function and does not require the correct specification of the baseline function. Therefore, the proposed approach is robust against model misspecification. We propose to estimate the contrast functions using partial linear models, which offer flexibility and reasonable efficiency in modeling a wide range of data. In addition, to cope with the high dimensional data that often appears in clinical studies, we incorporate shrinkage methods to carry out variable selection. Furthermore, we utilize the inverse probability of censoring weights and propensity scores to account for the censored nature of the data and the potential confounding factors, respectively. Thus, the proposed method can provide consistent estimations of the contrast function in the presence of data from both RCT and observational studies.

The chapter 4 is organized as follows. Section 4.1 introduces the response model and describes the proposed estimator, which employs a modified loss function. Section 4.2 contains extensive simulation studies under various scenarios to demon-

strate the performance of our method in selecting optimal treatment. In section 4.3, we demonstrate the application of our method using data obtained from the Kentucky Medicaid database on the patients diagnosed with cirrhosis. Section 4.4 concludes with a discussion and a few closing remarks.

CHAPTER 2

CONDITIONAL KAPLAN-MEIER ESTIMATOR WITH FUNCTIONAL COVARIATES FOR TIME-TO-EVENT DATA

2.1 Model setup and estimation method

We begin with introducing some notations to present our proposed procedure. For generic variables U and V , let $F_U(\cdot)$ and $S_U(\cdot) = 1 - F_U(\cdot)$ denote the cumulative distribution function and the survival function of U , respectively. Additionally, $F_U(\cdot|V)$ and $S_U(\cdot|V)$ denote the conditional cumulative distribution and survival functions, respectively, of U given V . Moreover, the conditional hazard and cumulative hazard functions of U given V are denoted by $\lambda_U(\cdot|V)$ and $\Lambda_U(\cdot|V)$ respectively. We denote the L_2 norm of a functional covariate x by $\|x\|$ and denote the cardinality of a set A by $|A|$. Given two sequences s_{1n} and s_{2n} , we use the notation $s_{1n} \simeq s_{2n}$ to denote $s_{1n} = O(s_{2n})$ and $s_{2n} = O(s_{1n})$.

2.1.1 The proposed method

In this section, we describe the proposed procedure for estimating $S_T(\cdot|\mathbf{X})$, where T is the time-to-event of interest, subject to the right censoring by C and $\mathbf{X} = (X^{(1)}(s), \dots, X^{(p)}(s))^T, s \in \mathcal{S}$ is a p -dimensional vector of functional covariates corresponding to the patient. Without loss of generality, we assume that $\mathcal{S} = [0, 1]$. Here, any scalar covariate Z can also be represented as a constant function $Z(s) = Z, \forall s \in \mathcal{S}$. For the simplicity of presentation, we only consider $\mathbf{X} = X(s), s \in \mathcal{S}$ as a 1-dimensional functional covariate in this work. However, the proposed method

can be readily applied to scenarios with $p > 1$, as demonstrated in our numerical analysis. Throughout the rest of this paper, we may write the functional covariate $X(s), s \in \mathcal{S}$ as X for simplicity in notation when there is no confusion. We also denote the functional space of \mathbf{X} by \mathcal{X} .

Let $Y = \min\{T, C\}$ and $\delta = 1\{T < C\}$ be the observed outcome variable and the censoring indicator respectively, where $1\{\cdot\}$ is an indicator function. The observed data consists of n i.i.d replicates of (Y, δ, X) , denoted by $\{(Y_i, \delta_i, X_i), i = 1, \dots, n\}$. Under the conditional independence between T and C given X , the conditional survival function of Y given X is $S_Y(\cdot|X) = S_T(\cdot|X)S_C(\cdot|X)$. By simple algebra,

$$\Lambda_T(t|X) = -\log S_T(t|X) = -\int_0^t \frac{dS_T(u|X)}{S_T(u|X)} = \int_0^t \frac{dH(u|X)}{S_Y(u|X)}, \quad (2.1)$$

where $H(t|X) = P(Y \leq t, \delta = 1|X)$ is the sub-distribution of Y in the absence of censoring. As $H(\cdot|X)$ and $S_Y(\cdot|X)$ in Equation (2.1) involve only the observed variables, we can estimate them by kernel-type methods (see, e.g., Parzen, 1962; Nadaraya, 1964; Watson, 1964; Gasser and Müller, 1979).

A common approach to dealing with functional covariates is utilizing the Karhunen-Loève expansion (see, e.g., Ma, 2016; Kong et al., 2018). Namely, we first find L orthogonal basis functions defined on \mathcal{S} and represent each $X_i(\cdot)$ by scores $\{\xi_{il}, i = 1, \dots, n; l = 1, \dots, L\}$ obtained from projecting $X_i(\cdot)$ onto the space generated by L basis functions. However, as L is required to increase with the sample size n (de Boor, 2001), the typical kernel estimation based on ξ_{il} 's would inevitably suffer from the curse of dimensionality and lead to inefficient estimation.

To overcome this challenge, we follow Ferraty et al. (2007) and employ the functional kernel estimator directly. Let $K(\cdot)$ be some kernel function and h_n be a sequence of positive real numbers. We may suppress the subscript of h_n when there is no confusion. We obtain Nadaraya-Watson type weights $\{B_{nj}(x), j = 1, \dots, n, x \in$

\mathcal{X} as

$$B_{nj}(x) = \frac{K(h^{-1} \|X_j - x\|)}{\sum_{r=1}^n K(h^{-1} \|X_r - x\|)}.$$

Subsequently, the kernel type estimators of $H(t|x)$ and $S_Y(t|x)$ can be constructed as $\hat{H}(t|x) = \sum_{j=1}^n 1\{Y_j \leq t, \delta_j = 1\} B_{nj}(x)$ and $\hat{S}_Y(t|x) = \sum_{j=1}^n 1\{Y_j \geq t\} B_{nj}(x)$, for $x \in \mathcal{X}$. Given that the argument inside the kernel function K above is positive, K is typically an asymmetric probability density function. Following Dabrowska (1987, 1989), we acquire a natural estimator of $\Lambda_T(\cdot|x)$

$$\hat{\Lambda}_T(t|x) = \int_0^t \frac{d\hat{H}(u|x)}{\hat{S}_Y(u|x)} = \sum_{j=1}^n \frac{1\{Y_j \leq t, \delta_j = 1\} B_{nj}(x)}{\sum_{r=1}^n 1\{Y_r \geq Y_j\} B_{nr}(x)}, \quad (2.2)$$

where the second equality follows from the fact that $\hat{H}(\cdot|x)$ and $\hat{S}_Y(\cdot|x)$ are piecewise constant functions that only jump at Y_j 's. Then by Equation (2.1), a generalized conditional KM estimator of $S_T(t|x)$ can be immediately obtained as

$$\hat{S}_T(t|x) = \begin{cases} \prod_{j=1}^n \exp\left(-\frac{1\{Y_j \leq t, \delta_j = 1\} B_{nj}(x)}{\sum_{r=1}^n 1\{Y_r \geq Y_j\} B_{nr}(x)}\right) & , t \leq Y_{(n)} \\ 0 & , t > Y_{(n)} \end{cases} \quad (2.3)$$

Remark 2.1.1. *Our proposed method can also be applied to settings where multiple functional or regular covariates are present. Let Z denote an additional covariate. We can construct multi-dimensional Nadaraya-Watson type weights $B_{nj}(x, z)$ as*

$$B_{nj}(x, z) = \frac{K_1(h_1^{-1} \|X_j - x\|) \times K_2(h_2^{-1} \|Z_j - z\|)}{\sum_{j=1}^n K_1(h_1^{-1} \|X_j - x\|) \times K_2(h_2^{-1} \|Z_j - z\|)},$$

where K_1 is an asymmetric kernel, and K_2 is either an asymmetric kernel (can be K_1) in case Z is a functional covariate or a symmetric kernel in case Z is a scalar covariate. Here, h_1 and h_2 are the bandwidths associated respectively. We can then obtain $\hat{S}_T(t|x, z)$ by replacing $B_{nj}(x)$ with $B_{nj}(x, z)$ in Equation (2.3). It should be noted that convergence rates are negatively impacted when we have a product weight

such as the above.

2.1.2 Bandwidth selection

It is well-known that the bandwidth selection is crucial to the performance of kernel-type estimator (see, e.g., Ferraty et al., 2007; Kara-Zaitri et al., 2017). One appealing approach is to study the asymptotic properties of $\hat{S}_T(t|x)$ and derive the optimal bandwidth by minimizing the mean integrated squared errors (Berg and Suaray, 2010). However, it is very challenging to obtain a closed form of the asymptotic variance of a generalized KM estimator (see, e.g., Gonzalez-Manteiga and Cadarso-Suarez, 1994). We thus propose to select the optimal bandwidth by a data-driven m -fold cross validation as follows:

1. Randomly split the index set $\{1, 2, \dots, n\}$ into m equal-size blocks: $\mathcal{I}_1, \dots, \mathcal{I}_m$.
Let \mathcal{I}_{-k} be the collection of indices that are not contained in \mathcal{I}_k .
2. Given a bandwidth h , for each $k = 1, \dots, m$,
 - (a) obtain $\hat{S}_T(t|x)$, the estimates of the survival probability based on the observations $\{(Y_i, \delta_i, X_i), i \in \mathcal{I}_{-k}\}$.
 - (b) obtain the fitness score $E_k(h)$ for the estimates $\hat{S}_T(t|x)$ in 2(a) following certain model fitness metric E , based on the observations $\{(Y_i, \delta_i, X_i), i \in \mathcal{I}_k\}$.
3. Summarize the overall fitness as $E_A(h) = m^{-1} \sum_{k=1}^m E_k(h)$.
4. Choose $\hat{h}_n = \operatorname{argmin}_h E_A(h)$ as the selected bandwidth.

For survival data, many fitness metrics often used for model selection may not be suitable, as they fail to account for censoring. The concordance index (Harrell et al., 2015) and time-dependent Brier scores (Graf et al., 1999; Gerds and Schumacher, 2006) are commonly used to evaluate the fitness of survival models (Kattan and Gerds, 2018). In this study, we chose to use the Brier score, which takes into account

both discrimination and calibration to assess the model fitness. In contrast, the concordance index reflects only discrimination (Zhang et al., 2018). The estimated Brier scores of observations with indices in \mathcal{I}_k at time t can be obtained as follows:

$$\widehat{BS}(t) = \frac{1}{|\mathcal{I}_k|} \sum_{i \in \mathcal{I}_k} \widehat{W}_i(t) (1\{Y_i > t\} - \widehat{S}_T(t|X_i))^2, \quad (2.4)$$

where $\widehat{W}_i(t)$ is the inverse probability censoring weight (IPCW) of subject i at time t , given by,

$$\widehat{W}_i(t) = \frac{1\{Y_i \leq t, \delta_i = 1\}}{1 - \widehat{S}_C(Y_i|\mathbf{X}_i)} + \frac{1\{Y_i > t\}}{1 - \widehat{S}_C(t|\mathbf{X}_i)}. \quad (2.5)$$

$\widehat{S}_T(t|x)$ and $\widehat{S}_C(t|x)$ in (2.5) are the estimated survival probabilities of T and C from 2(a). We further adopted a more general version of the IPCW Brier score (Kvamme and Borgan, 2019) with $|\mathcal{I}_k|$ in 2.4 replaced by $\sum \widehat{W}_i(t)$. Now we can calculate the evaluation score $E_k(h)$ in step (2.b), averaging the Brier scores over a range of $t > 0$. Then following steps 3 and 4, we can select the optimal bandwidth.

2.2 Theoretical properties

In this section, we establish the theoretical properties of the proposed conditional KM estimator. We begin with imposing the following theoretical conditions, which facilitate our technical derivations.

(C1) Let $\mathcal{T} = [0, \tau]$ for some constant $\tau > 0$. Given $x \in \mathcal{X}$, let $B(x, \varepsilon) = \{x' \in \mathcal{X}, \|x - x'\| \leq \varepsilon\}$ be a ball being centered at x and of radius ε (Ferraty and Vieu, 2006). There exists some $\varepsilon_* > 0$, such that,

$$\sup_{x \in \mathcal{X}} \sup_{x_1, x_2 \in B(x, \varepsilon_*)} \sup_{t_1, t_2 \in \mathcal{T}} |S_T(t_1|x_1) - S_T(t_2|x_2)| \leq C(\|x_1 - x_2\|^2 + |t_1 - t_2|^2).$$

(C2) The kernel function $K(\cdot) > 0$ is Lipschitz-continuous over its support $[0, 1]$,

satisfying $\int_0^1 K(v)dv = 1$ and $0 < \inf_{v \in [0,1]} K(v) \leq \sup_{v \in [0,1]} K(v) < \infty$.

(C3) Let $\phi_x(\varepsilon) = P(X \in B(x, \varepsilon)) > 0$ denote the probability of the functional variable X in $B(x, \varepsilon)$. There exists a function $\phi(\cdot)$ and constants $C_1, C_2, A > 0$ such that $0 < C_1\phi(\varepsilon) \leq \inf_{x \in \mathcal{X}} \phi_x(\varepsilon) \leq \sup_{x \in \mathcal{X}} \phi_x(\varepsilon) \leq C_2\phi(\varepsilon) < \infty$, and $\phi'(\varepsilon) < A, \forall \varepsilon < \varepsilon_*$.

(C4) Let $\psi(\varepsilon) = \log(N_\varepsilon(\mathcal{X}))$, where $N_\varepsilon(\mathcal{X})$ is the minimal number of $B(x, \varepsilon)$'s to cover \mathcal{X} . This is called the Kolmogorov's ε -entropy of \mathcal{X} (Ferraty et al., 2010). For n large enough, $(\log n)^2/n\phi(h) < \psi(\log n/n) < n\phi(h)/\log n$ and for some $\beta > 1$,

$$\sum_{j=1}^{\infty} j \exp \left[(1 - \beta) \psi \left(\frac{\log j}{j} \right) \right] < \infty.$$

The lipschitz continuous condition (C1) has been widely adopted in the literature (see, e.g., Ferraty and Vieu, 2006; Kara-Zaitri et al., 2017) to ensure the smoothness of functional operators. The conditions on kernel function in (C2) have been adopted in the functional nonparametric estimation literature (Ferraty et al., 2007; Bouzebda and Nemouchi, 2020). $K(\cdot)$ is chosen to be an asymmetric kernel because $\|X_j - x\|$ is always positive. The bounded support of $K(\cdot)$ and that $K(\cdot)$ is bounded away from 0 are technical conditions to simplify the theoretical derivations. In the numerical studies, we chose the asymmetric Gaussian kernel and the results showed that it works quite well.

Conditions (C3) and (C4) follow from Ferraty et al. (2010). They are needed to establish the uniform consistency of the proposed conditional KM estimator over \mathcal{X} . $\phi(\varepsilon)$ in Condition (C3) controls the concentration of the probability measure of the functional variable X , which is related to all the asymptotic results in nonparametric statistics for functional variables, as indicated by Ferraty and Vieu (2006). It is analogous to the assumed density condition when X is a scalar or vector (see, e.g., Dabrowska, 1989). $\psi(\varepsilon)$ in condition (C4) is a measure of the complexity of \mathcal{X} . A

larger $\psi(\varepsilon)$ means that \mathcal{X} is a more complex function space. Condition (C4) essentially requires \mathcal{X} to have some suitable complexity so that local smoothing can be applied. It is analogous to the entropy condition that is often assumed in empirical process (see, e.g., Van Der Vaart and Wellner, 1996; Kosorok, 2008). Conditions (C3) and (C4) are often satisfied in practice. We refer the reader to Section 2 in Ferraty et al. (2010) for some common examples where these two conditions are met.

We first establish the estimation consistency results of \hat{H} and \hat{S}_Y .

Theorem 2.2.1. *Under Conditions (C1)-(C4), if $h \rightarrow 0$ and $(n\phi(h))^{-1}\psi(\log n/n) \rightarrow 0$, then*

$$\sup_{x \in \mathcal{X}} \sup_{t \in \mathcal{T}} |\hat{H}(t|x) - H(t|x)| = o \left(h^2 + \left(\frac{\psi(\log n/n)}{n\phi(h)} \right)^{1/2} \right) \quad a.s.$$

$$\sup_{x \in \mathcal{X}} \sup_{t \in \mathcal{T}} |\hat{S}_Y(t|x) - S_Y(t|x)| = o \left(h^2 + \left(\frac{\psi(\log n/n)}{n\phi(h)} \right)^{1/2} \right) \quad a.s.$$

If \mathcal{X} is a compact set in \mathbb{R} and the density of X is bounded below and above, then $\psi(\log n/n) \simeq \log n$ and $\phi(h) \simeq h$. Thus, Theorem 2.2.1 boils down to the results for the ordinary conditional KM estimator (see, e.g., Dabrowska, 1989; Gonzalez-Manteiga and Cadarso-Suarez, 1994).

Next, we derive an almost sure representation for the cumulative hazard function $\Lambda_T(t|x)$, in terms of a sum of independent random variables as follows.

Theorem 2.2.2. *Under the same conditions as in Theorem 2.2.1,*

$$\hat{\Lambda}_T(t|x) - \Lambda_T(t|x) = S_T(t|x)^{-1} \sum_{j=1}^n B_{nj}(x) \xi(Y_j, \delta_j, t, x) + o \left(h^2 + \left(\frac{\psi(\log n/n)}{n\phi_x(h)} \right)^{3/4} \right) \quad a.s.,$$

where

$$\xi(Y_j, \delta_j, t, x) = S_T(t|x) \left[- \int_0^{\min\{Y_j, t\}} \frac{dH(u|x)}{S_Y(u|x)^2} + \frac{1\{Y_j \leq t, \delta_j = 1\}}{S_Y(Y_j|x)} \right].$$

There are two remainder terms in Theorem 2.2.1, One of them, h^2 , is the bias term, and the other one, $\left(\frac{\psi(\log n/n)}{n\phi_x(h)}\right)^{3/4}$, is a dispersion component. Since they increase and decrease, respectively as the bandwidth increases, we need to chose a suitable bandwidth to balance this trade-off. Noting that $\hat{S}_T(t|x) = \exp(-\hat{\Lambda}_T(t|x))$, we can obtain the following corollary.

Corollary 2.2.1. *Under the same assumptions as in Theorem 2.2.2,*

$$\hat{S}_T(t|x) - S_T(t|x) = \sum_{j=1}^n B_{nj}(x)\xi(Y_j, \delta_j, t, x) + o\left(h^2 + \left(\frac{\psi(\log n/n)}{n\phi_x(h)}\right)^{3/4}\right) \quad a.s$$

Moreover, if $n\phi_x(h)h^4 \rightarrow 0$ and $(n\phi_x(h))^{-1}(\psi(\log n/n))^3 \rightarrow 0, \forall x \in \mathcal{X}$,

$$(n\phi_x(h))^{1/2}[\hat{S}_T(t|x) - S_T(t|x)] \rightarrow_d N(0, V(x, t))$$

for some variance function $V(x, t)$.

The form of $V(x, t)$ is quite complicated and the estimation of $V(x, t)$ is beyond the scope of this work.

2.3 Simulation study

In this section, we conduct extensive simulation studies to examine the finite sample properties of our proposed procedure. We consider the following four different Scenarios.

- Scenario 1: $T(X) = \int_{-1}^{+1} |X(s)|(1 - \cos(\pi s))ds + \epsilon$, where $X(s) = \sin(\omega s) + (A + 2\pi)s + B, s \in (-1, 1), A, B \sim \text{Unif}(0, 1), \omega \sim \text{Unif}(0, 2\pi)$, and $\epsilon \sim N(0, 2)$ distribution.
- Scenario 2: $T(X) = \int_{-1}^{+1} |X(s)|(1 - \cos(\pi s))ds + 2.5Z + \epsilon$, where $X(s)$ and ϵ are generated in the same way as in scenario 1, and Z follows a standard normal

distribution.

- Scenario 3: $T(X) = 1 + 2.5 \int_{-1}^{+1} (1 - \cos(\pi s)) ds + \epsilon$, where $X(s)$ and ϵ generated in the same way as in scenario 1.
- Scenario 4: $T(X) \sim \exp(h_0(t) \exp\{\int_0^1 X(s)\beta_0(s)ds\})$, where $h_0(t) = 1$, $X(s) = U_1 + U_2s + \sum_{j=1}^{10} [\nu_{j1} \sin\{2(2j - 1)\pi s\} + \nu_{j2} \cos\{2(2j - 1)\pi s\}]$, with $U_1, U_2 \sim N(0, 1)$, $\nu_{j1}, \nu_{j2} \sim N(0, 1/j)$, and $\beta_0(s) = 0.6[\sin(\pi s) - \cos(\pi s) + \sin(3\pi s/10) - \cos(3\pi s) + \sin(5\pi s)/9 - \cos(5\pi s)/9 + \sin(7\pi s)/16 - \cos(7\pi s)/16 + \sin(9\pi s)/25 - \cos(9\pi s)/25 + (2\pi)^{-1/2} \exp\{-2^{-1}(s - 0.5)^2\}]$ for $0 \leq s \leq 1$.

Scenario 1 follows from Ferraty et al. (2007) where the survival time depends on the functional covariates. In Scenario 2, we considered an extra covariate in addition to functional covariates to elaborate what we discussed in **Remark 2.1**. Scenario 3 is considered to examine the performance of the proposed method when the time is independent of the covariates. Scenario 4 is a functional Cox regression model and was considered in Kong et al. (2018)

The censoring time in each scenario was generated independently from a uniform distribution $\text{Unif}(0, c_0)$, where c_0 is chosen to achieve the desired censoring rates of 15% and 25%, representing low and mild censoring, respectively. In addition, we consider two sample sizes $n = 100$ and 400, simulating the small and moderate sample sizes, respectively. For each combination of scenario, censoring rate, and sample size, we generate 100 replications.

In each replication, we standardize the functional covariates by first centering them according to their means and then scaling them by the standard deviation of their L^2 norms. The standardization of the covariates is critical for us to specify a uniform grid of bandwidth. We chose the kernel function $K(\cdot)$ to be the asymmetrical Gaussian kernel. To speed up locating the optimal bandwidth associated with the kernel function, we carried out a 2-fold search. We first considered a coarse grid

of bandwidth, $\{0.5, 1, \dots, 20\}$ and selected a pilot bandwidth \tilde{h} , according to the procedure described in Section 2.2. Then we constructed a refined grid $(\tilde{h} - 1, \tilde{h} + 1)$ of size 20 to select the optimal bandwidth.

In Scenario 2, we consider an additional grid of bandwidth for the Gaussian kernel function associated with the scalar covariate, Z . According to the silverman’s rule of thumb (Silverman, 2018), the optimal choice is approximately $1.06\sigma n^{-1/5} \approx 0.42$ ($n = 100$). We thus consider a grid of bandwidth $\{0.20, 0.25, \dots, 1\}$. We conduct the cross validation method in section 2.2 to obtain a pair of optimal bandwidths for the two kernel functions simultaneously. In scenario 3, we only conducted the search on the coarse grid as we expect the bandwidth to be large.

To evaluate the performance of our proposed bandwidth selection procedure, we compare the selected bandwidth to a hypothetical one obtained by using the mean squared error (MSE)

$$\text{MSE}(t) = \frac{1}{m} \sum_{k=1}^m \sum_{i \in \mathcal{I}_k} [S_T(t|\mathbf{X}_i) - \hat{S}_T(t|\mathbf{X}_i)]^2 \quad (2.6)$$

as the fitness metric E in our proposed cross validation procedure in Section 2.2. This can be done since $S_T(t|\mathbf{X})$ is known in the simulations.

Figures 2.1 and 2.2 plot the average Brier score over 100 replications at different bandwidths against the bandwidth under four scenarios for sample sizes 100 and 400 respectively. The vertical lines in Figures 2.1 and 2.2 indicate the average optimal bandwidths selected from using Brier score (dotted) and MSE (dashed).

Figures 2.1 and 2.2 indicates a good performance of our proposed bandwidth selector. For scenarios 1,2, and 4, it can be seen that the optimal bandwidth selected using the Brier score is close to the “oracle” optimal bandwidth selected based on MSE, which assumes that the true conditional survival probabilities are known in advance. As the censorship rate decreases, the difference between the two selected

bandwidths becomes smaller. In Scenario 3, since the survival time is independent of the covariates, the regular KM estimator should be used and the theoretical optimal bandwidth for our proposed conditional KM estimator is infinite so that all observations would be used to estimate the survival probability. Large bandwidths were selected by our proposed bandwidth selector as expected, and thus the resulting estimator would be similar to regular Kaplan-Meier estimator.

We compare the proposed method to two benchmark methods: the regular KM estimator and FLCRM (Kong et al., 2018). We considered the regular KM estimator for all scenario and FLCRM for Scenario 4. The functional Cox regression model was implemented using the R codes provided by Kong et al. (2018). We assess the predictive performance of the three methods as follows: in each replication, we generate additional test data set of sample size 100. For the proposed method, we compute $\hat{S}_T(Y_i|X_i)$ for each (Y_i, X_i) in the testing data, based on (2.3) with the training data and the selected optimal bandwidth from the training data set. Then we calculated the mean squared prediction error (MSPE) of the estimates as $\sum_{i=1}^{100} (\hat{S}_T(Y_i|X_i) - S_T(Y_i|X_i))^2/100$. For the benchmark methods, we also obtained their corresponding predicted survival probabilities and MSPE. The summary of the results are presented in Figure 2.3 and Table 2.1.

Figure 2.3 shows that for Scenarios 1, 2, and 4, the proposed method has comparatively lower MSPEs than the other methods. Furthermore, we can observe that the performance of the proposed estimator based on the bandwidth selected using the Brier score and “oracle” MSE (2.6) is comparable, confirming a good performance of our proposed bandwidth selector. Moreover, we note that as the sample size increases, the performance of our proposed conditional functional KM estimator enhances with lower MSPEs in all scenarios. On the contrary, the MSPE from the regular KM estimator does not necessarily gets lower as the sample size increases. Table 2.1 shows that the MSPE of our conditional functional KM estimator decreases

at a lower censoring rate, as expected. When the survival time is independent of covariates (Scenario 3), the regular KM estimator is expected to achieve the best performance. But the proposed estimator performs on par with the regular KM estimator because our bandwidth selector chose a large bandwidth and the conditional KM estimator converges to KM estimator as the bandwidth increases. Therefore, regardless of the various scenarios considered in this study, we can claim that the proposed estimator performs the same or better than the comparison methods.

2.4 Case study

In this section, we illustrate the practical use of our proposed method by analyzing the Alzheimer’s Disease Neuroimaging Initiative (ADNI) data (Kong et al., 2018). Alzheimer’s disease is one of the most common causes of memory loss and dementia in which roughly more than 5 million Americans are affected, and is the 6th leading cause of death in the USA. It is a progressive disease. In earlier stages of the disease, the symptoms are mild and the treatment is more likely to be beneficial as the symptoms gradually worsen over time. Therefore an earlier and more accurate diagnosis is one of the most important goals in this area of research. The phase of mild cognitive impairment (MCI) is considered as the initial stage of dementia, and the time that takes an individual to convert from MCI to AD is of primary interest in various studies (see, e.g., Jack et al., 1999; Fjell et al., 2010; Barnes et al., 2014; Li et al., 2017).

The hippocampus is an area in the brain that is important for learning and memory. It is also vulnerable to affect at the early stage of AD. Multiple studies (Thompson et al., 2004; Apostolova et al., 2006; Blanken et al., 2017) have proposed to use hippocampal radial distances for studying the changes in the hippocampus of the AD patients, as hippocampal radial distances are the distances between the medial core of the hippocampus and the corresponding vertex, and can reflect the hippocampal shape and size. In this study, we use the hippocampal radial distances

of 30,000 surface points on the left and right hippocampal surfaces at baseline as functional covariates. In Figure 2.4, we plotted the hippocampal radial distance curves for two randomly chosen patients ((a) and (b)) and the curves of all the patients in an overlaid plot (c). Additionally, we also consider the Alzheimer’s Disease Assessment Scale-Cognitive Subscale (ADAS-Cog) score as it was identified to be one of the most significant scalar covariates in predicting the time of conversion from MCI to AD in Kong et al. (2018). The data consists of 373 MCI patients where 161 of them had developed AD before study completion.

The functional covariate (hippocampal radial distances) and the scalar covariate (ADAS-Cog score) were both scaled prior to the estimation. We split the data into a training and testing set. The training set contains 273 randomly chosen observations and was used to calculate the optimal bandwidth. The testing set is of sample size 100, to which we apply the proposed method and compare the performance of other methods considered in this work. To select the optimal bandwidths for the functional covariates and scalar covariate, we employed the same approach used in Scenario 2 of our simulation studies and used the same grids of bandwidths for the functional and scalar covariates. The optimal bandwidth for the functional and scalar covariates were found to be 1.1 and 0.6, respectively. Then we computed the predicted survival probability for the testing data and subsequently obtained the Brier scores. To compare the performance of the proposed method, we also used FLCRM and regular KM methods to estimate the survival probabilities of the testing data and calculated their corresponding Brier scores. Noting that a smaller value of the Brier score indicates a more accurate estimation of survival probability, Figure 2.5 demonstrates that the performance of the proposed method is superior to the other two methods at most of the time points in the range of T . Furthermore, we estimated the area under the brier score curve (AUC) for each method. The proposed conditional functional KM has a significantly lower AUC (219.5) than FLCRM (326.7) and

the regular KM method (418.7).

2.5 Discussion

Recent technological advancement has made functional data widely available in multiple disciplines, especially biomedical studies, where the response variable is often the time-to-event time in the presence of censoring. Therefore, it would be practically appealing to develop a conditional KM estimator that takes the functional covariates into account. In this paper, we rise to this challenge and propose a kernel-based conditional generalized KM estimator to analyze time-to-event data in the presence of functional covariates. We rigorously establish the proposed estimator's asymptotic properties and develop a Brier scores-based bandwidth selector. The numerical studies in this paper evince the satisfactory performance of our proposed estimator when the functional covariate is present.

Wang and Wang (2009) and Leng and Tong (2013) studied the weighted quantile regression for censored survival data with weights constructed from the conditional KM estimator. The quantile regression can accommodate and investigate the heterogeneous effects of covariates on the survival time. It is possible to develop a quantile regression for functional covariates and examine their varying effects, which often entail significant practical implications (see, e.g., Peng and Huang, 2008; Zheng et al., 2018). The detailed development is beyond the scope of this paper and will be studied in our forthcoming work.

2.6 Tables and Figures

Table 2.1: The MSPEs of the survival probability in the test data using conditional functional KM, regular KM, and FLCRM under different scenarios.

	n	Method	15% Censoring		25% Censoring	
			Mean	SD	Mean	SD
Scenario1	100	Cond.KM.MSE	0.0588	0.0118	0.0618	0.0106
		Cond.KM.Brier	0.0617	0.0123	0.0644	0.0113
		KM	0.1034	0.0064	0.1035	0.0063
	400	Cond.KM.MSE	0.0381	0.0047	0.0421	0.0060
		Cond.KM.Brier	0.0393	0.0051	0.0437	0.0067
		KM	0.0990	0.0052	0.0992	0.0053
Scenario2	100	Cond.KM.MSE	0.0817	0.0095	0.0886	0.0103
		Cond.KM.Brier	0.0853	0.0103	0.0936	0.0129
		KM	0.2064	0.0124	0.2073	0.0108
	400	Cond.KM.MSE	0.0556	0.0059	0.0600	0.0062
		Cond.KM.Brier	0.0570	0.0063	0.0624	0.0070
		KM	0.2050	0.0110	0.2046	0.0095
Scenario3	100	Cond.KM.MSE	0.0378	0.0130	0.0417	0.0149
		Cond.KM.Brier	0.0392	0.0129	0.0437	0.0149
		KM	0.0362	0.0122	0.0398	0.0133
	400	Cond.KM.MSE	0.0210	0.0066	0.0237	0.0082
		Cond.KM.Brier	0.0227	0.0072	0.0251	0.0083
		KM	0.0204	0.0064	0.0228	0.0079
Scenario4	100	Cond.KM.MSE	0.0817	0.0103	0.0946	0.0172
		Cond.KM.Brier	0.0860	0.0128	0.1000	0.0170
		KM	0.1633	0.0115	0.1726	0.0173
		FLCRM	0.1503	0.1011	0.1942	0.1173
	400	Cond.KM.MSE	0.0601	0.0075	0.0703	0.0111
		Cond.KM.Brier	0.0626	0.0081	0.0767	0.0112
		KM	0.1616	0.0111	0.1677	0.0124
		FLCRM	0.1666	0.1157	0.1842	0.1185

Cond.KM.Brier= Conditional Kaplan-Meier (Bandwidth selection based on Brier scores),
 Cond.KM.MSE= Conditional Kaplan-Meier (Bandwidth selection based on MSE), KM= Kaplan-Meier and FLCRM= Functional Linear Cox Regression Model

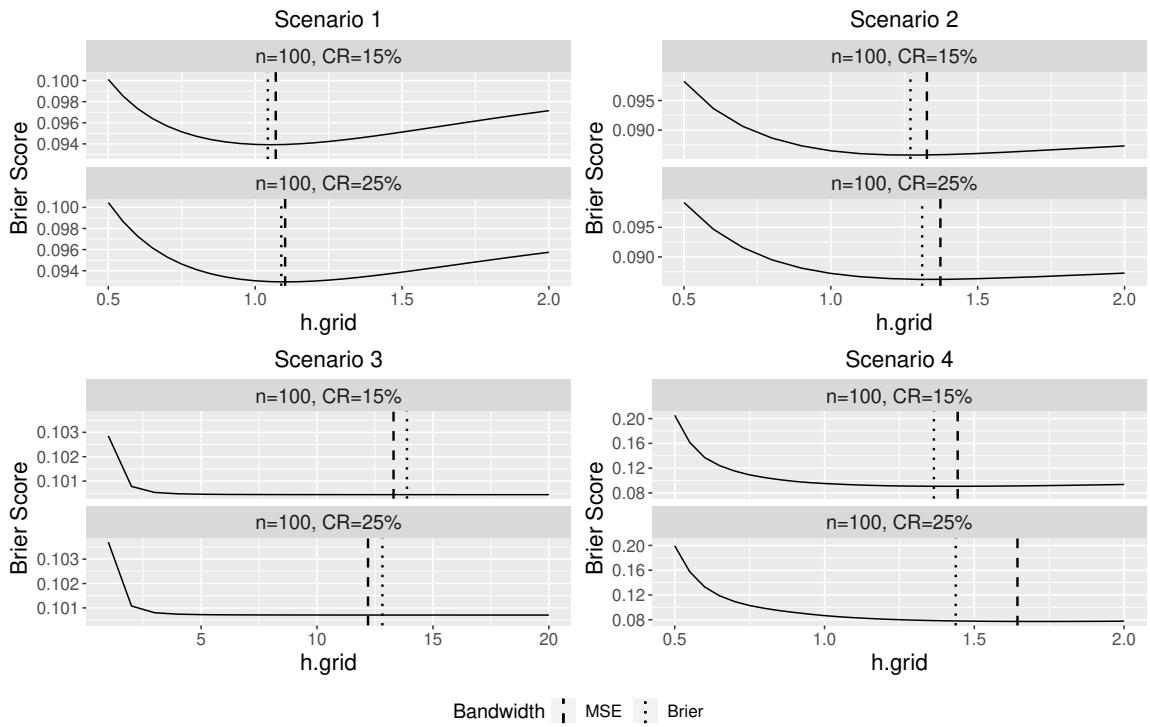


Figure 2.1: Simulation results of the average Brier score for sample size 100 over 100 replications plotted against the grid of bandwidth for different scenarios. The vertical lines indicate the optimal bandwidth based on Brier scores and MSE.

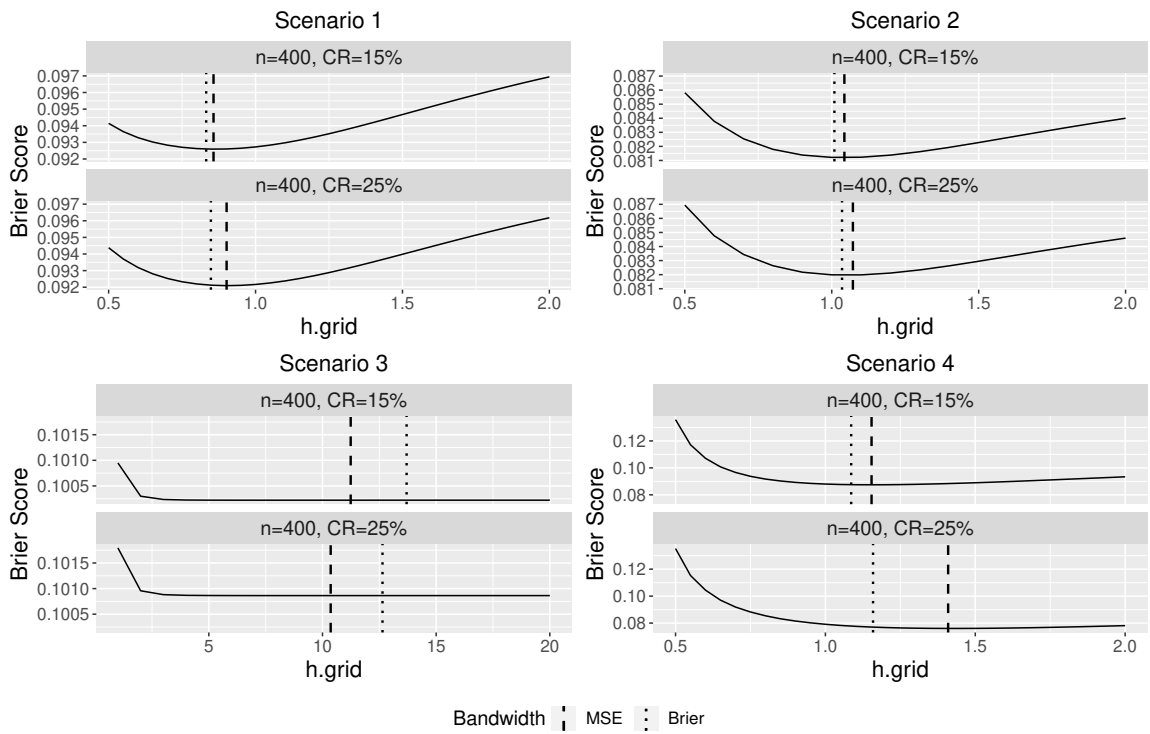


Figure 2.2: Simulation results of the average Brier score for sample size 400 over 100 replications plotted against the grid of bandwidth for different scenarios. The vertical lines indicate the optimal bandwidth based on Brier scores and MSE.

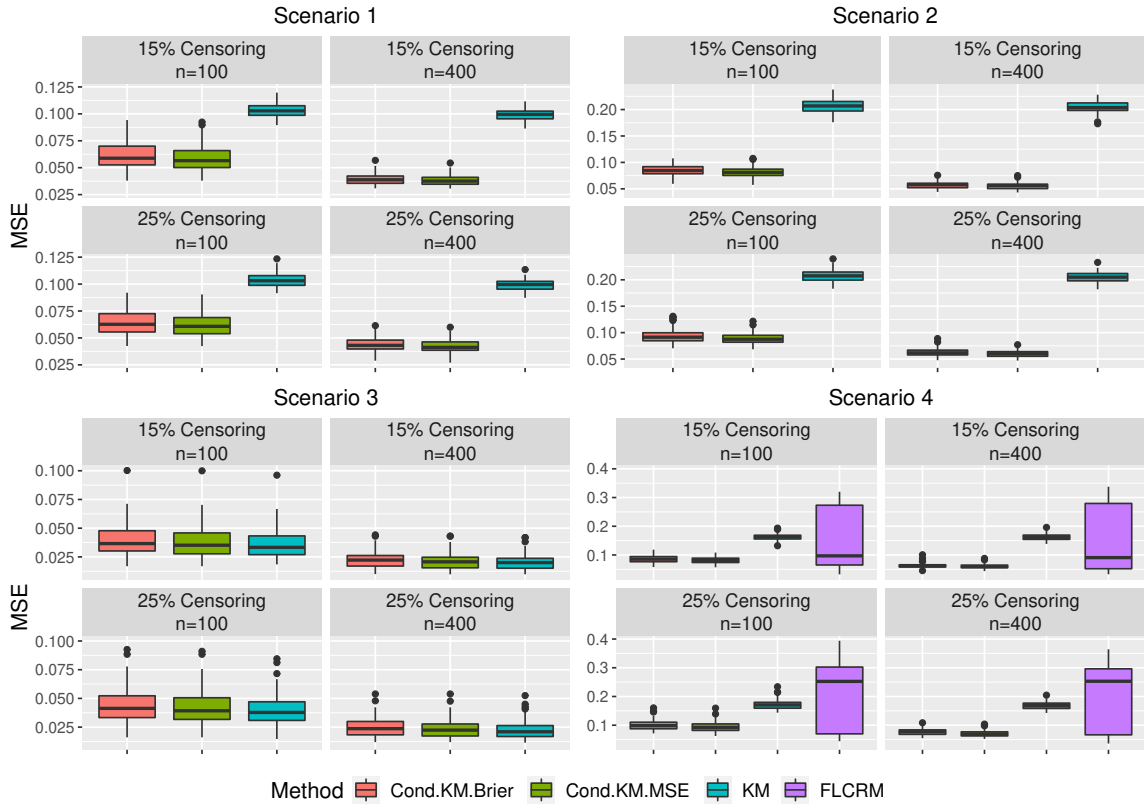
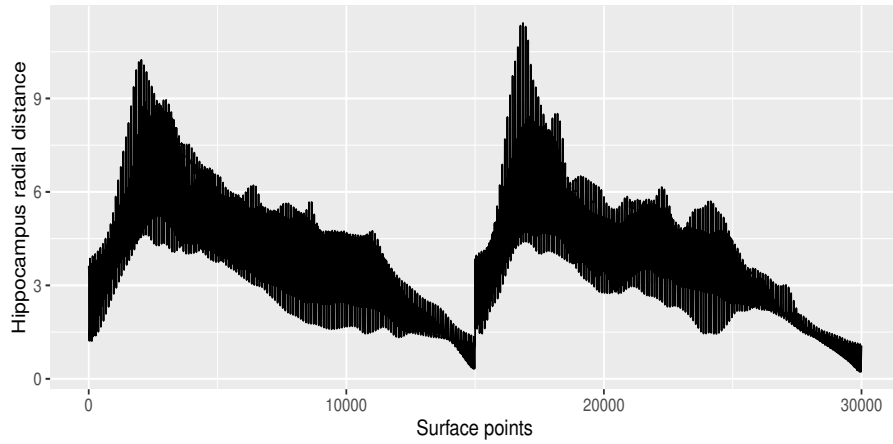
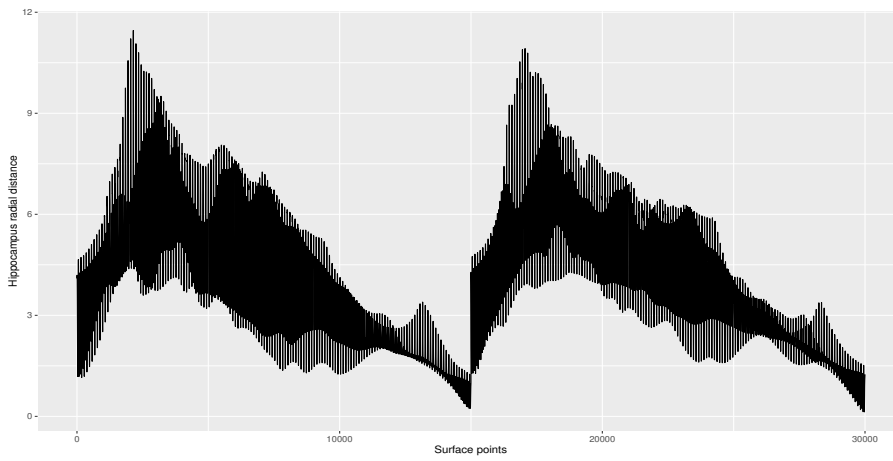


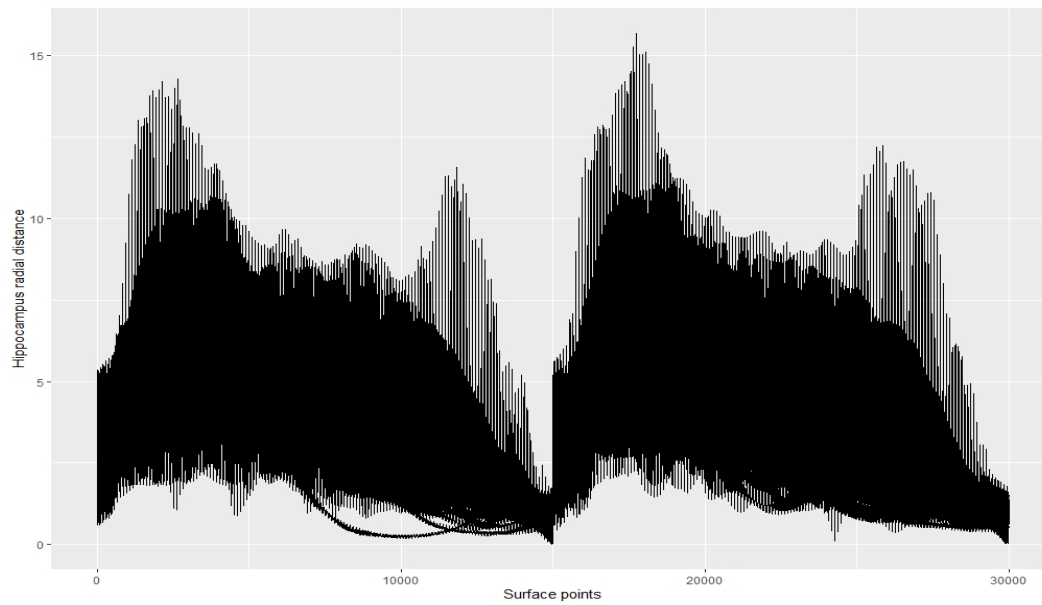
Figure 2.3: The boxplots represent the sampling distribution of the MSE based on the 100 simulation test sets using different methods: Cond.KM.Brier= Conditional Kaplan-Meier (Bandwidth selection based on Brier scores), Cond.KM.MSE= Conditional Kaplan-Meier (Bandwidth selection based on MSE), KM= Kaplan-Meier and FLCRM= Functional Linear Cox Regression Model



(a) Hippocampus radial distance curve of 19th patient



(b) Hippocampus radial distance curve of 207th patient



(c) Hippocampus radial distance curves of all the patients

Figure 2.4: Hippocampus radial distance curves

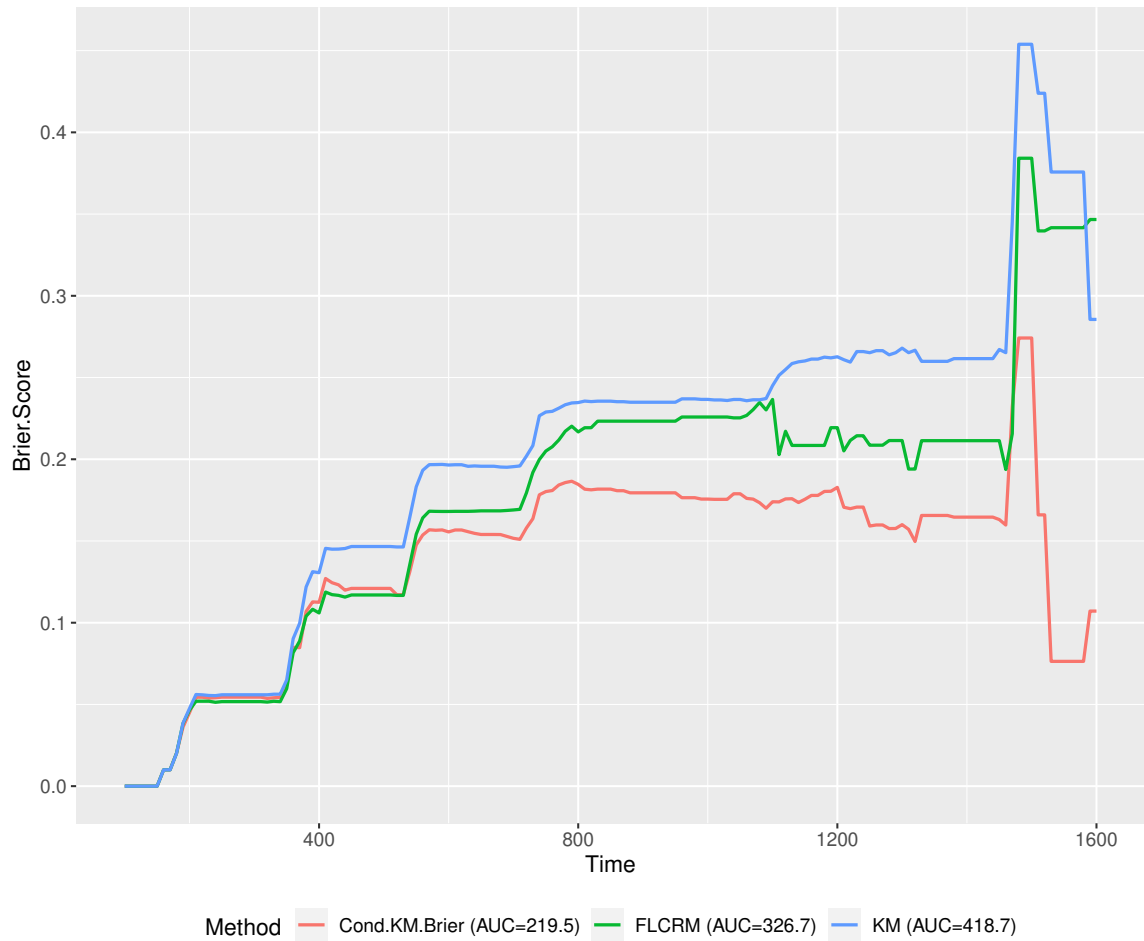


Figure 2.5: Brier scores on the ADNI data

CHAPTER 3

PERSONALIZED TREATMENT SELECTION USING OBSERVATIONAL DATA

1

3.1 Treatment selection method

In this section, we describe the proposed procedure for the selection of optimal treatment. Let us denote the observed triplet for a patient as (Y, \mathbf{X}, T) , where Y is the outcome variable, \mathbf{X} is a vector of r covariates, and T is the treatment received among the K treatment choices, say $T \in \{1, \dots, K\}$. Note that each subject has potentially K treatment choices. Let $(Y_1^*, \dots, Y_K^*)'$ be the hypothetical (counterfactual, potential) responses for a patient where he/she can have given one of K treatments where larger values of the responses are indicative of better outcomes. Although there are K potential responses for K treatment choices, in practice one can not observe the whole vector $(Y_1^*, \dots, Y_K^*)'$ for a single patient. Instead, one can only observe the outcome (say Y) corresponding to the treatment received (say T). That is, $Y = \sum_{k=1}^K I_{\{T=k\}} Y_k^*$. Thus, we cannot sample from the joint distribution of $(Y_1^*, \dots, Y_K^*, \mathbf{X})'$. In a randomized trial, we may consider pairs of random variables (Y, \mathbf{X}) with $T = k$, denoted as (Y_k, \mathbf{X}_k) , drawn from marginal distributions of (Y_k^*, \mathbf{X}_k) ($k = 1, \dots, K$). Then, in methods based on conditional means, one would use $E[Y_k | \mathbf{X}_k = x]$ ($k = 1, \dots, K$) to select

¹The work has been published in *Journal of Applied Statistics*. The citation is "Kulasekera, K. B., Tholkage, S., Kong, M. (2022). Personalized treatment selection using observational data. *Journal of Applied Statistics*, 1-13."

the best treatment. In an observational study, this may not be true, and the optimal treatment selection based on $E[Y_k|\mathbf{X}_k = x]$ ($k = 1, \dots, K$) may be inappropriate. Here we use the notation \mathbf{X}_k to indicate that the sampling is done from each group. In addition, when \mathbf{X} has a very high dimension, a natural choice is to use a composite score $U(\mathbf{X})$ that has a much smaller dimension.

If the available data had resulted from a randomized clinical trial (RCT), then the treatment selection based on pairs (Y_k, \mathbf{X}_k) , $k = 1, \dots, K$ has been addressed by many authors (Cai et al., 2011; Siriwardhana et al., 2019). In such data there are no confounding covariates and therefore the treatment assignment would not have been impacted by covariates. However, when the pairs (Y_k, \mathbf{X}_k) are from an observational study, treatment selection can be highly impacted by confounding covariates and (Y_k, \mathbf{X}_k) can not be considered as a random observation drawn from marginal distributions of (Y_k^*, \mathbf{X}_k) ($k = 1, \dots, K$). Therefore, the methods based on RCT data for optimal treatment selection are no longer applicable. To account for confounding effects we propose to use the generalized propensity score (Imbens, 2000) in our development below. Given there are K possible treatments, the generalized propensity score for a given set of covariates \mathbf{X} is defined as

$$p_k(x) = P[T = k|\mathbf{X} = x]; \quad k = 1, \dots, K \tag{3.1}$$

where T is the assigned treatment in conducting the observational study. There is abundant literature on the properties of generalized propensity scores and their applications in balancing covariates (Rosenbaum and Rubin, 1983; Franklin et al., 2014; Abdia et al., 2017; Yan et al., 2019). One powerful approach is to use the inverse probability of treatment weighting scheme, which is adopted here in our proposed method.

In our proposed treatment selection method, we start with the assumption that

a part of the r dimensional covariate vector \mathbf{X} is providing contributing information and the remainder are nuisance variables. In this, we assume there are unknown r_0 contributing covariates and the remaining $r - r_0$ covariates are junk variables. The r_0 covariates are either confounders or predictors. Literature has shown that including both confounders and predictors in the propensity score model increases the precision of the causal parameter estimation (see Craycroft et al., 2020, and references therein). Using

$$Y_k = g_k(\mathbf{X}) + \epsilon_k, \quad (3.2)$$

we model responses in relation to covariates for each treatment k , where $k = 1, \dots, K$. In the above model (2), $\epsilon_k \sim N(0, \sigma^2)$ and $g_k(\mathbf{X})$ is the mean of Y_k given \mathbf{X} where each g_k is assumed to be a smooth function. Given that we have data from each model above, our goal is to devise a method to estimate the best treatment for a new patient with r dimensional covariate value \mathbf{X}_0 . In particular, let

$$Y_{ki} = g_k(\mathbf{X}_{ki}) + \epsilon_{ki}; i = 1, \dots, n_k \quad k = 1, \dots, K \quad (3.3)$$

be the outcome model for k^{th} group based on the set of n_k observations.

Our first step is to select contributing variables to the outcome, which include confounding variables and predictor variables. We further use the inverse probability of treatment weightings to create K weighted samples such that the distributions of the the contributing variables are similar across the K weighted samples. Thus, the predicted model based on each sample can be applicable to the entire population. Assuming a linear approximation to $g_k(\mathbf{X}_{ki})$ we can use many existing approaches such as Adaptive LASSO (Zou, 2006) or generalized boosted method (GBM) (Greenwell et al., 2019) for variable selection. LASSO assumes a linear relationship between covariates and outcome variable, while GBM assumes a possibly non-linear relationship. In the following we describe our approach using the GBM while a similar approach

can be carried out using LASSO.

GBM is a tree-based machine learning method and has several parameters which can be tuned. We tune the shrinkage parameter, which is also called the learning rate, using a grid of (0.3, 0.1, 0.05, 0.01, 0.005). We use a preset tuning parameter `interaction.depth=3` to incorporate interactions and higher order main effects for each group. We apply a five-fold cross validation approach to obtain the optimal shrinkage parameter and the number of trees that minimize the root mean squares for errors (RMSE). Once the optimal tuning parameters are obtained, a GBM model with the selected tuning parameters is obtained. The important variables are then selected based on the relative influence of each variable. More specifically, we obtain the GBM model for treatment group k using all the covariates \mathbf{X}_k in the models to estimate $g_k(X)$ ($k = 1, \dots, K$). We select the variables where the contribution to the model is more than 5%. The variables selected by the GBM may not be the same for all groups. Suppose the union of the set of covariates selected from each group is $\tilde{\mathbf{X}}$ with a dimension \tilde{r} . Now, instead of using \mathbf{X} , we estimate the generalized propensity score using $\tilde{\mathbf{X}}$ as

$$p_k(\tilde{\mathbf{X}}) = P[T = k | \tilde{\mathbf{X}}], \quad k = 1, \dots, K \quad (3.4)$$

via an available method such as multinomial regression or the boosted logistic regression (Ridgeway et al., 2020).

Now, generalizing the approach in Cai et al. (2011), we define an appropriate treatment-specific score U for each patient in each treatment group as follows. First we define,

$$S_k(\mathbf{X}) = \hat{g}_k(\mathbf{X}) - \max_{j \neq k} \{\hat{g}_j(\mathbf{X})\}$$

where $\hat{g}_k(\mathbf{X})$ is the predicted mean from the GBM for observations in the k th group at a given vector of covariates \mathbf{X} . Note that here we use all covariate values for

the estimation of g_k in each group and also calculating $S_k(k = 1, \dots, K)$. Next we define the overall score to be the combination of the maximum of these treatment-specific scores, and an index that indicates for which treatment the maximum has been achieved for the particular covariate value. That is, we define

$$S(\mathbf{X}) = \max_{k \in \{1, \dots, K\}} \{S_k(\mathbf{X})\} \text{ and } \delta(\mathbf{X}) = \operatorname{argmax}_{k \in \{1, \dots, K\}} \{S_k(\mathbf{X})\}.$$

Then for a patient with covariate value \mathbf{X} , we define the patient score as $U(\mathbf{X}) = (S(\mathbf{X}), \delta(\mathbf{X}))'$. Note that S_k is actually a measure of regret (Murphy, 2003), which provides the decrease (regret) in the benefit-to-go that we forego by making decision k rather than the optimal decision $\delta(\mathbf{X})$, i.e. the predicted effect of the k th treatment from the optimal treatment effect. In our approach we are generalizing this regret to the $K > 2$ setting and choose to use $\max S_k$. One could instead use the minimum regret and in that case we get the negative value for S . Now, we use the patient outcome conditional on patient specific scores to obtain patient-level outcome models for each treatment group. That is, we estimate

$$\mu_k(u) = E[Y_k^* | U(\mathbf{X}) = u], \quad k = 1, \dots, K, \quad (3.5)$$

and the optimal treatment is the one which has the largest estimated value of $\mu_k(u)$ for $k = 1, \dots, K$ for a given U-score. Note that if one chooses not to develop a lower dimensional score, i.e., $U(\mathbf{X}) = \mathbf{X}$, then $\mu_k(U) = g_k(\mathbf{X})$. We estimate $\mu_k(u)$ using either the Nadaraya-Watson (NW) (Li and Racine, 2007) smoothing method or local linear estimation (Li and Racine, 2007) using the inverse of probability of treatment weighted sample to make the distribution of a covariate at k th sample similar to the distribution of the covariate in the population (i.e., balance covariates) so that we can use observed sample to estimate $E[Y_k^* | U(\mathbf{X}_k) = u]$. For example, for a given

$u = (s, \delta)$, we define our NW type estimator of $\mu_k(u)$ as,

$$\hat{\mu}_k(u) = \frac{\sum_{i=1}^{n_k} Y_{ki} \phi\left(\frac{\hat{S}(\mathbf{X}_{ki}) - s}{h_{k\delta}}\right) I(\delta(\mathbf{X}_{ki}) = \delta) w_{ki}}{\sum_{i=1}^{n_k} \phi\left(\frac{\hat{S}(\mathbf{X}_{ki}) - s}{h_{k\delta}}\right) I(\delta(\mathbf{X}_{ki}) = \delta) w_{ki}} ; i = 1, \dots, n_k; k = 1, \dots, K \quad (3.6)$$

where we use standard Gaussian density $\phi(\cdot)$ as the kernel function. Here $h_{k\delta}$ is the bandwidth for the NW estimator, which is calculated using the Asymptotic Mean Integrated Squared Error (AMISE) minimized with respect to the smoothing parameter as given in Scott(Scott, 2015) for each group. The variable δ in U is a discrete variable with values $1, \dots, K$ and weights w_{ki} are defined as $w_{ki} = 1/p_k(\tilde{\mathbf{X}}_{ki})$ where $p_k(\tilde{\mathbf{X}}_{ki})$ s are estimated using a suitable method as described subsequent to (3.4) above. The optimal bandwidths can be selected using the *h.amise* function in the *kedd* R-package.

Alternatively, we may fit a local linear model instead of the NW estimator to estimate each conditional mean $\mu_k(u)$. In that case, our estimator is

$$\hat{\mu}_k(u) = e_1' (\mathbf{Z}'_k \mathcal{W}_k \mathbf{Z})^{-1} (\mathbf{Z}'_k \mathcal{W}_k \mathbf{Y}_k) \quad (3.7)$$

where,

$$\mathbf{Z}_k = \begin{pmatrix} 1 & (\mathbf{S}(\mathbf{X}_{k1}) - \mathbf{s}) \\ 1 & (\mathbf{S}(\mathbf{X}_{k2}) - \mathbf{s}) \\ \cdot & \cdot \\ 1 & (\mathbf{S}(\mathbf{X}_{kn_k}) - \mathbf{s}) \end{pmatrix},$$

\mathcal{W}_k is a $n_k \times n_k$ diagonal matrix whose diagonal elements are $w_{11}, \dots, w_{n_k n_k}$ with $w_{ii} = \phi\left(\frac{\hat{S}(\mathbf{X}_{ki}) - s}{h_{k\delta}}\right) I(\delta(\mathbf{X}_{ki}) = \delta) / p_k(\tilde{\mathbf{X}}_{ki})$, $\mathbf{Y}_k = (Y_{k1}, \dots, Y_{kn_k})'$ and $e_1 = (1, 0)'$. The smoothing parameter $h_{k\delta}$ is selected using the AMISE based smoothing parameter selection method given by ScottScott (2015).

Now, for a new patient with a covariate value \mathbf{X}_0 , we can estimate the corresponding realization of the score u_0 by $\hat{u}_0 = (\hat{s}_0 = \hat{S}(\mathbf{X}_0), \hat{\delta}_0 = \hat{\delta}(\mathbf{X}_0))$ and estimate

$\mu_k(u_0), k = 1, \dots, K$ by $\hat{\mu}_k(\hat{u}_0)$ to find

$$\hat{k}^* = \operatorname{argmax} \hat{\mu}_k(\hat{u}_0).$$

Now, we select the treatment \hat{k}^* as the optimal treatment for that patient.

3.2 Simulation study

In this section, we conduct a detailed simulation study to examine finite sample properties of the proposed procedures introduced in the previous section.

We carried out the simulation study to investigate the accuracy of the proposed treatment selection procedure using the frequency of correct selection of the optimal treatment. We used three treatments ($K = 3$) in the simulations with $n_1 + n_2 + n_3 = 500$ as the total sample size. Our primary focus is on the accuracy of the treatment assignment, where larger values of the responses indicate better outcomes. The models for each treatment group have been defined in a manner that no model will dominate others over the whole covariate domain, which is the primary reason for choosing the best treatment among several based on underlying covariate information.

In this study, we first simulate $n = 500$ iid multivariate normal random vectors $\mathbf{X}_i, i = 1, \dots, 500$ of dimension $r = 10$ from $MVN(0, I_r)$ distribution. For each covariate value \mathbf{X}_i , we calculate a probability $\tilde{p}_k(\mathbf{X}_i); k = 1, 2, 3$ where $\sum_k \tilde{p}_k = 1$. Then we assign each patient with a covariate value \mathbf{X}_i into one of the three treatment groups according to a multinomial distribution with corresponding probabilities $\tilde{p}_1(\mathbf{X}_i), \tilde{p}_2(\mathbf{X}_i)$ and $\tilde{p}_3(\mathbf{X}_i)$. Here we used

$$\tilde{p}_k(\mathbf{X}_i) = \frac{\exp(-2 + \alpha'_k \mathbf{X}_i)}{1 + \sum_{k=1}^2 \exp(-2 + \alpha'_k \mathbf{X}_i)} \text{ for } k = 1, 2,$$

and

$$\tilde{p}_3(\mathbf{X}_i) = 1 - \tilde{p}_1(\mathbf{X}_i) - \tilde{p}_2(\mathbf{X}_i)$$

with $\alpha'_1 = (3, 0_7, 2.5, 2)$ and $\alpha'_2 = (-3, 0_7, 1.5, -3)$ with 0_7 being a vector of zeros of length 7. We consider three different functional forms for the outcome models (3) for each treatment. The errors ϵ_{ki} in each outcome model were generated from a normal distribution with zero mean and standard deviation 0.1. We used three different scenarios to increase the complexity of outcome models from simple linear form to a complex non-linear form containing interactions and higher order terms of the covariates (Table 3.1). While we have conducted simulations using numerous models, we are only presenting variations of these selected few models that have also been used in a previous article by Lu et al. (2013) for evaluating a selection procedure for data from a randomized clinical trial. We feel that these models represent the variety needed for establishing the required accuracy of selecting a treatment from multiple choices.

Table 3.1: Three different simulation scenarios which correspond to different complexities of outcome models.

Outcome models		
Scenario 1: Linear Outcomes	Group-1	$1 + \gamma'_1 \mathbf{X}_i + \beta'_1 \mathbf{X}_i$
	Group-2	$1 + \gamma'_1 \mathbf{X}_i + \beta'_2 \mathbf{X}_i$
	Group-3	$1 + (\gamma'_1 \mathbf{X}_i)$
Scenario 2: Quadratic Outcomes	Group-1	$1 + (\gamma'_1 \mathbf{X}_i)(\gamma'_2 \mathbf{X}_i) + \beta'_1 \mathbf{X}_i$
	Group-2	$1 + (\gamma'_1 \mathbf{X}_i)(\gamma'_2 \mathbf{X}_i) + \beta'_2 \mathbf{X}_i$
	Group-3	$1 + (\gamma'_1 \mathbf{X}_i)(\gamma'_2 \mathbf{X}_i)$
Scenario 3: Nonlinear Outcomes	Group-1	$1 + 0.5 \sin(\pi \gamma'_1 \mathbf{X}_i) + 0.25(1 + \gamma'_1 \mathbf{X}_i)^2 + \beta'_1 \mathbf{X}_i$
	Group-2	$1 + 0.5 \sin(\pi \gamma'_1 \mathbf{X}_i) + 0.25(1 + \gamma'_1 \mathbf{X}_i)^2 + \beta'_2 \mathbf{X}_i$
	Group-3	$1 + 0.5 \sin(\pi \gamma'_1 \mathbf{X}_i) + 0.25(1 + \gamma'_1 \mathbf{X}_i)^2$

$$\gamma'_1 = (-2, 0_7, 0.8, -1.1), \gamma'_2 = (-1, 0_7, -2, 0.8), \beta'_1 = (1, 0_7, 1.5, 2) \text{ and } \beta'_2 = c(-1, 0_7, -1, 2).$$

Once the samples were generated, we first estimated mean functions $g_k(\mathbf{X})$ for each treatment group using the GBM method (or LASSO) and select the union $\tilde{\mathbf{X}}$ of contributing covariates from the three groups to estimate propensity scores

$p_k(\tilde{\mathbf{X}}_i)$ for $k = 1, 2, 3$ and $i = 1, \dots, n$. Then we used the estimated mean functions $g_k(\mathbf{X}), k = 1, 2, 3$ to estimate the scores $(U(\mathbf{X}_i) = (S(\mathbf{X}_i), \delta(\mathbf{X}_i))')$ for $i = 1, \dots, n$. In the case of variables selected from the GBM method, we used the *mnps* function from the R package *twang* to estimate the propensity scores with boosted logistic regression. If variables were selected from LASSO method, we used the *multinom* function from the R package *nnet* to estimate the propensity scores with multinomial logistic regression.

Now, a new covariate vector \mathbf{X}_0 was generated from the same multivariate normal distribution above, and the corresponding score $\hat{\mathbf{u}}_0$ was estimated to calculate $\hat{\mu}_k(\hat{\mathbf{u}}_0)$ for $k = 1, 2, 3$. The kernel function in this estimation was taken to be the standard normal pdf while the optimal bandwidths in (5) were calculated using Asymptotic Mean Integrated Squared Error (AMISE) method given by Scott (1992) using the *h.amise* function from the R package *kedd* (Guidoum, 2015). Then, corresponding to this \mathbf{X}_0 , we generated treatment responses $Y_{k0}^*; k = 1, 2, 3$ for each treatment group using the outcome models in Table 3.1. We define the treatment assignment to be correct if

$$\operatorname{argmax}_k \{\hat{\mu}_k(\hat{u}_0)\} = \operatorname{argmax}_k \{Y_{k0}^*\}.$$

We generated 1000 such test cases and calculated the relative frequency of correct treatment assignment for each setting and repeated this procedure 500 times to get a sample distribution of these relative frequencies. For comparison purposes, we also carried out the analysis without using propensity score weighting to estimate the $\hat{\mu}_k(\hat{u}_0)$. The boxplots of the predicted accuracies based on the 500 simulation test sets are reported in Figure 3.1, and their means are summarized in Table 3.2, for different methods used.

We have additionally assessed the performance of the proposed method using

the composite average gain of responses. This measure helps us to understand the impact of possible wrong assignments by comparing the treatment chosen by our method (the treatment with the largest $\hat{\mu}$) with its nearest competitor as well as its worst competitor. Suppose that for a new covariate value X_0 , the ordered $\hat{\mu}_i(\hat{\mathbf{u}}_0)$ s are $\hat{\mu}_{i_1}(\hat{\mathbf{u}}_0) \geq \hat{\mu}_{i_2}(\hat{\mathbf{u}}_0) \dots \geq \hat{\mu}_{i_K}(\hat{\mathbf{u}}_0)$. Define $\lambda_{12}(\hat{\mathbf{u}}_0)$ and $\lambda_{1K}(\hat{\mathbf{u}}_0)$ as

$$\lambda_{12}(\hat{\mathbf{u}}_0) = \hat{\mu}_{i_1}(\hat{\mathbf{u}}_0) - \hat{\mu}_{i_2}(\hat{\mathbf{u}}_0)$$

and

$$\lambda_{1K}(\hat{\mathbf{u}}_0) = \hat{\mu}_{i_1}(\hat{\mathbf{u}}_0) - \hat{\mu}_{i_K}(\hat{\mathbf{u}}_0).$$

Now letting C be the maximum difference between any pair of μ_{i_k} s within the whole covariate domain, we average λ_{12}/C and λ_{1K}/C for new test cases and denote them as Λ_{12} and Λ_{1K} respectively. Positive values of Λ_{12} and Λ_{1K} indicate relative average gains in the expected treatment outcome by the treatment selection technique. Then we get sampling distribution of these Λ_{12} and Λ_{1K} by repeating the procedure for 500 times. Table 3.2 reports the sample means of these estimates.

To our knowledge, there is no literature on selecting a treatment based on observational data using propensity scores for the case $K > 2$. Tables and graphs above show the selection accuracy of selecting a treatment for multiple possible variations of the proposed procedure based on observational data (see Table 3.2 and 3.3; Figure 3.1). Second and third columns of Tables 3.2 and 3.3 show various combinations that can be used in the proposed procedure. Based on these results we conclude that, under Scenario 1, the proposed procedure with Nadaraya-Watson estimation technique seems to show higher accuracy compared with the local linear choice for this novel approach. We can especially observe that the propensity score weighting has improved the prediction accuracy in all methods. Even though the method using the LASSO-NW combination has a slightly higher average prediction accuracy than

the combination of GBM-NW, the latter appears to produce more consistent results according to box-plots. Under Scenarios 2 and 3, the GBM method seems to perform better. However, weighting on propensity scores have neither decreased nor improved the prediction accuracy under Scenarios 2 and 3.

3.3 Case study

In this section, we illustrate the use of our proposed method for the variety of choices using an observational data set obtained from a computerized pharmacy database on statin use (Joosten et al., 2014). Statins are one of most commonly prescribed lipid-lowering medications to help reduce cholesterol and reduce the risk of cardiovascular diseases. The primary objective of the study done by Joosten et al. (2014) was to evaluate the association between statin use and cognitive function. According to the literature, statin use has been recommended over a longer period to have a positive effect on cognitive function. Therefore, long-term observational studies are preferred to evaluate statin use on cognitive function since RCTs of longer duration are generally not feasible. Our objective in this analysis is merely to show the applicability of our method using this data set. We are not critiquing medical aspects of the above study in our discussion below.

In this study, a total of 4,095 community-dwelling participants aged 35-82 years were included and 904 participants (about 22%) used statin. The statins can be categorized based on the solubility as hydrophilic and lipophilic. In general, lipophilic statin tend to have a high central nervous system penetration while hydrophilic statins tend to have less central nervous system penetration. In this study, we consider three treatment groups: treatment 1 is the use of lipophilic statin (470 patients), treatment 2 is the use of hydrophilic statin (340 patients) and 3 is no statin use (3165 patients).

The outcome variable was considered as the cognitive function, which was measured by the Ruff Figural Fluency Test (RFFT: the worst score at 0 points to the

best score at 175 points). In this study, we used predictor variables such as demographic information of patients (age, sex, ethnicity, and educational level), history of cardiovascular events, diabetes mellitus, smoking status, hypertension, BMI, systolic blood pressure (mmHg), diastolic blood pressure (mmHg), mean arterial pressure (mmHg), estimated glomerular filtration rate (MDRD), albuminuria in three categories ($0 = \text{“0 to } < 10\text{”}$, $1 = \text{“10 to } < 30\text{”}$, $2 = \text{“} \leq 30 \text{ mg/24hr”}$), total cholesterol (mmol/L) and HDL cholesterol (mmol/L).

We conducted the analysis using a five-fold cross-validation. First we randomly partitioned patients from k^{th} ($k = 1, 2, 3$) treatment group into five folds. In the first iteration, we kept the first fold of each treatment group for testing and the remaining data for training. We estimated the mean function $g_k(\mathbf{X})$ ($k = 1, 2, 3$) using the GBM method and selected the union of contributing covariates from the three groups (say, $\tilde{\mathbf{X}}$) to estimate propensity scores $p_k(\tilde{\mathbf{X}}_i)$ for $k = 1, 2, 3$ combining the three training data sets. Then using the estimated mean functions $g_k(\mathbf{X})$ s we estimated the scores for patients in the training set. Then using the proposed weighted Nadaraya-Watson method we assigned the patients in the testing data to a treatment based on their estimated scores. The predicted optimal treatments for the testing fold in the first iteration is reported in Table 3.4A. We repeated the process for each fold, and the treatment assignment based on this repeated 5-fold cross-validation is summarized in Table 3.4B. The intermediate estimation results for the first iteration of the 5-fold cross validation are reported in the Appendix B.

The assignment probabilities seem to be consistent on optimal treatment assignments resulted from one-fold testing (Table 3.4A) versus five fold testing (Table 3.4B). Among the patients who were originally given lypophilic statin (treatment 1), the proposed optimal assignment remained unchanged for 33.8% of the patients while the rest of the patients were recommended to receive the other two options. Among the patients who were originally given hydrophilic statin (treatment 2), the

proposed optimal assignment remained unchanged for 32.4% of the patients while the rest of the patients were recommended to receive the other two options. For the patients who were originally not given a statin, the proposed method assigned 12.7% to the lipophilic statin, 27.9% to the hydrophilic statin, 59.4% of the patients remained not to give any statins. Overall, we recommend switching the treatments to gain a better outcome for some patients based on their covariate information. We also calculated the composite average gain of response, averaging the Λ_{12} and Λ_{13} values of the five folds in the 5-fold cross validation as $\Lambda_{12} = 0.271$ and $\Lambda_{13} = 0.378$.

3.4 Discussion

In this paper, we proposed a novel method to estimate the optimal personalized treatment based on observational data. This framework allows the proposed method to focus on the most important covariates and the use of inverse probability of treatment weighting helps to adjust for bias due to confounding. In the empirical study, the proposed method was tested under different scenarios and the GBM-NW combination appears to outperform other compared methods in selecting the optimal treatment in a multiple treatment setting. The sampling distributions of prediction accuracy were considered to compare the methods in a broader perspective. Our method was applied on a real observational data set with multiple treatment options to observe how the treatments could be assigned based on patient characteristics in order to gain a better outcome. Although in the real data analyses the proposed method doesn't provide a general optimal treatment, rather it recommends patients to stay on the current treatment or switch from the current treatment to other available treatments based on their characteristics at individual level, in practice this method proposes the best treatment at an individual patient level.

The proposed method is based on a single outcome measure and for future work we would extend our method to explore the situations with multiple outcome

measures on observational data. Time to event data is also another aspect that requires attention on the problem we discussed in this paper and will be considered in future work.

3.5 Tables and Figures

Table 3.2: The average prediction accuracy based on 500 test sets using different methods under different scenarios.

			Unweighted	Weighted
Scenario 1	LASSO	NW	0.5180	0.8515
		LL	0.4788	0.7358
	GBM	NW	0.7169	0.8243
		LL	0.6510	0.7571
Scenario 2	LASSO	NW	0.7269	0.6973
		LL	0.7278	0.7076
	GBM	NW	0.8130	0.8128
		LL	0.7955	0.7919
Scenario 3	LASSO	NW	0.5672	0.6477
		LL	0.5788	0.6366
	GBM	NW	0.7175	0.7175
		LL	0.6996	0.6977

GBM= GBM for variable selection; LASSO=LASSO for variable selection; LL= Local Linear Estimator; NW= Nadaraya-Watson type estimator.

Table 3.3: The composite average gain of responses to choose the optimal versus the second optimal treatment (Λ_{12}), and the optimal versus the worst treatment (Λ_{13}).

			Unweighted		Weighted	
			Λ_{12}	Λ_{13}	Λ_{12}	Λ_{13}
Scenario 1	LASSO	NW	0.2240	0.3692	0.2094	0.3733
		LLE	0.0309	0.0653	0.0356	0.0807
	GBM	NW	0.1934	0.3144	0.1987	0.2938
		LLE	0.0371	0.0745	0.0505	0.0943
Scenario 2	LASSO	NW	0.0572	0.2865	0.0471	0.2642
		LLE	0.0305	0.2229	0.0255	0.2166
	GBM	NW	0.1698	0.3023	0.1570	0.2761
		LLE	0.0406	0.1032	0.0385	0.1032
Scenario 3	LASSO	NW	0.1565	0.3671	0.1279	0.3423
		LLE	0.0196	0.1511	0.0178	0.1452
	GBM	NW	0.1216	0.2589	0.1159	0.2512
		LLE	0.0270	0.1331	0.0314	0.1383

GBM= GBM for variable selection; LASSO=LASSO for variable selection; LL= Local Linear Estimator; NW= Nadaraya-Watson type estimator.

Table 3.4: Summarized optimal treatment assignments compared with the original assignments based on one-fold testing data as well as based on 5-folds testing data.

A: Proposed optimal assignment based on the 1st iteration of 5-fold CV						
			1	2	3	Total
Original Assignment	1: lipo.	count	32	36	26	94
	statin	%	34.0%	38.3%	27.7%	100.0%
	2: hydro.	count	13	22	33	68
	statin	%	19.1%	32.4%	48.5%	100.0%
	3: no	count	83	184	366	633
	statin	%	13.1%	29.1%	57.8%	100.0%
B: Proposed optimal assignment based on all the iterations of 5-fold CV						
			1	2	3	Total
Original Assignment	1: lipo.	count	159	170	141	470
	statin	%	33.8%	36.2%	30.0%	100.0%
	2: hydro.	count	78	110	152	340
	statin	%	22.9%	32.4%	44.7%	100.0%
	3: no	count	401	884	1880	3165
	statin	%	12.7%	27.9%	59.4%	100.0%

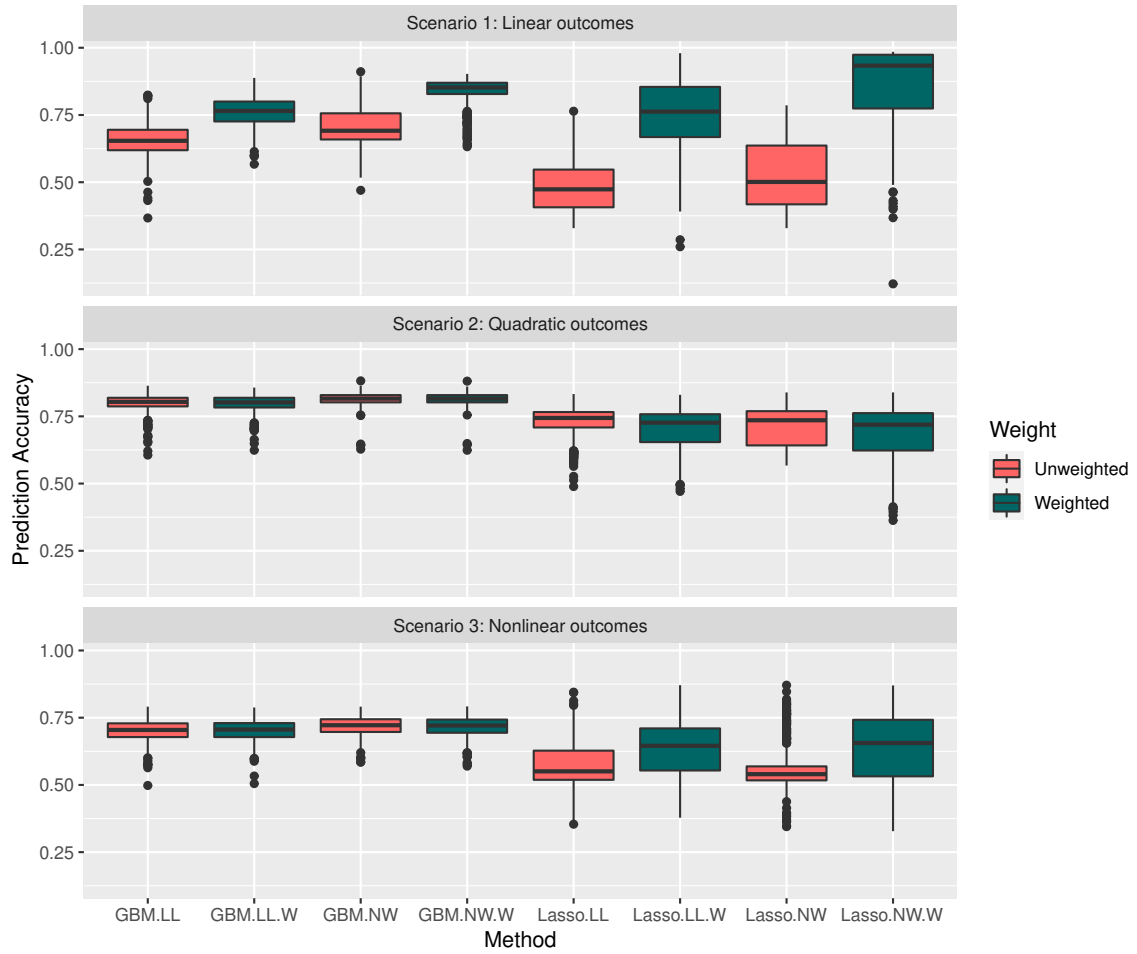


Figure 3.1: The boxplots of the predicted accuracy based on the 500 simulation test sets using different methods under three different scenarios. GBM= GBM for variable selection; LASSO=LASSO for variable selection; LL= Local Linear Estimator; NW= Nadaraya-Watson type estimator; .W=Methods that used inverse probability of treatment weights

CHAPTER 4

IDENTIFYING OPTIMAL TREATMENT REGIME USING
SINGLE INDEX MODELS FOR SURVIVAL DATA

4.1 Treatment selection method

In this section, we describe the proposed procedure for identifying the optimal treatment. Let T denote the survival time of a patient, which is subject to random right censoring C . Thus, the observed information for a patient is $\tilde{T} = \min(T, C)$ and $\Delta = 1\{T \leq C\}$, where $1\{\cdot\}$ is the indicator function. We use $(\mathbf{X}, \mathbf{Z}) \in \mathbb{R}^p \times \mathbb{R}^q$ to denote the covariate information of a patient with $\mathbf{X} \in \mathbb{R}^p$ being continuous covariates and $\mathbf{Z} \in \mathbb{R}^q$ being categorical covariates. Suppose there are $K + 1$ treatments available indexed by $k = 0, 1, \dots, K$. Let A denote the treatment that a patient received, and $A \in \{0, 1, \dots, K\}$. We impose the independent censoring assumption that the censoring time C is independent of T , (\mathbf{X}, \mathbf{Z}) , and A . The observed data consists of n i.i.d. replicates of $(\tilde{T}, \Delta, (\mathbf{X}, \mathbf{Z}), A)$, denoted by $\{(\tilde{T}_i, \Delta_i, (\mathbf{X}_i, \mathbf{Z}_i), A_i)\}_{i=1}^n$.

Let $Y = \log T$ and $\tilde{Y} = \log \tilde{T}$. In addition, let $Y^{(k)}$ be the potential (i.e., counterfactual) log-survival time of a patient of receiving the k th treatment, $k = 0, 1, \dots, K$. Let $A_{(k)} = 1\{A = k\}$ denote the dummy variable of a patient receiving treatment k ($k = 0, 1, \dots, K$). Since a patient is given only one of $K + 1$ treatments, we naturally have $Y = \sum_{k=0}^K A_{(k)} Y^{(k)}$, which is coincided as the consistency assumption in the causal inference literature.

In this work, we consider a semiparametric partial linear model for the coun-

terfactual log-survival time of receiving the k th treatment, namely,

$$E[Y^{(k)}|\mathbf{X}, \mathbf{Z}] = h_0^*(\mathbf{X}, \mathbf{Z}) + \mathbf{Z}^T \boldsymbol{\theta}_k^* + g_k^*(\mathbf{X}^T \boldsymbol{\beta}_k^*), \quad k = 1, \dots, K, \quad (4.1)$$

where $h_0^*(\cdot) = E[Y|A = 0, \mathbf{X} = x, \mathbf{Z} = \mathbf{z}]$ is a baseline mean function for $k = 0$, $\boldsymbol{\theta}_k^* = (\theta_{k1}^*, \dots, \theta_{kq}^*)^T$ is a q -dimensional vectors of unknown coefficients for \mathbf{Z} for the k th treatment, and $g_k^*(\cdot)$ is an unknown smooth function with $\boldsymbol{\beta}_k^* = (\beta_{k1}^*, \dots, \beta_{kp}^*)^T$ as a p -dimensional vector of unknown coefficients for the k th treatment. Thus, $\mathbf{Z}^T \boldsymbol{\theta}_k^* + g_k^*(\mathbf{X}^T \boldsymbol{\beta}_k^*)$ is the contrast function between treatment k and control. The consistency assumption $Y = \sum_{k=0}^K A_{(k)} Y^{(k)}$ and (4.1) together lead to

$$E[Y|A, \mathbf{X}, \mathbf{Z}] = h_0^*(\mathbf{X}, \mathbf{Z}) + \sum_{k=1}^K A_{(k)} [\mathbf{Z}^T \boldsymbol{\theta}_k^* + g_k^*(\mathbf{X}^T \boldsymbol{\beta}_k^*)]. \quad (4.2)$$

We assume that $\|\boldsymbol{\beta}_k^*\|^2 = 1$ and $\beta_{k1}^* > 0$ in order for the model to be identifiable. Let $g_0^*(\cdot) = 0$ and $\boldsymbol{\theta}_0^* = \mathbf{0}$. Under model (4.2), the optimal treatment regime is $\operatorname{argmax}_{0 \leq k \leq K} \mathbf{Z}^T \boldsymbol{\theta}_k^* + g_k^*(\mathbf{X}^T \boldsymbol{\beta}_k^*)$.

Let $\underline{\boldsymbol{\theta}} = (\boldsymbol{\theta}_1^T, \dots, \boldsymbol{\theta}_K^T)^T$, $\mathbf{g} = (g_1, \dots, g_K)^T$ and $\underline{\boldsymbol{\beta}} = (\boldsymbol{\beta}_1^T, \dots, \boldsymbol{\beta}_K^T)^T$. We propose to estimate the optimal treatment regime by minimizing the following objective function

$$\frac{1}{n} \sum_{i=1}^n \frac{\Delta_i}{G(T_i)} \left[\tilde{Y}_i - \phi(\mathbf{X}_i, \mathbf{Z}_i; \boldsymbol{\gamma}) - \sum_{k=1}^K (A_{i(k)} - \pi_k(\mathbf{X}_i, \mathbf{Z}_i)) [\mathbf{Z}_i^T \boldsymbol{\theta}_k + g_k(\mathbf{X}_i^T \boldsymbol{\beta}_k)] \right]^2, \quad (4.3)$$

with respect to $\boldsymbol{\gamma}$, \mathbf{g} , $\underline{\boldsymbol{\theta}}$, and $\underline{\boldsymbol{\beta}}$. In (4.3), $Y_i = \log(T_i)$, $\pi_k(x, \mathbf{Z}) = P(A_i = k | \mathbf{X}_i = x, \mathbf{Z}_i = \mathbf{z})$ is the propensity score, $G(\cdot)$ is the survival function of censoring time C , and $\phi(x, \mathbf{z}; \boldsymbol{\gamma})$ is a posited parametric/semiparametric function with parameters $\boldsymbol{\gamma} = (\boldsymbol{\gamma}_1^T, \boldsymbol{\gamma}_2^T)^T$, where $\boldsymbol{\gamma}_1 \in \mathbb{R}^p$ and $\boldsymbol{\gamma}_2 \in \mathbb{R}^q$. $\phi(\cdot; \boldsymbol{\gamma})$ can take various forms. For example, we can choose $\phi(\cdot; \boldsymbol{\gamma})$ as a constant function or a linear function (Lu et al., 2013), (*i.e.*, $\phi(\mathbf{X}, \mathbf{Z}; \boldsymbol{\gamma}) = \mathbf{X}^T \boldsymbol{\gamma}_1 + \mathbf{Z}^T \boldsymbol{\gamma}_2$) or a partial linear function (*i.e.*, $\phi(\mathbf{X}, \mathbf{Z}; \boldsymbol{\gamma}) =$

$m(\mathbf{X}^T \boldsymbol{\gamma}_1) + \mathbf{Z}^T \boldsymbol{\gamma}_2$, for some known/unknown link function $m(\cdot)$). We can show that as long as $\pi_k(\mathbf{X}, \mathbf{Z})$ is correctly specified, the estimation of $\underline{\boldsymbol{\theta}}$, $\underline{\boldsymbol{\beta}}$ and \mathbf{g} would be consistent regardless of the choice of $\phi(\cdot; \boldsymbol{\gamma})$. Thus, we can use $\tilde{\boldsymbol{\gamma}}$, a working value of $\boldsymbol{\gamma}$ in (4.3). In practice, the censoring probability $G(\cdot)$ and the propensity scores $\pi_k(x, \mathbf{Z})$ are typically unknown. But they can be replaced by their corresponding consistent estimators \hat{G} and $\hat{\pi}_k(x, \mathbf{Z})$. For example, we can obtain $\hat{G}(\cdot)$ using Kaplan-Meier method (Kaplan and Meier, 1958) and implement multinomial logistic regression to estimate $\pi_k(x, \mathbf{Z})$ (Yan et al., 2019). As a result, we minimize $L_n(\mathbf{g}, \underline{\boldsymbol{\theta}}, \underline{\boldsymbol{\beta}}; \tilde{\boldsymbol{\gamma}})$, which is the objective function (4.3) with $\phi(\mathbf{X}_i, \mathbf{Z}_i; \boldsymbol{\gamma})$, G , and $\pi_k(x, \mathbf{Z})$ replaced by $\phi(\mathbf{X}_i, \mathbf{Z}_i; \tilde{\boldsymbol{\gamma}})$, \hat{G} , and $\hat{\pi}_k(x, \mathbf{Z})$, respectively.

$$L_n(\mathbf{g}, \underline{\boldsymbol{\theta}}, \underline{\boldsymbol{\beta}}; \tilde{\boldsymbol{\gamma}}) = \frac{1}{n} \sum_{i=1}^n \frac{\Delta_i}{\hat{G}(T_i)} \left[\tilde{Y}_i - \phi(\mathbf{X}_i, \mathbf{Z}_i; \tilde{\boldsymbol{\gamma}}) - \sum_{k=1}^K (A_{i(k)} - \hat{\pi}_k(\mathbf{X}_i, \mathbf{Z}_i)) [\mathbf{Z}_i^T \boldsymbol{\theta}_k + g_k(\mathbf{X}_i^T \boldsymbol{\beta}_k)] \right]^2. \quad (4.4)$$

The contrast function between treatment k and control, $g_k(\cdot)$ ($k = 1, \dots, K$), is an unspecified smooth function, and can be approximated by B-splines (de Boor, 2001). Assume that $\max_{1 \leq k \leq K} \sup_{\mathbf{X}} |\mathbf{X}^T \boldsymbol{\beta}_k|$ is bounded above. Let

$$[a_k, b_k] = [\inf_{\mathbf{X}} (\mathbf{X}^T \boldsymbol{\beta}_k), \sup_{\mathbf{X}} (\mathbf{X}^T \boldsymbol{\beta}_k)]$$

denote the support of $g_k(\cdot)$, $1 \leq k \leq K$. The interior knots of B-splines can then be obtained by partitioning the $[a_k, b_k]$ with equally spaced knots, $a_k = t_{0,k} < t_{1,k} < \dots < t_{N_k,k} < b_k = t_{N_k+1,k}$. The number of internal knots is actually allowed to increase with n . But for notation simplicity, we suppress the dependence of N_k on n when there is no confusion (*i.e.*, $N_k = N_{k,n}$). Based on these knots, we then divide $[a_k, b_k]$ into sub-intervals $I_{l,k} = [t_{l,k}, t_{l+1,k})$, $0 \leq l \leq N_k - 1$ and $I_{N_k} = [t_{N_k,k}, t_{N_k+1,k}]$ satisfying $\max_{0 \leq l \leq N_k} |t_{l+1,k} - t_{l,k}| / \min_{0 \leq l \leq N_k} |t_{l+1,k} - t_{l,k}| \leq M$ uniformly in n for some constant

$0 < M < \infty$. Then we can define the normalized B-spline basis of this space as $\mathbf{B}_k(\cdot) = \{B_{l,k}(\cdot) : 1 \leq l \leq L_k\}^T$, where $L_k = N_k + v_k$ is the number of basis spline functions and $v_k - 1$ is the spline order. By de Boor (2001), we can approximate the nonparametric function g_k as $g_k(\mathbf{X}^T \boldsymbol{\beta}_k) \approx \mathbf{B}_k(\mathbf{X}^T \boldsymbol{\beta}_k)^T \boldsymbol{\delta}_k^*$, where $\boldsymbol{\delta}_k^*$ minimizes $\sup_{t \in [a_k, b_k]} |g_k(t) - \mathbf{B}_k(t)^T \boldsymbol{\delta}_k|$ over $\boldsymbol{\delta}_k \in \mathbb{R}^{L_k}$. In this work, we choose $N_k = 5$ and $v_k = 4(k = 1, \dots, K)$ for computational convenience. It has been shown that a large number of knots may lead to over-fitting the data and as small as five knots is sufficient for cubic splines (Gauthier et al., 2020). It is worth noting that $v_k = 4$ corresponds to cubic splines.

Let $\underline{\boldsymbol{\delta}} = (\boldsymbol{\delta}_1^T, \dots, \boldsymbol{\delta}_K^T)^T$. We can approximate (4.4) by

$$\begin{aligned} \tilde{L}_n(\underline{\boldsymbol{\delta}}, \underline{\boldsymbol{\theta}}, \underline{\boldsymbol{\beta}}; \tilde{\boldsymbol{\gamma}}) &= \frac{1}{n} \sum_{i=1}^n \frac{\Delta_i}{\hat{G}(T_i)} \left[\tilde{Y}_i - \phi(\mathbf{X}_i, \mathbf{Z}_i; \tilde{\boldsymbol{\gamma}}) \right. \\ &\quad \left. - \sum_{k=1}^K (A_{i(k)} - \hat{\pi}_k(\mathbf{X}_i, \mathbf{Z}_i)) \left[\mathbf{Z}_i^T \boldsymbol{\theta}_k + \mathbf{B}_k(\mathbf{X}_i^T \boldsymbol{\beta}_k)^T \boldsymbol{\delta}_k \right] \right]^2. \end{aligned} \quad (4.5)$$

Let $\boldsymbol{\beta}_{k,-1}$ be a vector obtained by removing the first element of $\boldsymbol{\beta}_k$. To obtain the estimates of $\underline{\boldsymbol{\delta}}$, $\underline{\boldsymbol{\theta}}$, and $\underline{\boldsymbol{\beta}}$, we employ an iterative algorithm as follows:

Step 1 *Obtain initial estimates:* the initial estimates of $\underline{\boldsymbol{\theta}}$ and $\underline{\boldsymbol{\beta}}$ are obtained by minimizing (4.8) by treating g_k as identity functions, i.e., $g_k(\mathbf{X}^T \boldsymbol{\beta}_k) = \mathbf{X}^T \boldsymbol{\beta}_k$.

Step 2 *Update $\underline{\boldsymbol{\delta}}$, $\underline{\boldsymbol{\theta}}$, and $\underline{\boldsymbol{\beta}}$:* denote the current estimates of $\boldsymbol{\theta}_k$ by $\boldsymbol{\theta}_k^{old}$ and $\boldsymbol{\beta}_k$ by $\boldsymbol{\beta}_k^{old}$ for $k = 1, \dots, K$. Let $\boldsymbol{\beta}_{k,-1}$ be a vector obtained by removing the first element of $\boldsymbol{\beta}_k$.

- (a) *Update $\underline{\boldsymbol{\delta}}^{new}$ given $\underline{\boldsymbol{\theta}}^{old}$ and $\underline{\boldsymbol{\beta}}^{old}$:* given $\underline{\boldsymbol{\theta}}^{old}$ and $\underline{\boldsymbol{\beta}}^{old}$, the estimate of $\underline{\boldsymbol{\delta}}$ can be updated by $\underline{\boldsymbol{\delta}}^{new} = (\mathbb{B}^T \mathbb{W} \mathbb{B})^{-1} \mathbb{B}^T \mathbb{W} \mathbf{D}_1$, where \mathbb{W} is a diagonal matrix with diagonal elements $w_{ii} = \hat{G}(T_i)^{-1} \Delta_i$, \mathbf{D}_1 is a $n \times 1$ vector with the i th element being $\tilde{Y}_i - \phi(\mathbf{X}_i, \mathbf{Z}_i; \tilde{\boldsymbol{\gamma}}) - \sum_{k=1}^K (A_{i(k)} - \hat{\pi}_k(\mathbf{X}_i, \mathbf{Z}_i)) \mathbf{Z}_i^T \boldsymbol{\theta}_k^{old}$, and \mathbb{B} is

a $n \times KL$ matrix with the i th row being

$$(A_{i(1)} - \hat{\pi}_1(\mathbf{X}_i, \mathbf{Z}_i))\mathbf{B}_1^\top(\mathbf{X}_i^\top \boldsymbol{\beta}_1^{old}), \dots, (A_{i(K)} - \hat{\pi}_K(\mathbf{X}_i, \mathbf{Z}_i))\mathbf{B}_K^\top(\mathbf{X}_i^\top \boldsymbol{\beta}_K^{old}).$$

- (b) Update $\underline{\boldsymbol{\beta}}^{new}$ given $\underline{\boldsymbol{\delta}}^{new}$, $\underline{\boldsymbol{\theta}}^{old}$, and $\underline{\boldsymbol{\beta}}^{old}$: given $\underline{\boldsymbol{\delta}}^{new}$ and $\underline{\boldsymbol{\beta}}^{old}$, we can approximate $\tilde{g}_k(\mathbf{X}^\top \boldsymbol{\beta}_k) := B(\mathbf{X}^\top \boldsymbol{\beta}_k)^\top \boldsymbol{\delta}_k^{new}$ as

$$\tilde{g}_k(\mathbf{X}^\top \boldsymbol{\beta}_k) \approx \tilde{g}_k(\mathbf{X}^\top \boldsymbol{\beta}_k^{old}) + \tilde{g}'_k(\mathbf{X}^\top \boldsymbol{\beta}_k^{old}) \mathbf{X}^\top \mathbb{J}(\boldsymbol{\beta}_k^{old})(\boldsymbol{\beta}_{k,-1} - \boldsymbol{\beta}_{k,-1}^{old})$$

where

$$\mathbb{J}(\boldsymbol{\beta}_k) = \frac{\partial \boldsymbol{\beta}_k}{\partial \boldsymbol{\beta}_{k,-1}} = \begin{pmatrix} -\boldsymbol{\beta}_{k,-1}^\top / \sqrt{1 - \|\boldsymbol{\beta}_{k,-1}\|_2^2} \\ \mathbb{I}_{p-1} \end{pmatrix}$$

is the $p \times (p-1)$ Jacobian matrix, and \mathbb{I}_t is a t -dimensional identity matrix.

Let $\underline{\boldsymbol{\beta}}_{-1} = (\boldsymbol{\beta}_{1,-1}^\top, \boldsymbol{\beta}_{2,-1}^\top, \dots, \boldsymbol{\beta}_{K,-1}^\top)^\top \in \mathbb{R}^{K(p-1)}$ and $R_{ik} = \tilde{g}'_k(\mathbf{X}_i^\top \boldsymbol{\beta}_k^{old}) \mathbf{X}_i^\top \mathbb{J}(\boldsymbol{\beta}_k^{old}) \in \mathbb{R}^{p-1}$ ($k = 1, \dots, K$). Now we can obtain $\underline{\boldsymbol{\beta}}_{-1}^{new}$ as a minimizer of the objective function

$$\frac{1}{n} \sum_{i=1}^n (D_{2i} - \mathbf{V}_i^\top \underline{\boldsymbol{\beta}}_{-1})^2 \quad (4.6)$$

where $D_{2i} = w_{ii}^{1/2}(\tilde{Y}_i - \phi(\mathbf{X}_i, \mathbf{Z}_i; \tilde{\gamma}) - \sum_{k=1}^K (A_{i(k)} - \hat{\pi}_k(\mathbf{X}_i, \mathbf{Z}_i))[\mathbf{Z}_i^\top \boldsymbol{\theta}_k^{old} + \tilde{g}_k(\mathbf{X}_i^\top \boldsymbol{\beta}_k^{old}) - R_{ik}^\top \boldsymbol{\beta}_{k,-1}^{old}])$ and $\mathbf{V}_i = w_{ii}^{1/2}((A_{i(1)} - \hat{\pi}_1(\mathbf{X}_i, \mathbf{Z}_i))R_{i1}^\top, \dots, (A_{i(K)} - \hat{\pi}_K(\mathbf{X}_i, \mathbf{Z}_i))R_{iK}^\top)^\top$.

Subsequently, we obtain $\boldsymbol{\beta}_k^{new} = (\sqrt{1 - \|\boldsymbol{\beta}_{k,-1}^{new}\|_2^2}, \boldsymbol{\beta}_{k,-1}^{new})^\top$.

- (c) Update $\underline{\boldsymbol{\theta}}^{new}$ given $\underline{\boldsymbol{\delta}}^{new}$ and $\underline{\boldsymbol{\beta}}^{new}$: given $\underline{\boldsymbol{\delta}}^{new}$ and $\underline{\boldsymbol{\beta}}^{new}$, we can obtain

$\underline{\boldsymbol{\theta}}^{new}$ as a minimizer of the objective function

$$\frac{1}{n} \sum_{i=1}^n (D_{3i} - \mathbf{U}_i^T \underline{\boldsymbol{\theta}})^2 \quad (4.7)$$

where $D_{3i} = w_{ii}^{1/2} (\tilde{Y}_i - \phi(\mathbf{X}_i, \mathbf{Z}_i; \tilde{\boldsymbol{\gamma}}) - \sum_{k=1}^K (A_{i(k)} - \hat{\pi}_k(\mathbf{X}_i, \mathbf{Z}_i)) \mathbf{B}_k(\mathbf{X}_i^T \boldsymbol{\beta}_k^{new})^T \boldsymbol{\delta}_k^{new})$
and $\mathbf{U}_i = w_{ii}^{1/2} ((A_{i(1)} - \hat{\pi}_1(\mathbf{X}_i, \mathbf{Z}_i)) \mathbf{Z}_i^T, \dots, (A_{i(K)} - \hat{\pi}_K(\mathbf{X}_i, \mathbf{Z}_i)) \mathbf{Z}_i^T)^T$.

Step 3 Repeat Step 2 (a), (b), and (c) until convergence.

After the convergence of the algorithm, we obtain the final estimates $\hat{\underline{\boldsymbol{\theta}}}$, $\hat{\underline{\boldsymbol{\beta}}}$ and $\hat{\underline{\boldsymbol{\delta}}}$, and consequently $\hat{g}_k(\cdot) = \mathbf{B}_k(\cdot)^T \hat{\boldsymbol{\delta}}_k$. Let $\hat{g}_0(\cdot) = 0$ and $\hat{\boldsymbol{\theta}}_0 = \mathbf{0}$. Then for a given patient with covariate information (x, \mathbf{z}) ,

$$\hat{k} = \operatorname{argmax}_{0 \leq k \leq K} \mathbf{z}^T \hat{\boldsymbol{\theta}}_k + \hat{g}_k(x^T \hat{\boldsymbol{\beta}}_k),$$

is selected as the optimal treatment for that patient.

When \mathbf{X} and \mathbf{Z} are high dimensional, we impose parameter regularization to explore the sparsity and consider a penalized version of $\tilde{L}_n(\mathbf{g}, \underline{\boldsymbol{\theta}}, \underline{\boldsymbol{\beta}}; \tilde{\boldsymbol{\gamma}})$ in (4.9) as

$$\tilde{L}_n(\mathbf{g}, \underline{\boldsymbol{\theta}}, \underline{\boldsymbol{\beta}}; \tilde{\boldsymbol{\gamma}}) + \sum_{k=1}^K P_{1k}(\boldsymbol{\theta}_k; \lambda_{1k}) + \sum_{k=1}^K P_{2k}(\boldsymbol{\beta}_{k,-1}; \lambda_{2k}), \quad (4.8)$$

where $P_{tk}(\cdot; \lambda_{tk})$ are appropriate penalty functions with tuning parameters λ_{tk} , ($t = 1, 2; k = 1, \dots, K$). For example, we can choose $P_{tk}(\cdot; \lambda_{tk})$ as adaptive-LASSO (Zou, 2006), MCP (Zhang, 2010), or SCAD (Fan and Li, 2001) functions. The estimates $\hat{\underline{\boldsymbol{\theta}}}$, $\hat{\underline{\boldsymbol{\beta}}}$ and $\hat{\underline{\boldsymbol{\delta}}}$ can be obtained using the same iterative algorithm with (4.6) and (4.7) replaced by their penalized versions $n^{-1} \sum_{i=1}^n (D_{2i} - \mathbf{V}_i^T \underline{\boldsymbol{\beta}}_{-1})^2 + \sum_{k=1}^K P_{2k}(\boldsymbol{\beta}_{k,-1}; \lambda_{2k})$ and $n^{-1} \sum_{i=1}^n (D_{3i} - \mathbf{U}_i^T \underline{\boldsymbol{\theta}})^2 + \sum_{k=1}^K P_{1k}(\boldsymbol{\theta}_k; \lambda_{1k})$.

$$\begin{aligned}
& \tilde{L}_n(\boldsymbol{\delta}^{(a)}, \boldsymbol{\theta}^{(a)}, \boldsymbol{\beta}^{(a)}; \tilde{\boldsymbol{\gamma}}) \\
&= \frac{1}{n} \sum_{i=1}^n \frac{\Delta_i}{\hat{G}(T_i)} \left[\tilde{Y}_i - \phi(\mathbf{X}_i, \mathbf{Z}_i; \tilde{\boldsymbol{\gamma}}) - \sum_{k=1}^K (A_{i(k)} - \hat{\pi}_k(\mathbf{X}_i, \mathbf{Z}_i)) \left[\mathbf{Z}_i^T \boldsymbol{\theta}_k + \mathbf{B}_k(\mathbf{X}_i^T \boldsymbol{\beta}_k)^T \boldsymbol{\delta}_k \right] \right]^2 \\
&\quad + \sum_{k=1}^K P_{1k}(\boldsymbol{\theta}_k; \lambda_{1k}) + \sum_{k=1}^K P_{2k}(\boldsymbol{\beta}_{k,-1}; \lambda_{2k}). \tag{4.9}
\end{aligned}$$

4.2 Simulation study

In this section, we conduct extensive simulation studies to investigate the empirical performance of the proposed method on optimal treatment selection under various settings. We consider three treatments (*i.e.*, $K = 2$) in the simulation studies. The dimensions of continuous and discrete covariates are chosen as 10 and 2, (*i.e.*, $p = 10$ and $q = 2$).

We first generate $\tilde{\mathbf{X}} = (\tilde{X}_1, \dots, \tilde{X}_p)^T$ following a multivariate normal distribution with mean 0 and covariance $Corr(\tilde{X}_j, \tilde{X}_l) = 0.5^{|j-l|}$, $1 \leq j \leq l \leq 10$. Then the continuous covariates vector \mathbf{X} is generated by truncating $\tilde{\mathbf{X}}$ between $(-2, 2)$. The discrete variables, $\mathbf{Z} = (Z_1, Z_2)^T$ are generated as $Z_1 \sim \text{Bernoullie}(0.6)$ and $Z_2 \sim \text{Bernoullie}(0.2)$. To simulate observational data, we assign a patient with covariates (\mathbf{X}, \mathbf{Z}) into one of the three treatment groups ($k = 0, 1, 2$), according to a multinomial distribution with probabilities $\pi_k(\mathbf{X}, \mathbf{Z})$, where $\pi_0(\mathbf{X}, \mathbf{Z}) = 1 - \pi_1(\mathbf{X}, \mathbf{Z}) - \pi_2(\mathbf{X}, \mathbf{Z})$,

$$\pi_k(\mathbf{X}, \mathbf{Z}) = \frac{\exp(\log(0.4/0.6) + (\mathbf{X}, \mathbf{Z})^T \boldsymbol{\alpha}_k)}{1 + \sum_{l=1}^2 \exp(\log(0.4/0.6) + (\mathbf{X}, \mathbf{Z})^T \boldsymbol{\alpha}_l)} \quad \text{for } k = 1, 2,$$

$\boldsymbol{\alpha}_1 = (1, 0_7, -0.5, 1, 1.2, -0.7)^T$, $\boldsymbol{\alpha}_2 = (0.5, 0_7, -0.8, -1, -0.2, 0.5)^T$ and 0_l denotes a vector of zeros of length l .

Recall that $A_{(k)} = 1_{\{A=k\}}$ is the indicator variable on whether the patient receives treatment k . For the simulations we used slightly modified versions of the

outcome models that was designed for binary-valued outcomes with binary treatments used in Guo et al. (2021). We consider the following outcome models with different complexities:

Model 1: $\log(T) = 1 + \mathbf{X}^T \boldsymbol{\gamma}_1^* + \mathbf{Z}^T \boldsymbol{\gamma}_2^* + \sum_{k=1}^2 A_{(k)} [\mathbf{Z}^T \boldsymbol{\theta}_k^* + \mathbf{X}^T \boldsymbol{\beta}_k^*] + \epsilon_1,$

Model 2: $\log(T) = 1 + (\mathbf{X}^T \boldsymbol{\gamma}_1^*)(1 - \mathbf{X}^T \boldsymbol{\gamma}_1^*) + \mathbf{Z}^T \boldsymbol{\gamma}_2^* + \sum_{k=1}^2 A_{(k)} [\mathbf{Z}^T \boldsymbol{\theta}_k^* + \mathbf{X}^T \boldsymbol{\beta}_k^* (1 - \mathbf{X}^T \boldsymbol{\beta}_k^*)] + \epsilon_2,$

Model 3: $\log(T) = 1 + (\mathbf{X}^T \boldsymbol{\gamma}_1^*)(1 - \mathbf{X}^T \boldsymbol{\gamma}_1^*) + \mathbf{Z}^T \boldsymbol{\gamma}_2^* + A_{(1)} [\mathbf{Z}^T \boldsymbol{\theta}_1^* + \mathbf{X}^T \boldsymbol{\beta}_1^* (1 - \mathbf{X}^T \boldsymbol{\beta}_1^*)] + A_{(2)} [\mathbf{Z}^T \boldsymbol{\theta}_2^* + \sin(\pi(\mathbf{X}^T \boldsymbol{\beta}_2^*)/2)] + \epsilon_3.$

In the three models, $\boldsymbol{\gamma}_1^* = \frac{1}{\sqrt{2}}(1, 0_8, 1)^T$, $\boldsymbol{\gamma}_2^* = (0.3, -0.6)^T$, $\boldsymbol{\theta}_1^* = (0.6, 0.5)^T$, $\boldsymbol{\theta}_2^* = (-0.4, 0.4)^T$, $\boldsymbol{\beta}_1^* = \frac{1}{\sqrt{4.25}}(1.5, 0_7, -1, 1)^T$, $\boldsymbol{\beta}_2^* = \frac{1}{\sqrt{6}}(1, 0_7, 1, -2)^T$, and the error terms ϵ_1, ϵ_2 and ϵ_3 follow normal distributions with mean 0 and standard deviations $\sigma_1 = 0.4$ or 0.6 , $\sigma_2 = 0.5$ or 0.7 and $\sigma_3 = 0.5$ or 0.7 , respectively. The two choices for the error standard deviations in each model represent high (3.2) and low (2.2) signal/noise ratios respectively. The censoring times are independently generated from a uniform distribution $U(0, \tau)$, where τ is chosen to achieve 10% or 30% censoring rates representing low and high rates of censoring. We also consider two sample sizes $n=600$ and 1200 . Thus, we carried out simulations under the following 24 settings: 3 outcome models \times 2 signal/noise ratios \times 2 censoring rates \times 2 sample sizes. For each setting, we run 500 replications.

The B-spline basis functions and their derivatives used in the estimation process were calculated using the *splineDesign* function in R package *splines*. We considered three choices for the baseline function $\phi(\mathbf{X}, \mathbf{Z}; \boldsymbol{\gamma})$:

1. Constant function: $\phi(\mathbf{X}, \mathbf{Z}; \boldsymbol{\gamma}) = \gamma$
2. Linear function: $\phi(\mathbf{X}, \mathbf{Z}; \boldsymbol{\gamma}) = \mathbf{X}^T \boldsymbol{\gamma}_1 + \mathbf{Z}^T \boldsymbol{\gamma}_2$
3. Partial linear function: $\phi(\mathbf{X}, \mathbf{Z}; \boldsymbol{\gamma}) = m(\mathbf{X}^T \boldsymbol{\gamma}_1) + \mathbf{Z}^T \boldsymbol{\gamma}_2$

We obtain $\tilde{\gamma}$, a working value of γ by minimizing the following objective function

$$\frac{1}{n} \sum_{i=1}^n \frac{\Delta_i}{\hat{G}(T_i)} \left[\tilde{Y}_i - \phi(\mathbf{X}, \mathbf{Z}; \gamma) \right]^2.$$

The estimation of baseline function under the 1st choice (*i.e.*, the constant function), was simply the weighted least squares method with intercept only model. To estimate the baseline function under the 2nd choice (*i.e.*, the linear function), we used the weighted least squares method with all the covariates. The estimation of the 3rd choice (*i.e.*, the partial linear function) was based on the same iterative approach we described in the methodology section for estimating the contrast functions, where we used B-splines regression to estimate $m(\cdot)$ without involving treatment information.

In the simulation studies, since \mathbf{Z} was only two-dimensional, we only obtained the sparse estimates for β_k . We choose to use the adaptive -LASSO penalties, that is, $P_2(\beta_{k,-1}; \lambda_{2k}) = \lambda_{2k} \sum_{l=2}^p w_{kl} |\beta_{kl}|$, where $w_{kl}^{-1} = |\tilde{\beta}_{kl}|$ and $\tilde{\beta}_k = (\tilde{\beta}_{k1}, \dots, \tilde{\beta}_{kp})^T$ are some pilot estimates of β_k^* . We obtained $\tilde{\beta}_k$'s by minimizing the unpenalized version of loss function (4.9) using LARS algorithm (Efron et al., 2004). To select the tuning parameters, we used a BIC-type criteria (Zou, 2006). We estimated the propensity scores using multinomial logistic regression and $G(\cdot)$ using Kaplan-Meier method.

We compare the proposed semiparametric method with estimated propensity scores, denoted by SC.Est, to another two approaches. The first one is actually the proposed method but without the propensity score being set to 1/3 for each treatment, *i.e.*, assuming that the data came from a randomized study. It is denoted by SC.const. The second one is a penalized A-learning method developed by Lu et al. (2013), which assumes the linear contrast functions. It is denoted by LC.est.

We compare the three methods by their performances in variable selection and optimal treatment assignment. For the performance in variable selection, we calculate the proportion of zero coefficients correctly identified (Correct zeros) and

the proportion of non-zero coefficients correctly identified (Correct non-zeros) through 500 replications. For the performance in the optimal treatment assignment, we obtain the proportion of correct decisions (PCD) in each replication as

$$\frac{1}{n} \sum_{i=1}^n 1 \left\{ \operatorname{argmax}_{0 \leq k \leq K} \{ \mathbf{Z}_i^T \boldsymbol{\theta}_k^* + g_k^*(\mathbf{X}_i^T \boldsymbol{\beta}_k) \} = \operatorname{argmax}_{0 \leq k \leq K} \{ \mathbf{Z}_i^T \hat{\boldsymbol{\theta}}_k + \hat{g}_k(\mathbf{X}_i^T \hat{\boldsymbol{\beta}}_k) \} \right\},$$

and average the PCDs over 500 replications.

The simulation results under different conditions were summarized in Tables 4.1–4.4. Tables 4.1 and 4.2 reported the summarized results for high signal/noise ratio (around 3.2), under censoring rates 10% and 30% respectively, while Tables 4.3 and 4.4 reported the summarized results lower signal/noise ratio (around 2.2), under censoring rates 10% and 30% respectively.

In the case of the linear contrast function (model 1), the 2nd choice with the linear model for the baseline function $\phi(\cdot)$ had a higher PCD in all three contrast function estimation methods. However, the LC.est method with the 2nd choice for $\phi(\cdot)$ had the best PCD among all the combinations. When 2nd choice was used to estimate $\phi(\cdot)$, the proportion of correct identification of non-zero coefficients was comparatively high in the LC.est method. We can also see that the 3rd choice for $\phi(\cdot)$ with the LC.est method had a very close PCD (0.876) to the one with the 2nd choice (0.895). In the case of the non-linear contrast function (model 2 & 3), the 3rd choice with the partial linear model for the baseline function $\phi(\cdot)$ had a significantly higher PCD in all three contrast function estimation methods. However, the best PCD was reported when the contrast function was estimated using SC.est, while $\phi(\cdot)$ was estimated with the 3rd choice. We can also see that in Models 2 & 3, the 3rd choice for $\phi(\cdot)$ with the LC.est method had higher accuracy regarding the correct identification of both zero and non-zero coefficients. However, when the sample size was increased, the proportions of correct identification of both zero and non-zero

coefficients were increased significantly compared to LC.est and SC.const methods. All in all, we can say that even though a correct specification of the baseline function is not required to estimate the optimal treatment regime, a better estimation of $\phi(\cdot)$ improves the accuracy of the method.

When the censoring rate was increased from 10% to 30%, we can observe the same combinations of estimating $\phi(\cdot)$ and contrast function dominating both PCD and variable selection measures under all three models with a slight reduction in the measures. When the signal/noise ratio decreased by half (from ≈ 10 to ≈ 5), the same patterns of PCD and variable selection measures were reported with a slight reduction in accuracy for the case of lower signal/noise ratio.

When the sample size was increased from 600 to 1200, the PCD and the variable selection measures improved significantly, as expected. Overall, in both linear and non-linear scenarios, we can see substantially better performance when the estimated propensity scores are used instead of fixed ones. The performance of the LC.est method in Model 1 is expected to be better as the linear contrast is the true model. However, the SC.est method is a good competitor in estimating the contrast function in Model 1. In conclusion, we can say that regardless of the situation, the combination of 3rd choice for estimating $\phi(\cdot)$ and the SC.est for estimating the contrast function gives desired results in terms of both PCD and variable selection.

4.3 Case study

In this section, we illustrated the use of our proposed method using data obtained from the Kentucky Medicaid database on the patients diagnosed with cirrhosis. Cirrhosis of the liver is identified to be a chronic liver damage that leads to scarring and liver failure due to various causes. The most common causes of cirrhosis are known as chronic alcohol abuse and hepatitis. Damage to the liver caused by cirrhosis can hinder it from performing key functions such as eliminating toxins from the body

and aiding digestion. Furthermore, it can lead to complications such as portal hypertension, varices, fluid buildup, liver cancer and hepatic encephalopathy (Heidelbaugh and Sherbondy, 2006). Even though cirrhosis isn't curable, it can be treated. The patients we considered in this study are known to be of the diagnostic domains of alcohol abuse and/or alcohol dependence.

In this study we obtained data from the Kentucky Medicaid database of the patients diagnosed with cirrhosis in years 2015/2016 based on international classification of diseases (ICD) 9th edition and 10th edition clinical modification codes until the last observed follow-up date, 12/31/2020. The main variable of interest, the time to death was calculated from the difference of the date of diagnosed to the date of death. The patients who had not experienced death by the end of the follow-up period were considered as censored observations. The initial cohort was targeted on studying the prevalence of alcohol use disorder (AUD), and we considered the use of both pharmacotherapy and psychosocial treatments for the patients diagnosed with cirrhosis. If a patient has received any of the FDA-approved drugs for treating AUD, such as naltrexone, disulfiram, acamprosate, or topiramate, we considered them to have had pharmacotherapy treatment. The patients received psychosocial and behavioral therapies, such as AUD counseling and rehabilitation/detoxification were considered to have received psychosocial treatments. The said treatment options were identified via ICD-9 procedure codes and HCPCS procedure codes. Due to the lack of patients who received both treatments, we include patients who had received either pharmacotherapy or psychosocial treatment but not both. A total of 264 cirrhosis patients, ranging in age from 24-81 years, were enrolled in this study, with 92 of them receiving pharmacotherapy treatments, 72 receiving psychosocial treatments and 100 receiving neither of the treatments during the year of diagnosis. Among 264 patients, 57.6% were identified as censored. The covariates observed at the baseline contain demographic information (age in years, gender (male and female) and Rural-Urban

Continuum (RUC)), tobacco use, alcohol abuse, mental disorder (anxiety and/or major depressive disorder) and Charlson score that measures comorbidity of the patients at the baseline (Murray et al., 2006).

The baseline function, $\phi(\cdot)$ was estimated using the bsplines. Considering Z is high dimensional, we use adaptive-LASSO penalty to obtain sparse estimates for θ_k and γ_2 . The mental disorder variable appears to be the only binary covariate included in the model based on the baseline function. In the estimation of contrast functions, no binary covariates were included in the model when the adaptive-LASSO penalty was considered. The Table 4.5 summarizes the proposed optimal treatment for the patients with their original assignment. Among the patients who were originally given pharmacotherapy treatment, the proposed optimal treatment didn't change for 33.7% of the patients, while 33.7% patients were recommended to receive psychosocial treatment. Among the patients who were originally given psychosocial treatment, the proposed optimal treatment didn't change for 16.7% of the patients, while 40.3% patients were recommended to receive pharmacotherapy treatment. Among the patients who didn't receive any treatment, 44% and 33% were recommended to receive pharmacotherapy and psychosocial treatments respectively. In Table 4.6, we present the estimation results for two sets of patients with similar characteristics to investigate the behavior of proposed optimal treatment. Patient 1 and patient 2, both of whom were 55 years old at the time of the baseline, had an RUC of 5, a Charlson score of 0, and under the alcohol abuse, were initially assigned to pharmacotherapy and received no treatment, respectively. Patient 1, who underwent pharmacotherapy treatment, appears to have a longer survival time than patient 2, who didn't received treatment. For both patients with similar characteristics, the proposed method suggests pharmacotherapy treatment. This means that, even if patients with similar features received different treatment options, the proposed method will assign the treatment that maximizes survival time to both patients. The same results can be observed

for patients 3 and 4 in Table 4.6. Overall, based on the covariate information, we recommend switching treatments for some patients to achieve a better outcome.

Furthermore, in Figure 4.1, we compared the Kaplan-Meier survival curves of the patients in three treatment groups with the patients whose estimated treatment using the proposed method agreed with the original treatment assignment. In order to adjust the bias due to confounding, we weight the responses by their propensity scores. According to the plot, we can see that the overall survival of the optimal treatment group estimated using the proposed method is better compared to the individual treatment groups. This result suggested that the estimated optimal treatment regime can lead to greater survival compared to the original treatment assigned for the patients who were diagnosed with cirrhosis.

4.4 Discussion

This study proposes a novel treatment selection method to estimate the optimal treatment from multiple treatments that maximize the mean potential log survival time. The proposed loss function that corresponds to a form of A-learning makes our approach more robust to model misspecification as opposed to Q-learning since the treatment decision is hinged upon the estimation of the contrast function. The estimation is robust as the baseline mean function does not require a correct specification as long as the propensity scores are correctly specified. Nevertheless, a more complex baseline model can usually enhance the efficiency and accuracy of the estimation. The proposed method is based on semi-parametric Single Index Models, which provide a great deal of flexibility and reasonable efficiency that can be used to model a wide range of data. To account for the censored nature of the data and potential confounding factors, we proposed to use the inverse probability of censoring weights and propensity score, respectively. Furthermore, we incorporate shrinkage methods in the loss function to select important variables associated with the optimal decision.

The numerical studies provided satisfactory performance based on the probability of correct decisions under different simulation settings. The proposed method was applied to a real observational data set with multiple treatment options to see how the treatments could be assigned based on patient characteristics that can lead to great survival.

Future work could concentrate on constructing a doubly robust estimator to estimate the optimal treatment regime in the same context, where the correct specification of either the posited baseline model or the propensity score model is sufficient to obtain a better estimator.

4.5 Tables and Figures

Table 4.1: Summarized simulation results for the settings with 10% censoring rate and a high signal-noise ratio (≈ 3.2).

	Sample Size n	Baseline $\hat{\phi}(\cdot)$	Correct zeros			Correct non-zeros			PCD		
			LC.Est	SC.Const	SC.Est	LC.Est	SC.Const	SC.Est	LC.Est	SC.Const	SC.Est
Model 1	600	Const	0.990	0.915	0.870	0.429	0.711	0.620	0.644	0.661	0.688
		Lin.model	0.975	0.978	0.982	0.998	0.950	0.924	0.937	0.841	0.897
		Bspline	0.976	0.971	0.979	0.998	0.927	0.926	0.935	0.813	0.895
	1200	Const	0.978	0.923	0.941	0.885	0.797	0.691	0.848	0.678	0.775
		Lin.model	0.987	0.991	0.989	1.000	0.990	0.992	0.958	0.854	0.939
		Bspline	0.986	0.986	0.988	1.000	0.984	0.992	0.957	0.833	0.938
Model 2	600	Const	0.997	0.739	0.689	0.105	0.552	0.542	0.355	0.540	0.551
		Lin.model	0.996	0.883	0.757	0.233	0.557	0.590	0.435	0.443	0.611
		Bspline	0.949	0.843	0.928	0.821	0.748	0.765	0.724	0.726	0.787
	1200	Const	0.992	0.817	0.759	0.274	0.576	0.610	0.461	0.547	0.653
		Lin.model	0.986	0.887	0.843	0.592	0.623	0.673	0.626	0.460	0.712
		Bspline	0.962	0.914	0.955	0.912	0.909	0.927	0.766	0.815	0.877
Model 3	600	Const	0.998	0.763	0.708	0.045	0.535	0.552	0.251	0.505	0.526
		Lin.model	0.996	0.919	0.795	0.170	0.561	0.585	0.333	0.433	0.584
		Bspline	0.956	0.951	0.970	0.905	0.810	0.809	0.736	0.738	0.813
	1200	Const	0.993	0.856	0.810	0.237	0.577	0.592	0.373	0.507	0.623
		Lin.model	0.986	0.943	0.897	0.732	0.641	0.667	0.651	0.450	0.717
		Bspline	0.969	0.969	0.986	0.960	0.955	0.945	0.770	0.806	0.903

LC.est= Linear contrast function estimated with penalized regression and estimated propensity scores.

SC.const= Semiparametric contrast function estimated with Bspline regression with fixed propensity scores 1/3.

SC.est= Semiparametric contrast function estimated with Bspline regression with estimated propensity scores.

Table 4.2: Summarized simulation results for the settings with 30% censoring rate and a high signal-noise ratio (≈ 3.2).

	Sample Size n	Baseline $\hat{\phi}(\cdot)$	Correct zeros			Correct non-zeros			PCD		
			LC.Est	SC.Const	SC.Est	LC.Est	SC.Const	SC.Est	LC.Est	SC.Const	SC.Est
Model 1	600	Const	0.976	0.851	0.789	0.330	0.616	0.553	0.419	0.616	0.549
		Lin.model	0.951	0.968	0.960	0.975	0.951	0.904	0.895	0.856	0.856
	1200	Bspline	0.951	0.969	0.963	0.961	0.938	0.885	0.876	0.843	0.840
		Const	0.954	0.878	0.892	0.672	0.680	0.615	0.647	0.628	0.613
		Lin.model	0.968	0.983	0.979	0.998	0.994	0.978	0.930	0.884	0.911
		Bspline	0.969	0.982	0.979	0.993	0.987	0.969	0.913	0.872	0.899
Model 2	600	Const	0.999	0.711	0.625	0.051	0.503	0.490	0.311	0.504	0.415
		Lin.model	0.997	0.878	0.700	0.105	0.495	0.529	0.330	0.380	0.473
	1200	Bspline	0.943	0.770	0.897	0.736	0.681	0.696	0.633	0.640	0.719
		Const	0.996	0.802	0.707	0.115	0.540	0.543	0.324	0.526	0.473
		Lin.model	0.989	0.909	0.780	0.289	0.553	0.595	0.393	0.392	0.573
		Bspline	0.943	0.887	0.945	0.896	0.844	0.866	0.707	0.781	0.830
Model 3	600	Const	0.997	0.725	0.669	0.033	0.506	0.516	0.237	0.471	0.446
		Lin.model	0.998	0.897	0.729	0.066	0.484	0.549	0.252	0.388	0.502
	1200	Bspline	0.936	0.922	0.951	0.864	0.715	0.741	0.675	0.673	0.744
		Const	0.993	0.834	0.739	0.089	0.556	0.548	0.261	0.489	0.510
		Lin.model	0.986	0.931	0.825	0.317	0.590	0.584	0.371	0.400	0.600
		Bspline	0.948	0.955	0.973	0.936	0.904	0.902	0.719	0.785	0.853

LC.est= Linear contrast function estimated with penalized regression and estimated propensity scores.

SC.const= Semiparametric contrast function estimated with Bspline regression with fixed propensity scores 1/3.

SC.est= Semiparametric contrast function estimated with Bspline regression with estimated propensity scores.

Table 4.3: Summarized simulation results for the settings with 10% censoring rate and a low signal-noise ratio (≈ 2.2).

	Sample Size n	Baseline $\hat{\phi}(\cdot)$	Correct zeros			Correct non-zeros			PCD		
			LC.Est	SC.Const	SC.Est	LC.Est	SC.Const	SC.Est	LC.Est	SC.Const	SC.Est
Model 1	600	Const	0.990	0.924	0.844	0.356	0.686	0.611	0.587	0.654	0.672
		Lin.model	0.963	0.968	0.969	0.981	0.860	0.825	0.901	0.810	0.845
	1200	Bspline	0.960	0.968	0.966	0.977	0.836	0.821	0.897	0.785	0.841
		Const	0.979	0.925	0.940	0.814	0.772	0.665	0.815	0.672	0.756
		Lin.model	0.977	0.982	0.981	0.999	0.945	0.932	0.938	0.839	0.905
Bspline	0.978	0.980	0.982	0.999	0.930	0.931	0.938	0.815	0.904		
Model 2	600	Const	0.999	0.709	0.673	0.081	0.554	0.525	0.337	0.536	0.524
		Lin.model	0.997	0.894	0.723	0.171	0.530	0.558	0.392	0.432	0.569
	1200	Bspline	0.956	0.774	0.905	0.678	0.660	0.661	0.655	0.652	0.718
		Const	0.996	0.807	0.750	0.213	0.563	0.591	0.420	0.545	0.625
		Lin.model	0.985	0.906	0.836	0.516	0.586	0.636	0.580	0.449	0.681
Bspline	0.955	0.904	0.958	0.879	0.806	0.818	0.746	0.760	0.826		
Model 3	600	Const	0.998	0.742	0.706	0.036	0.536	0.544	0.244	0.500	0.509
		Lin.model	0.996	0.918	0.770	0.110	0.520	0.579	0.293	0.426	0.559
	1200	Bspline	0.946	0.938	0.953	0.823	0.666	0.688	0.687	0.661	0.732
		Const	0.995	0.849	0.788	0.192	0.565	0.583	0.339	0.505	0.602
		Lin.model	0.983	0.949	0.890	0.595	0.612	0.618	0.565	0.436	0.678
Bspline	0.967	0.968	0.981	0.920	0.857	0.836	0.745	0.769	0.845		

LC.est= Linear contrast function estimated with penalized regression and estimated propensity scores.

SC.const= Semiparametric contrast function estimated with Bspline regression with fixed propensity scores 1/3.

SC.est= Semiparametric contrast function estimated with Bspline regression with estimated propensity scores.

Table 4.4: Summarized simulation results for the settings with 30% censoring rate and a low signal-noise ratio (≈ 2.2).

	Sample Size n	Baseline $\hat{\phi}(\cdot)$	Correct zeros			Correct non-zeros			PCD		
			LC.Est	SC.Const	SC.Est	LC.Est	SC.Const	SC.Est	LC.Est	SC.Const	SC.Est
Model 1	600	Const	0.975	0.838	0.745	0.247	0.579	0.551	0.350	0.604	0.517
		Lin.model	0.940	0.950	0.950	0.896	0.793	0.740	0.836	0.787	0.780
	1200	Bspline	0.944	0.954	0.951	0.870	0.802	0.728	0.814	0.782	0.760
		Const	0.958	0.877	0.852	0.540	0.645	0.582	0.526	0.624	0.567
		Lin.model	0.947	0.970	0.958	0.964	0.929	0.873	0.887	0.845	0.848
		Bspline	0.949	0.970	0.961	0.950	0.925	0.861	0.872	0.837	0.836
Model 2	600	Const	0.995	0.697	0.628	0.051	0.492	0.474	0.308	0.497	0.410
		Lin.model	0.996	0.868	0.666	0.097	0.460	0.513	0.323	0.370	0.457
	1200	Bspline	0.959	0.715	0.825	0.527	0.582	0.606	0.517	0.554	0.631
		Const	0.995	0.791	0.685	0.109	0.527	0.537	0.318	0.520	0.457
		Lin.model	0.990	0.923	0.770	0.255	0.516	0.581	0.374	0.379	0.541
		Bspline	0.934	0.873	0.942	0.827	0.726	0.736	0.657	0.707	0.755
Model 3	600	Const	0.996	0.703	0.651	0.039	0.495	0.497	0.236	0.462	0.424
		Lin.model	0.997	0.883	0.699	0.047	0.455	0.529	0.244	0.382	0.471
	1200	Bspline	0.941	0.888	0.918	0.674	0.578	0.616	0.556	0.579	0.641
		Const	0.990	0.820	0.705	0.087	0.526	0.541	0.254	0.478	0.480
		Lin.model	0.990	0.930	0.793	0.216	0.545	0.566	0.316	0.394	0.555
		Bspline	0.930	0.947	0.959	0.888	0.754	0.763	0.674	0.704	0.767

LC.est= Linear contrast function estimated with penalized regression and estimated propensity scores.

SC.const= Semiparametric contrast function estimated with Bspline regression with fixed propensity scores 1/3.

SC.est= Semiparametric contrast function estimated with Bspline regression with estimated propensity scores.

Table 4.5: Summarized optimal treatment assignments compared with the original assignments.

			Proposed			Total
			1	2	0	
Original treatment	1: Pharmacotherapy	Count	31	31	30	92
		%	33.7%	33.7%	32.6%	
	2: Psychosocial	Count	29	12	31	72
		%	40.3%	16.7%	43.1%	
	0: None	Count	44	33	23	100
		%	44.0%	33.0%	23.0%	

Table 4.6: Comparison of optimal treatment assignment for two sets of patients with similar characteristics.

	log(T)	Age	RUC	Comorbidity	Abuse	Δ	A	Contrast1	Contrast2	Opt.treatment
Patient1	5.44	55	5	0	Yes	1	1	0.65	0.52	1
Patient2	4.91	55	5	0	Yes	1	0	0.65	0.52	1
Patient3	4.74	56	1	0	No	1	2	-1.12	-0.40	0
Patient4	5.41	56	1	0	No	1	0	-1.12	-0.40	0

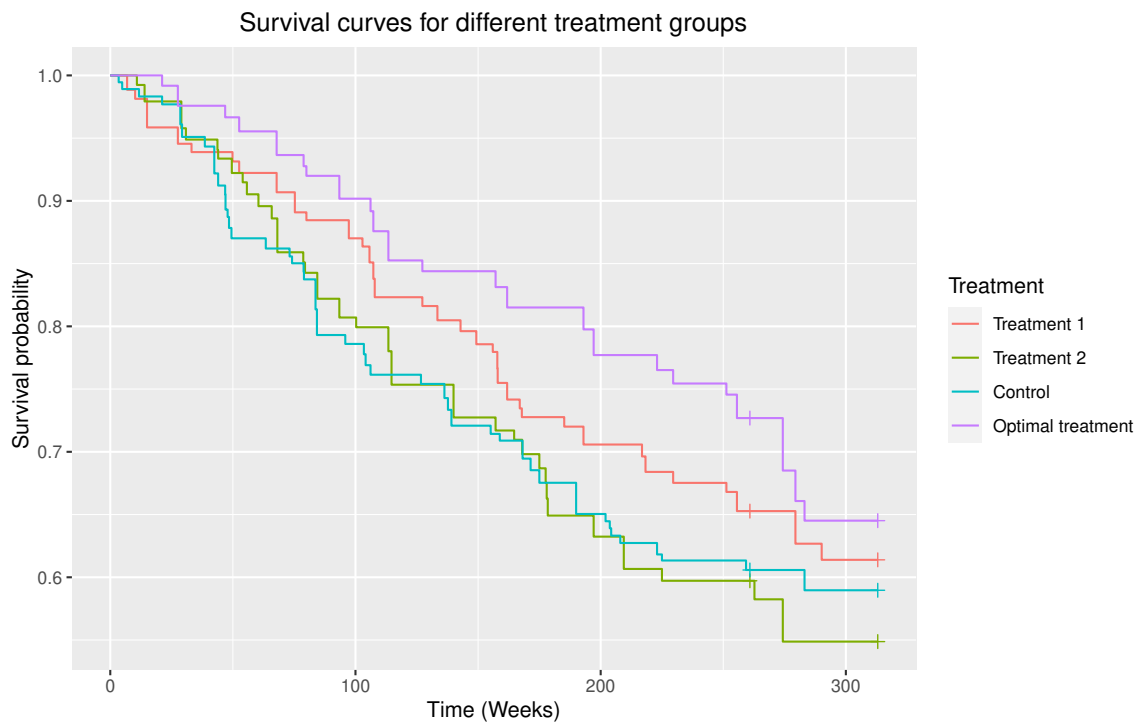


Figure 4.1: Kaplan-Meier survival curves for the three treatment groups and the patients who received the estimated optimal treatment weighted by the respective propensity scores.

REFERENCES

- Abdia, Y., Kulasekera, K., Datta, S., Boakye, M., and Kong, M. (2017). Propensity scores based methods for estimating average treatment effect and average treatment effect among treated: A comparative study. *Biometrical Journal*, 59(5):967–985.
- Apostolova, L. G., Dinov, I. D., Dutton, R. A., Hayashi, K. M., Toga, A. W., Cummings, J. L., and Thompson, P. M. (2006). 3d comparison of hippocampal atrophy in amnesic mild cognitive impairment and alzheimer’s disease. *Brain*, 129(11):2867–2873.
- Barnes, D. E., Cenzer, I. S., Yaffe, K., Ritchie, C. S., Lee, S. J., Initiative, A. D. N., et al. (2014). A point-based tool to predict conversion from mild cognitive impairment to probable alzheimer’s disease. *Alzheimer’s & Dementia*, 10(6):646–655.
- Beran, R. (1981). Nonparametric regression with randomly censored survival data. *Technical Report, Univ. California, Berkeley*.
- Berg, A. and Suaray, K. (2010). Bootstrap bandwidth selection for a smooth survival function estimator from censored data. *Journal of Statistical Research*, 44(2):207.
- Blanken, A. E., Hurtz, S., Zarow, C., Biado, K., Honarpisheh, H., Somme, J., Brook, J., Tung, S., Kraft, E., Lo, D., et al. (2017). Associations between hippocampal morphometry and neuropathologic markers of alzheimer’s disease using 7 t mri. *NeuroImage: Clinical*, 15:56–61.
- Borggaard, C. and Thodberg, H. H. (1992). Optimal minimal neural interpretation of spectra. *Analytical chemistry*, 64(5):545–551.

- Bouzebda, S. and Nemouchi, B. (2020). Uniform consistency and uniform in bandwidth consistency for nonparametric regression estimates and conditional u-statistics involving functional data. *Journal of Nonparametric Statistics*, 32(2):452–509.
- Cai, T., Tian, L., Wong, P. H., and Wei, L. (2011). Analysis of randomized comparative clinical trial data for personalized treatment selections. *Biostatistics*, 12(2):270–282.
- Cardot, H., Ferraty, F., and Sarda, P. (1999). Functional linear model. *Statistics & Probability Letters*, 45(1):11–22.
- Cardot, H., Ferraty, F., and Sarda, P. (2003). Spline estimators for the functional linear model. *Statistica Sinica*, pages 571–591.
- Cardot, H. and Sarda, P. (2005). Estimation in generalized linear models for functional data via penalized likelihood. *Journal of Multivariate Analysis*, 92(1):24–41.
- Craycroft, J. A., Huang, J., and Kong, M. (2020). Propensity score specification for optimal estimation of average treatment effect with binary response. *Statistical Methods in Medical Research*, 29(12):3623–3640.
- Dabrowska, D. M. (1987). Non-parametric regression with censored survival time data. *Scandinavian Journal of Statistics*, pages 181–197.
- Dabrowska, D. M. (1989). Uniform consistency of the kernel conditional kaplan-meier estimate. *The Annals of Statistics*, pages 1157–1167.
- de Boor, C. (2001). *A Practical Guide to Splines (Applied Mathematical Sciences Vol. 27)*. Springer-Verlag, New York.
- Efron, B., Hastie, T., Johnstone, I., and Tibshirani, R. (2004). Least angle regression. *The Annals of statistics*, 32(2):407–499.

- Fan, J. and Li, R. (2001). Variable selection via nonconcave penalized likelihood and its oracle properties. *Journal of the American statistical Association*, 96(456):1348–1360.
- Fang, H.-B., Wu, T. T., Rapoport, A. P., and Tan, M. (2016). Survival analysis with functional covariates for partial follow-up studies. *Statistical methods in medical research*, 25(6):2405–2419.
- Febrero, M., Galeano, P., and González-Manteiga, W. (2008). Outlier detection in functional data by depth measures, with application to identify abnormal nox levels. *Environmetrics: The official journal of the International Environmetrics Society*, 19(4):331–345.
- Ferraty, F., Laksaci, A., Tadj, A., and Vieu, P. (2010). Rate of uniform consistency for nonparametric estimates with functional variables. *Journal of Statistical planning and inference*, 140(2):335–352.
- Ferraty, F., Mas, A., and Vieu, P. (2007). Nonparametric regression on functional data: inference and practical aspects. *Australian & New Zealand Journal of Statistics*, 49(3):267–286.
- Ferraty, F. and Vieu, P. (2003). Curves discrimination: a nonparametric functional approach. *Computational Statistics & Data Analysis*, 44(1-2):161–173.
- Ferraty, F. and Vieu, P. (2006). *Nonparametric functional data analysis: theory and practice*. Springer Science & Business Media.
- Fjell, A. M., Walhovd, K. B., Fennema-Notestine, C., McEvoy, L. K., Hagler, D. J., Holland, D., Brewer, J. B., Dale, A. M., Initiative, A. D. N., et al. (2010). Csf biomarkers in prediction of cerebral and clinical change in mild cognitive impairment and alzheimer’s disease. *Journal of Neuroscience*, 30(6):2088–2101.

- Franklin, J. M., Rassen, J. A., Ackermann, D., Bartels, D. B., and Schneeweiss, S. (2014). Metrics for covariate balance in cohort studies of causal effects. *Statistics in medicine*, 33(10):1685–1699.
- Gasser, T. and Müller, H.-G. (1979). Kernel estimation of regression functions. In *Smoothing techniques for curve estimation*, pages 23–68. Springer.
- Gauthier, J., Wu, Q., and Gooley, T. (2020). Cubic splines to model relationships between continuous variables and outcomes: a guide for clinicians.
- Gellar, J. E., Colantuoni, E., Needham, D. M., and Crainiceanu, C. M. (2015). Cox regression models with functional covariates for survival data. *Statistical modelling*, 15(3):256–278.
- Geng, Y., Zhang, H. H., and Lu, W. (2015). On optimal treatment regimes selection for mean survival time. *Statistics in Medicine*, 34(7):1169–1184.
- Gentleman, R. and Crowley, J. (1991). Graphical methods for censored data. *Journal of the American Statistical Association*, 86(415):678–683.
- Gerds, T. A. and Schumacher, M. (2006). Consistent estimation of the expected brier score in general survival models with right-censored event times. *Biometrical Journal*, 48(6):1029–1040.
- Goldberg, Y. and Kosorok, M. R. (2012). Q-learning with censored data. *Annals of statistics*, 40(1):529.
- Gonzalez-Manteiga, W. and Cadarso-Suarez, C. (1994). Asymptotic properties of a generalized kaplan-meier estimator with some applications. *Communications in Statistics-Theory and Methods*, 4(1):65–78.
- Graf, E., Schmoor, C., Sauerbrei, W., and Schumacher, M. (1999). Assessment

- and comparison of prognostic classification schemes for survival data. *Statistics in medicine*, 18(17-18):2529–2545.
- Greenwell, B., Boehmke, B., Cunningham, J., and Developers, G. (2019). *gbm: Generalized Boosted Regression Models*. R package version 2.1.5.
- Guidoum, A. (2015). *kedd: Kernel estimator and bandwidth selection for density and its derivatives*. R package version 1.0.3.
- Guo, W., Zhou, X.-H., and Ma, S. (2021). Estimation of optimal individualized treatment rules using a covariate-specific treatment effect curve with high-dimensional covariates. *Journal of the American Statistical Association*, 116(533):309–321.
- Harrell, F. E. et al. (2015). *Regression modeling strategies: with applications to linear models, logistic and ordinal regression, and survival analysis*, volume 3. Springer.
- Hasenstab, K., Scheffler, A., Telesca, D., Sugar, C. A., Jeste, S., DiStefano, C., and Şentürk, D. (2017). A multi-dimensional functional principal components analysis of eeg data. *Biometrics*, 73(3):999–1009.
- Heidelbaugh, J. J. and Sherbondy, M. (2006). Cirrhosis and chronic liver failure: part ii. complications and treatment. *American family physician*, 74(5):767–776.
- Huang, X., Goldberg, Y., and Xu, J. (2019). Multicategory individualized treatment regime using outcome weighted learning. *Biometrics*, 75(4):1216–1227.
- Imbens, G. W. (2000). The role of the propensity score in estimating dose-response functions. *Biometrika*, 87(3):706–710.
- Jack, C. R., Petersen, R. C., Xu, Y. C., O’Brien, P. C., Smith, G. E., Ivnik, R. J., Boeve, B. F., Waring, S. C., Tangalos, E. G., and Kokmen, E. (1999). Prediction of ad with mri-based hippocampal volume in mild cognitive impairment. *Neurology*, 52(7):1397–1397.

- James, G. M. (2002). Generalized linear models with functional predictors. *Journal of the Royal Statistical Society: Series B (Statistical Methodology)*, 64(3):411–432.
- Jiang, B., Song, R., Li, J., and Zeng, D. (2019). Entropy learning for dynamic treatment regimes. *Statistica Sinica*, 29(4):1633.
- Jiang, R., Lu, W., Song, R., and Davidian, M. (2017). On estimation of optimal treatment regimes for maximizing t-year survival probability. *Journal of the Royal Statistical Society: Series B (Statistical Methodology)*, 79(4):1165–1185.
- Joosten, H., Visser, S. T., van Eersel, M. E., Gansevoort, R. T., Bilo, H. J., Slaets, J. P., and Izaks, G. J. (2014). Statin use and cognitive function: population-based observational study with long-term follow-up. *PLoS One*, 9(12):e115755.
- Kang, S., Lu, W., and Zhang, J. (2018). On estimation of the optimal treatment regime with the additive hazards model. *Statistica Sinica*, 28(3):1539.
- Kaplan, E. L. and Meier, P. (1958). Nonparametric estimation from incomplete observations. *Journal of the American statistical association*, 53(282):457–481.
- Kara-Zaitri, L., Laksaci, A., Rachdi, M., and Vieu, P. (2017). Uniform in bandwidth consistency for various kernel estimators involving functional data. *Journal of Nonparametric Statistics*, 29(1):85–107.
- Kattan, M. W. and Gerds, T. A. (2018). The index of prediction accuracy: an intuitive measure useful for evaluating risk prediction models. *Diagnostic and prognostic research*, 2(1):1–7.
- Kong, D., Ibrahim, J. G., Lee, E., and Zhu, H. (2018). Flcrm: Functional linear cox regression model. *Biometrics*, 74(1):109–117.
- Kosorok, M. R. (2008). *Introduction to empirical processes and semiparametric inference*. Springer.

- Kulasekera, K., Tholkage, S., and Kong, M. (2022). Personalized treatment selection using observational data. *Journal of Applied Statistics*, pages 1–13.
- Kvamme, H. and Borgan, Ø. (2019). The brier score under administrative censoring: Problems and solutions. *arXiv preprint arXiv:1912.08581*.
- Leng, C. and Tong, X. (2013). A quantile regression estimator for censored data. *Bernoulli*, 19(1):344–361.
- Li, J., Li, Y., Jin, B., and Kosorok, M. R. (2021). Multithreshold change plane model: Estimation theory and applications in subgroup identification. *Statistics in medicine*.
- Li, K., Chan, W., Doody, R. S., Quinn, J., Luo, S., Initiative, A. D. N., et al. (2017). Prediction of conversion to alzheimer’s disease with longitudinal measures and time-to-event data. *Journal of Alzheimer’s Disease*, 58(2):361–371.
- Li, Q. and Racine, J. S. (2007). *Nonparametric econometrics: theory and practice*. Princeton University Press.
- Locantore, N., Marron, J., Simpson, D., Tripoli, N., Zhang, J., Cohen, K., Boente, G., Fraiman, R., Brumback, B., Croux, C., et al. (1999). Robust principal component analysis for functional data. *Test*, 8(1):1–73.
- Lu, W., Zhang, H. H., and Zeng, D. (2013). Variable selection for optimal treatment decision. *Statistical methods in medical research*, 22(5):493–504.
- Ma, J., Hobbs, B. P., and Stingo, F. C. (2015). Statistical methods for establishing personalized treatment rules in oncology. *BioMed research international*, 2015.
- Ma, S. (2016). Estimation and inference in functional single-index models. *Annals of the Institute of Statistical Mathematics*, 68(1):181–208.

- Marx, B. D. and Eilers, P. H. (1999). Generalized linear regression on sampled signals and curves: a p-spline approach. *Technometrics*, 41(1):1–13.
- Moodie, E. E., Chakraborty, B., and Kramer, M. S. (2012). Q-learning for estimating optimal dynamic treatment rules from observational data. *Canadian Journal of Statistics*, 40(4):629–645.
- Müller, H.-G. and Stadtmüller, U. (2005). Generalized functional linear models. *the Annals of Statistics*, 33(2):774–805.
- Müller, H.-G. and Zhang, Y. (2005). Time-varying functional regression for predicting remaining lifetime distributions from longitudinal trajectories. *Biometrics*, 61(4):1064–1075.
- Murphy, S. A. (2003). Optimal dynamic treatment regimes. *Journal of the Royal Statistical Society: Series B (Statistical Methodology)*, 65(2):331–355.
- Murphy, S. A. (2005). An experimental design for the development of adaptive treatment strategies. *Statistics in medicine*, 24(10):1455–1481.
- Murray, S. B., Bates, D. W., Ngo, L., Ufberg, J. W., and Shapiro, N. I. (2006). Charlson index is associated with one-year mortality in emergency department patients with suspected infection. *Academic Emergency Medicine*, 13(5):530–536.
- Nadaraya, E. A. (1964). On estimating regression. *Theory of Probability & Its Applications*, 9(1):141–142.
- Parzen, E. (1962). On estimation of a probability density function and mode. *The annals of mathematical statistics*, 33(3):1065–1076.
- Peng, L. and Huang, Y. (2008). Survival analysis with quantile regression models. *Journal of the American Statistical Association*, 103(482):637–649.

- Qian, M. and Murphy, S. A. (2011). Performance guarantees for individualized treatment rules. *Annals of statistics*, 39(2):1180.
- Ramsay, J. O. and Silverman, B. W. (2002). *Applied functional data analysis: methods and case studies*, volume 77. Springer.
- Ridgeway, G., McCaffrey, D., Morral, A., Griffin, B. A., Burgette, L., and Cefalu, M. (2020). *twang: Toolkit for Weighting and Analysis of Nonequivalent Groups*. R package version 1.6.
- Robins, J. M. (2004). Optimal structural nested models for optimal sequential decisions. In *Proceedings of the second seattle Symposium in Biostatistics*, pages 189–326. Springer.
- Rosenbaum, P. R. and Rubin, D. B. (1983). The central role of the propensity score in observational studies for causal effects. *Biometrika*, 70(1):41–55.
- Rutikanga, J. U., Diop, A., et al. (2021). Functional kernel estimation of the conditional extreme quantile under random right censoring. *Open Journal of Statistics*, 11(01):162.
- Schmee, J. and Hahn, G. J. (1979). A simple method for regression analysis with censored data. *Technometrics*, 21(4):417–432.
- Schulte, P. J., Tsiatis, A. A., Laber, E. B., and Davidian, M. (2014). Q-and a-learning methods for estimating optimal dynamic treatment regimes. *Statistical science: a review journal of the Institute of Mathematical Statistics*, 29(4):640.
- Scott, D. W. (2015). *Multivariate density estimation: theory, practice, and visualization*. John Wiley & Sons.
- Silverman, B. W. (2018). *Density estimation for statistics and data analysis*. Routledge.

- Siriwardhana, C., Zhao, M., Datta, S., and Kulasekera, K. (2019). A probability based method for selecting the optimal personalized treatment from multiple treatments. *Statistical methods in medical research*, 28(3):749–760.
- Sorensen, T. I. (1996). Which patients may be harmed by good treatments? *The Lancet*, 348(9024):351–352.
- Tao, Y. and Wang, L. (2017). Adaptive contrast weighted learning for multi-stage multi-treatment decision-making. *Biometrics*, 73(1):145–155.
- Thompson, P. M., Hayashi, K. M., De Zubicaray, G. I., Janke, A. L., Rose, S. E., Semple, J., Hong, M. S., Herman, D. H., Gravano, D., Doddrell, D. M., et al. (2004). Mapping hippocampal and ventricular change in alzheimer disease. *Neuroimage*, 22(4):1754–1766.
- Van Der Vaart, A. W. and Wellner, J. (1996). *Weak Convergence and Empirical Processes: with Applications to Statistics*. Springer Science & Business Media.
- Van't Veer, L. J. and Bernards, R. (2008). Enabling personalized cancer medicine through analysis of gene-expression patterns. *Nature*, 452(7187):564–570.
- Vazquez, A. (2013). Optimization of personalized therapies for anticancer treatment. *BMC Systems Biology*, 7(1):1–11.
- Wang, H. J. and Wang, L. (2009). Locally weighted censored quantile regression. *Journal of the American Statistical Association*, 104(487):1117–1128.
- Wang, J., Li, J., Li, Y., and Wong, W. K. (2019). A model-based multithreshold method for subgroup identification. *Statistics in medicine*, 38(14):2605–2631.
- Watson, G. S. (1964). Smooth regression analysis. *Sankhyā: The Indian Journal of Statistics, Series A*, pages 359–372.

- Yan, X., Abdia, Y., Datta, S., Kulasekera, K., Ugiliweneza, B., Boakye, M., and Kong, M. (2019). Estimation of average treatment effects among multiple treatment groups by using an ensemble approach. *Statistics in medicine*, 38(15):2828–2846.
- Zamorski, M. A. and Albucher, R. (2002). What to do when ssris fail: eight strategies for optimizing treatment of panic disorder. *American Family Physician*, 66(8):1477–1485.
- Zhang, B., Tsiatis, A. A., Laber, E. B., and Davidian, M. (2012). A robust method for estimating optimal treatment regimes. *Biometrics*, 68(4):1010–1018.
- Zhang, C.-H. (2010). Nearly unbiased variable selection under minimax concave penalty. *The Annals of statistics*, 38(2):894–942.
- Zhang, Z., Cortese, G., Combescure, C., Marshall, R., Lee, M., Lim, H. J., Haller, B., et al. (2018). Overview of model validation for survival regression model with competing risks using melanoma study data. *Annals of translational medicine*, 6(16).
- Zhao, Y., Zeng, D., Rush, A. J., and Kosorok, M. R. (2012). Estimating individualized treatment rules using outcome weighted learning. *Journal of the American Statistical Association*, 107(499):1106–1118.
- Zhao, Y.-Q., Zeng, D., Laber, E. B., and Kosorok, M. R. (2015). New statistical learning methods for estimating optimal dynamic treatment regimes. *Journal of the American Statistical Association*, 110(510):583–598.
- Zhao, Y.-Q., Zhu, R., Chen, G., and Zheng, Y. (2020). Constructing dynamic treatment regimes with shared parameters for censored data. *Statistics in Medicine*, 39(9):1250–1263.

- Zheng, Q., Peng, L., and He, X. (2018). High dimensional censored quantile regression. *Annals of statistics*, 46(1):308.
- Zhou, Y. and Sedransk, N. (2009). Functional data analytic approach of modeling ecg t-wave shape to measure cardiovascular behavior. *The Annals of applied statistics*, pages 1382–1402.
- Zou, H. (2006). The adaptive lasso and its oracle properties. *Journal of the American statistical association*, 101(476):1418–1429.

APPENDICES

A First Appendix

Let $a_n \simeq \left(h^2 + [\psi(\log n/n)/(n\phi(h))]^{1/2} \right)$ and $b_n \simeq a_n^{-1/2}$.

Proof of Theorem 2.2.1: Since the proofs of the consistency of \hat{S}_Y and \hat{H} are similar, we only deal with \hat{S}_Y . According to Lemma 12 of Ferraty et al. (2010), under (C1) and (C4), we have

$$\sup_{x \in \mathcal{X}} \sup_{t \in \mathcal{T}} |E(\hat{S}_Y(t|x)) - S_Y(t|x)| = o(h^2).$$

Moreover, following Lemma 13 of Ferraty et al. (2010), under (C1)–(C4), we can obtain,

$$\sup_{x \in \mathcal{X}} \sup_{t \in \mathcal{T}} |\hat{S}_Y(t|x) - E(\hat{S}_Y(t|x))| = o\left(\sqrt{\frac{\psi(\log n/n)}{n\phi(h)}}\right) \quad \text{a.s.}$$

Combining the above two results together completes the proof of Theorem 2.2.1. \square

Proof of Theorem 2.2.2: By simple algebra, we obtain the following decomposition:

$$\begin{aligned} \hat{\Lambda}_T(t|x) - \Lambda_T(t|x) &= \left(\sum_{j=1}^n \frac{1\{y_j \leq t, \delta_j = 1\} B_{nj}(x)}{1 - \sum_{r=1}^n 1\{y_r < y_j\} B_{nr}(x)} - \sum_{j=1}^n \frac{1\{y_j \leq t, \delta_j = 1\} B_{nj}(x)}{1 - \sum_{r=1}^n 1\{y_r \leq y_j\} B_{nr}(x)} \right) \\ &\quad + \left(\int_0^t \frac{d\hat{H}(u|x)}{\hat{S}_Y(u|x)} - \int_0^t \frac{dH(u|x)}{S_Y(u|x)} \right) =: I + II \end{aligned}$$

By Theorem 2.2.1 and the fact that $\sup_j B_{nj}(x) = o(n^{-1}\phi(h)^{-1})$, we can write I as

follows

$$\begin{aligned}
I &= \sum_{j=1}^n \frac{1\{y_j \leq t, \delta_j = 1\}B_{nj}(x)}{1 - \sum_{r=1}^n 1\{y_r < y_j\}B_{nr}(x)} - \sum_{j=1}^n \frac{1\{y_j \leq t, \delta_j = 1\}B_{nj}(x)}{1 - \sum_{r=1}^n 1\{y_r \leq y_j\}B_{nr}(x)} \\
&= \sum_{j=1}^n \frac{1\{y_j \leq t, \delta_j = 1\}B_{nj}(x)[\sum_{r=1}^n 1\{y_r < y_j\}B_{nr}(x) - \sum_{r=1}^n 1\{y_r \leq y_j\}B_{nr}(x)]}{(1 - \sum_{r=1}^n 1\{y_r < y_j\}B_{nr}(x))(1 - \sum_{r=1}^n 1\{y_r \leq y_j\}B_{nr}(x))} \\
&= \sum_{j=1}^n \frac{1\{y_j \leq t, \delta_j = 1\}B_{nj}(x)^2}{(1 - \sum_{r=1}^n 1\{y_r < y_j\}B_{nr}(x))(1 - \sum_{r=1}^n 1\{y_r \leq y_j\}B_{nr}(x))} = o(n^{-1}\phi(h)^{-1}).
\end{aligned}$$

Now let us write $II = II_1 + II_2$, where

$$\begin{aligned}
II_1 &= \int_0^t \left(\frac{1}{\hat{S}_Y(u|x)} - \frac{1}{S_Y(u|x)} \right) dH(u|x) + \int_0^t \left(\frac{1}{S_Y(u|x)} \right) d(\hat{H}(u|x) - H(u|x)) \quad \text{and} \\
II_2 &= \int_0^t \left(\frac{1}{\hat{S}_Y(u|x)} - \frac{1}{S_Y(u|x)} \right) d(\hat{H}(u|x) - H(u|x)).
\end{aligned}$$

First, we deal with II_1 .

$$\begin{aligned}
II_1 &= \int_0^t \left(\frac{1}{S_Y(u|x)} \right) d(\hat{H}(u|x) - H(u|x)) + \int_0^t \frac{S_Y(u|x) - \hat{S}_Y(u|x)}{S_Y^2(u|x)} dH(u|x) \\
&\quad + \int_0^t \left[\frac{S_Y(u|x) - \hat{S}_Y(u|x)}{S_Y(u|x)\hat{S}_Y(u|x)} - \frac{S_Y(u|x) - \hat{S}_Y(u|x)}{S_Y^2(u|x)} \right] dH(u|x) \\
&= - \int_0^t \frac{\hat{S}_Y(u|x)}{S_Y^2(u|x)} dH(u|x) + \sum_{j=1}^n \frac{1\{y_j \leq t, \delta_j = 1\}B_{nj}(x)}{S_Y(Y_j|x)} \\
&\quad + \int_0^t \frac{[S_Y(u|x) - \hat{S}_Y(u|x)]^2}{S_Y^2(u|x)\hat{S}_Y(u|x)} dH(u|x) \\
&= - \int_0^t \frac{1 - \sum_{j=1}^n 1\{Y_j \leq u\}B_{nj}(x)}{S_Y^2(u|x)} dH(u|x) + \sum_{j=1}^n \frac{1\{y_j \leq t, \delta_j = 1\}B_{nj}(x)}{S_Y(Y_j|x)} + O(a_n^2) \quad \text{a.s.},
\end{aligned}$$

where the last equality follows from Theorem 2.2.1. Noting that $\sum_{j=1}^n B_{nj}(x) = 1$,

we have

$$\begin{aligned}
II_1 &= - \int_0^t \frac{\sum_{j=1}^n B_{nj}(x) - \sum_{j=1}^n B_{nj}(x) 1\{Y_j \leq u\}}{S_Y^2(u|x)} dH(u|x) \\
&\quad + \sum_{j=1}^n B_{nj}(x) \frac{1\{y_j \leq t, \delta_j = 1\}}{S_Y(Y_j|x)} + O(a_n^2) \\
&= - \int_0^t \frac{\sum_{j=1}^n B_{nj}(x) 1\{Y_j > u\}}{S_Y^2(u|x)} dH(u|x) + \sum_{j=1}^n B_{nj}(x) \frac{1\{y_j \leq t, \delta_j = 1\}}{S_Y(Y_j|x)} + O(a_n^2) \\
&= - \sum_{j=1}^n B_{nj}(x) \int_0^t \frac{1\{u < Y_j\}}{(S_Y(u|x))^2} dH(u|x) + \sum_{j=1}^n B_{nj}(x) \frac{1\{y_j \leq t, \delta_j = 1\}}{S_Y(Y_j|x)} + O(a_n^2) \\
&= - \sum_{j=1}^n B_{nj}(x) \int_0^{\min\{Y_j, t\}} \frac{1}{(S_Y(u|x))^2} dH(u|x) + \sum_{j=1}^n B_{nj}(x) \frac{1\{y_j \leq t, \delta_j = 1\}}{S_Y(Y_j|x)} + O(a_n^2) \\
&= \sum_{j=1}^n B_{nj}(x) \left[- \int_0^{\min\{Y_j, t\}} \frac{dH(u|x)}{(S_Y(u|x))^2} + \frac{1\{y_j \leq t, \delta_j = 1\}}{S_Y(Y_j|x)} \right] + O(a_n^2) \\
&= \sum_{j=1}^n B_{nj}(x) \frac{\xi(Y_j, \delta_j, t, x)}{S_T(t|x)} + O(a_n^2).
\end{aligned}$$

Next, we evaluate II_2 . Let $0 = t_1 < t_2 < \dots < t_{k_n+1} = t$ denote a partition for the interval $[0, t]$, where $k_n \simeq \{[\psi(\log n/n)/(n\phi(h))]^{1/2} + h^2\}^{-1}$. By integration by parts and Theorem 2.2.1,

$$\begin{aligned}
|II_2| &= \left| \left(\frac{1}{\hat{S}_Y(u|x)} - \frac{1}{S_Y(u|x)} \right) (\hat{H}(u|x) - H(u|x)) \right|_0^t \\
&\quad - \int_0^t (\hat{H}(u|x) - H(u|x)) d \left(\frac{1}{\hat{S}_Y(u|x)} - \frac{1}{S_Y(u|x)} \right) \Big| \\
&\leq \sup_{0 \leq u \leq t} \left| \frac{1}{\hat{S}_Y(u|x)} - \frac{1}{S_Y(u|x)} \right| \sum_{1 \leq i \leq k_n} \left| (\hat{H}(u|x) - H(u|x)) \Big|_{t_i}^{t_{i+1}} \right| \\
&\quad + \sup_{0 \leq s \leq t} |\hat{H}(u|x) - H(u|x)| \sum_{1 \leq i \leq k_n} \left| \int_{t_i}^{t_{i+1}} d \left(\frac{1}{\hat{S}_Y(u|x)} - \frac{1}{S_Y(u|x)} \right) \right| \\
&\leq k_n O(a_n) \left\{ \max_{1 \leq i \leq k_n} \left| \hat{H}(t_{i+1}|x) - H(t_{i+1}|x) - \hat{H}(t_i|x) + H(t_i|x) \right| \right. \\
&\quad \left. + \max_{1 \leq i \leq k_n} \sup_{y \in [t_i, t_{i+1}]} \left| \frac{1}{\hat{S}_Y(y|x)} - \frac{1}{S_Y(y|x)} - \frac{1}{\hat{S}_Y(t_i|x)} + \frac{1}{S_Y(t_i|x)} \right| \right\}.
\end{aligned}$$

According to Condition (C1), there exists a constant C_3 such that $|S_Y(t_{i+1}|x) - S_Y(t_i|x)| \leq C_3/k_n$. Now, divide each $[t_i, t_{i+1}]$ into b_n sub-intervals $[t_{ij}, t_{i(j+1)}], j = 1, \dots, b_n$. Then we have, $|S_Y(t_{i(j+1)}|x) - S_Y(t_{ij}|x)| = O(a_n^{3/2})$. By Theorem 2.2.1, we get

$$\sup_{0 < t < \tau} \sup_{x \in \mathcal{X}} |\hat{S}_Y(t|x) - S_Y(t|x)|^2 = O(a_n^2).$$

These two results and the monotonicity of $\hat{S}_Y(t|x)$ over t together yield that

$$\begin{aligned} & \sup_{y \in [t_i, t_{i+1}]} \left| \frac{1}{\hat{S}_Y(y|x)} - \frac{1}{S_Y(y|x)} - \frac{1}{\hat{S}_Y(t_i|x)} + \frac{1}{S_Y(t_i|x)} \right| \\ & \leq \sup_{y \in [t_i, t_{i+1}]} \left| \frac{\hat{S}_Y(y|x) - S_Y(y|x)}{S_Y(y|x)^2} - \frac{\hat{S}_Y(t_i|x) - S_Y(t_i|x)}{S_Y(t_i|x)^2} \right| + O(a_n^2) \\ & \leq \sup_{y \in [t_i, t_{i+1}]} \frac{1}{S_Y(t_{i+1}|x)^2} \left| \hat{S}_Y(y|x) - S_Y(y|x) - \hat{S}_Y(t_i|x) + S_Y(t_i|x) \right| + O(a_n^2) \\ & \leq C_4 \max_j \sup_{y \in [t_{ij}, t_{i(j+1)}]} \left| \hat{S}_Y(y|x) - S_Y(t_{ij}|x) - \hat{S}_Y(t_i|x) + S_Y(t_i|x) \right| + O(a_n^{3/2}) + O(a_n^2) \\ & \leq C_4 \max_j \left| \hat{S}_Y(t_{ij}|x) - S_Y(t_{ij}|x) - \hat{S}_Y(t_i|x) + S_Y(t_i|x) \right| + O(a_n^{3/2}), \end{aligned}$$

almost surely, where C_4 is some constant. Then we have,

$$\begin{aligned} |II_2| & \leq O(1) \max_{1 \leq i \leq k_n} \left| \hat{H}(t_{ij}|x) - H(t_{ij}|x) - \hat{H}(t_i|x) + H(t_i|x) \right| \\ & \quad + \max_{1 \leq i \leq k_n} \max_{1 \leq j \leq b_n} \left| (\hat{S}_Y(t_{ij}|x)) - (S_Y(t_{ij}|x)) - (\hat{S}_Y(t_i|x) + (S_Y(t_i|x))) \right| + O(a_n^{3/2}) \end{aligned}$$

As deduced in Gonzalez-Manteiga and Cadarso-Suarez (1994), we have

$$|II_2| = O(a_n^{3/2}) + h^2.$$

Combining the results of I, II_1 and II_2 together completes the proof of Theorem 3.2.

□

Proof of Corollary 2.2.1: By Taylor's expansion of the function $\exp(\cdot)$ around

$-\Lambda_T(t|x)$, there exists a $\tilde{\Lambda}(t|x)$ between $\hat{\Lambda}(t|x)$ and $\Lambda(t|x)$ such that

$$\begin{aligned}\hat{S}_T(t|x) - S_T(t|x) &= - \left(\exp\{-\hat{\Lambda}_T(t|x)\} - \exp\{-\Lambda_T(t|x)\} \right) \\ &= - \exp\{-\Lambda_T(t|x)\} - \exp\{-\Lambda_T(t|x)\} \times (-\hat{\Lambda}_T(t|x) + \Lambda_T(t|x)) \\ &\quad - \exp(-\tilde{\Lambda}(t|x))(-\tilde{\Lambda}_T(t|x) + \Lambda_T(t|x))^2 + \exp\{-\Lambda_T(t|x)\} \\ &= - S_T(t|x) \times (-\hat{\Lambda}_T(t|x) + \Lambda_T(t|x)) - \exp(-\tilde{\Lambda}(t|x))(-\hat{\Lambda}_T(t|x) + \Lambda_T(t|x))^2\end{aligned}$$

Noting that

$$\begin{aligned}\hat{\Lambda}_T(t|x) - \Lambda_T(t|x) &= \int_0^t \left(\frac{1}{S_Y(u|x)} \right) d(\hat{H}(u|x) - H(u|x)) \\ &\quad + \int_0^t \left(\frac{1}{\hat{S}_Y(u|x)} - \frac{1}{S_Y(u|x)} \right) d\hat{H}(u|x) + o(n^{-1}\phi_x(h)^{-1}) \quad \text{a.s.}\end{aligned}$$

by Theorem 2.2.1, we have,

$$\sup_{0 < t < \tau} \sup_{x \in \mathcal{X}} |\hat{\Lambda}_T(t|x) - \Lambda_T(t|x)| = o(a_n) \quad \text{a.s.}$$

Therefore,

$$\hat{S}_T(t|x) - S_T(t|x) = -S_T(t|x) \times (-\hat{\Lambda}_T(t|x) + \Lambda_T(t|x)) + o(a_n) \quad \text{a.s.}$$

By Theorem 2.2.2, we obtain

$$\hat{S}_T(t|x) - S_T(t|x) = \sum_{j=1}^n B_{nj}(x) \xi(Y_j, \delta_j, t, x) + o \left(h^2 + \left(\frac{\psi(\log n/n)}{n\phi_x(h)} \right)^{3/4} \right) \quad \text{a.s.}$$

If $nh^5 \rightarrow 0$ and $n^{-1}h^{-2}(\psi(\log n/n)/\phi_x(h))^3 \rightarrow 0$,

$$(nh)^{1/2} o \left(\left(\frac{\psi(\log n/n)}{n\phi(h)} \right)^{3/4} + h^2 \right) = o(1).$$

Therefore, $(nh)^{1/2}[\hat{S}_T(t|x) - S_T(t|x)]$ and $(nh)^{1/2} \sum_{j=1}^n B_{nj}(x)\xi(Y_j, \delta_j, t, x)$ have the same asymptotic distribution.

Since $\xi(Y_j, \delta_j, t, x)$ satisfies $E[\xi(Y_j, \delta_j, t, x)] = 0$ and $E[\xi^2(Y_j, \delta_j, t, x)] < \infty$, for $j = 1, \dots, n$ and it is easy to see that $E[h \{B_{nj}(x)\xi(Y_j, \delta_j, t, x)\}^2] < \infty$, we have

$$(nh)^{1/2} \sum_{j=1}^n B_{nj}(x)\xi(Y_j, \delta_j, t, x) \rightarrow_d N(0, V(x, t)),$$

by Central Limit Theorem, for some variance function $N(0, V(x, t))$. □

B Second Appendix

Intermediate estimation results from real data example.

In this section, we explain the proposed method using the real data example. The generalized boosted models (GBM) were used in estimating the $\hat{g}_k(\cdot)$, $k = 1, 2, 3$ and for variable selection in the proposed method. As mentioned in the section 4, we used a 5-fold cross validation method to summarize the optimal treatment assignment, comparing with the original treatment assignment. Now we describe the steps involved in selecting the optimal treatment using the data from the 1st step of the 5-fold cross validation method, i.e the 1st combination of training and testing data. First, we subset the training data in each of the 3 treatment groups. Then for each treatment group, we perform the gbm method as described in section 2, using all the covariates (X_k) to estimate $\hat{g}_k(\cdot)$, $k = 1, 2, 3$. After tuning the parameters of the gbm models under each treatment group, we observe the following parameters for the best models.

Table B.1: Parameters for the gbm model

Treatment k	Shrinkage	Number of trees
1	0.05	39
2	0.005	729
3	0.005	1085

From each of the gbm models, we select the variables, \tilde{X}_k , using the relative influence. The Figure B.1 illustrates the importance of the covariates in each treatment group based on the relative influence. The union of the selected covariates, $\{\tilde{X}_1 \cup \tilde{X}_2 \cup \tilde{X}_3\}$ is then used in the propensity score estimation. For treatment group 1 and group 2, the selected variables are $\tilde{X}_1 = \tilde{X}_2 = \{\text{Age, Education, BMI, Total cholesterol, estimated glomerular filtration rate}\}$ and for treatment group 3, the selected variables are $\tilde{X}_3 = \{\text{Age, Education}\}$. Therefore, the union of the variables selected in each group; Age, Education, BMI, Total cholesterol and estimated

glomerular filtration rate were then used to estimate the propensity scores, using boosted logistic regression. We use the `mnp` function from `twang` package using 5000 trees.

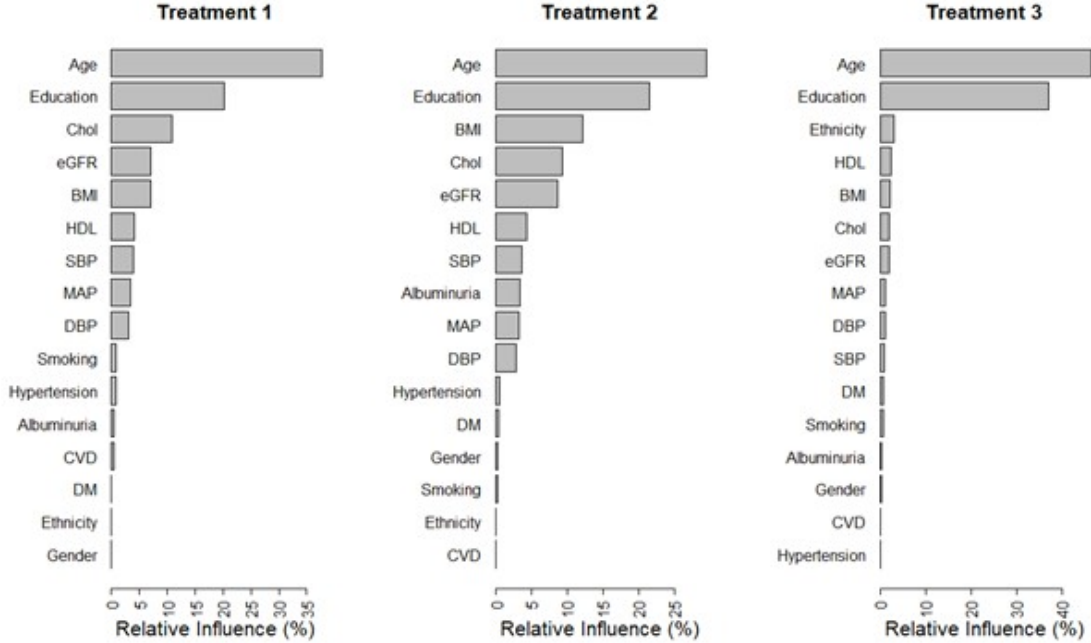


Figure B.1: Relative influence of the covariates obtained from the GBM models of the three treatment groups.

Then using the estimates of $\hat{g}_k(X)$ obtained from the GBM method, we calculate the patient level scores $U(X)$ that were defined in the section 2. In Table B.2, we have provided the estimated $U(X)$ scores for the first 10 patients in the training data.

Now we estimate the patient level scores $U(X_0)$ for the testing data. The Table B.3 shows the estimated scores for the first 10 patients in the testing data.

Then we estimate the $\mu_k(U(X_0)), k = 1, 2, 3$ for the patients in the testing data using the NW estimator described in the section 2. The optimal bandwidths were selected for each treatment group using the `h.amise` function in the `kedd` R-package. The selected bandwidths for the three treatment groups are 2.68, 3.36 and 2.69 respectively. The Table B.4 presents the estimated $\hat{\mu}_k(U(X_0))$ and the proposed

Table B.2: The estimated patient scores $U(X) = (S(X), \delta(X))^T$ for the first 10 patients in the training data

i	$S(X_i)$	$U(X_i)$
1	0.4382	3
2	8.8367	2
3	3.3064	2
4	1.9863	2
5	2.5895	2
6	4.4242	3
7	5.6317	1
8	1.9030	2
9	1.9600	2
10	7.7091	3

Table B.3: The estimated patient scores $U(X_0) = (S(X_0), \delta(X_0))^T$ for the first 10 patients in the training data

i	$S(X_{0i})$	$U(X_{0i})$
1	2.2899	3
2	14.0865	2
3	6.4727	2
4	7.0352	3
5	7.4772	3
6	7.2044	3
7	1.9484	3
8	8.1466	3
9	9.1050	3
10	11.4191	3

treatment for the first 10 patients.

Table B.4: Proposed treatment for the first 10 patients in the testing data

i	$\hat{\mu}_1(U(X_{0i}))$	$\hat{\mu}_1(U(X_{0i}))$	$\hat{\mu}_1(U(X_{0i}))$	Original	$\hat{k}^* = \operatorname{argmax}_k(\hat{\mu}_k(U(X_{0i})))$
1	67.0158	66.3098	76.1271	1	3
2	56.4334	105.8077	65.9183	1	2
3	55.8858	78.1317	65.1130	1	2
4	69.1504	67.7253	82.6819	1	3
5	69.7832	67.5299	83.2943	2	3
6	69.3898	67.6580	82.9180	2	3
7	67.1128	66.0590	75.7446	2	3
8	70.7465	67.1185	84.1944	2	3
9	71.9809	66.3231	85.4302	3	3
10	73.8878	63.8497	88.2359	3	3

C Third Appendix

The validity of the objective function (4.3)

We take the derivative of (4.3) with respect to $\boldsymbol{\theta}_k$ and $\boldsymbol{\beta}_k$ and obtain the following

$$S_k(\mathbf{g}, \underline{\boldsymbol{\theta}}, \underline{\boldsymbol{\beta}}; \gamma) = \begin{cases} S_{\boldsymbol{\beta}_k}(\mathbf{g}, \underline{\boldsymbol{\theta}}, \underline{\boldsymbol{\beta}}; \gamma) \\ S_{\boldsymbol{\theta}_k}(\mathbf{g}, \underline{\boldsymbol{\theta}}, \underline{\boldsymbol{\beta}}; \gamma) \end{cases} = \begin{cases} \frac{\partial L_n(\mathbf{g}, \underline{\boldsymbol{\theta}}, \underline{\boldsymbol{\beta}}; \gamma)}{\partial \boldsymbol{\beta}_k} \\ \frac{\partial L_n(\mathbf{g}, \underline{\boldsymbol{\theta}}, \underline{\boldsymbol{\beta}}; \gamma)}{\partial \boldsymbol{\theta}_k} \end{cases},$$

where

$$\begin{aligned} S_{\boldsymbol{\beta}_k}(\mathbf{g}, \underline{\boldsymbol{\theta}}, \underline{\boldsymbol{\beta}}; \gamma) &:= 2n^{-1} \sum_{i=1}^n (A_{i(k)} - \pi_k(\mathbf{X}_i, \mathbf{Z}_i)) g'_k(\mathbf{X}_i^T \boldsymbol{\beta}_k) \mathbf{X}_i \frac{\Delta_i}{G(T_i)} \\ &\times \left[Y_i - \phi(\mathbf{X}_i, \mathbf{Z}_i; \gamma) - \sum_{k=1}^k (A_{i(k)} - \pi_k(\mathbf{X}_i, \mathbf{Z}_i)) [\mathbf{Z}_i^T \boldsymbol{\theta}_k + g_k(\mathbf{X}_i^T \boldsymbol{\beta}_k)] \right] \end{aligned} \quad (4.10)$$

$$\begin{aligned} S_{\boldsymbol{\theta}_k}(\mathbf{g}, \underline{\boldsymbol{\theta}}, \underline{\boldsymbol{\beta}}; \gamma) &:= 2n^{-1} \sum_{i=1}^n (A_{i(k)} - \pi_k(\mathbf{X}_i, \mathbf{Z}_i)) \mathbf{Z}_i \frac{\Delta_i}{G(T_i)} \\ &\times \left[Y_i - \phi(\mathbf{X}_i, \mathbf{Z}_i; \gamma) - \sum_{k=1}^k (A_{i(k)} - \pi_k(\mathbf{X}_i, \mathbf{Z}_i)) [\mathbf{Z}_i^T \boldsymbol{\theta}_k + g_k(\mathbf{X}_i^T \boldsymbol{\beta}_k)] \right] \end{aligned} \quad (4.11)$$

We would like to show that the expectation of $S_k(\mathbf{g}, \underline{\boldsymbol{\theta}}, \underline{\boldsymbol{\beta}}; \gamma)$ is 0.

$$\begin{aligned}
E \begin{bmatrix} S_{\boldsymbol{\beta}_k}(\mathbf{g}, \underline{\boldsymbol{\theta}}, \underline{\boldsymbol{\beta}}; \gamma) \\ S_{\boldsymbol{\theta}_k}(\mathbf{g}, \underline{\boldsymbol{\theta}}, \underline{\boldsymbol{\beta}}; \gamma) \end{bmatrix} &= 2E \left[(A_{(k)} - \pi_k(\mathbf{X}, \mathbf{Z})) \begin{bmatrix} g'_k(\mathbf{X}^\top \boldsymbol{\beta}_k) \mathbf{X} \\ Z \end{bmatrix} \frac{\Delta}{G(T)} \right. \\
&\quad \left. \times \left[\tilde{Y} - \phi(\mathbf{X}, \mathbf{Z}; \gamma) - \sum_{k=1}^k (A_{(k)} - \pi_k(\mathbf{X}, \mathbf{Z})) [\mathbf{Z}^\top \boldsymbol{\theta}_k + g_k(\mathbf{X}^\top \boldsymbol{\beta}_k)] \right] \right] \\
&= 2E \left[(A_{(k)} - \pi_k(\mathbf{X}, \mathbf{Z})) \begin{bmatrix} g'_k(\mathbf{X}^\top \boldsymbol{\beta}_k) \mathbf{X} \\ Z \end{bmatrix} \frac{\Delta}{G(T)} \right. \\
&\quad \left. \times \left[Y - \phi(\mathbf{X}, \mathbf{Z}; \gamma) - \sum_{k=1}^k (A_{(k)} - \pi_k(\mathbf{X}, \mathbf{Z})) [\mathbf{Z}^\top \boldsymbol{\theta}_k + g_k(\mathbf{X}^\top \boldsymbol{\beta}_k)] \right] \right] \\
&= 2E \left[E \left[(A_{(k)} - \pi_k(\mathbf{X}, \mathbf{Z})) \begin{bmatrix} g'_k(\mathbf{X}^\top \boldsymbol{\beta}_k) \mathbf{X} \\ Z \end{bmatrix} \frac{1\{T < C\}}{G(T)} \right. \right. \\
&\quad \left. \left. \times \left[Y - \phi(\mathbf{X}, \mathbf{Z}; \gamma) - \sum_{k=1}^k (A_{(k)} - \pi_k(\mathbf{X}, \mathbf{Z})) [\mathbf{Z}^\top \boldsymbol{\theta}_k + g_k(\mathbf{X}^\top \boldsymbol{\beta}_k)] \right] \middle| T, \mathbf{X}, \mathbf{Z}, A \right] \right] \\
&= 2E \left[E \left[(A_{(k)} - \pi_k(\mathbf{X}, \mathbf{Z})) \begin{bmatrix} g'_k(\mathbf{X}^\top \boldsymbol{\beta}_k) \mathbf{X} \\ Z \end{bmatrix} \right. \right. \\
&\quad \left. \left. \times \left[Y - \phi(\mathbf{X}, \mathbf{Z}; \gamma) - \sum_{k=1}^k (A_{(k)} - \pi_k(\mathbf{X}, \mathbf{Z})) [\mathbf{Z}^\top \boldsymbol{\theta}_k + g_k(\mathbf{X}^\top \boldsymbol{\beta}_k)] \right] \middle| \mathbf{X}, \mathbf{Z}, A \right] \right] \\
&= 2E \left[(A_{(k)} - \pi_k(\mathbf{X}, \mathbf{Z})) \begin{bmatrix} g'_k(\mathbf{X}^\top \boldsymbol{\beta}_k) \mathbf{X} \\ Z \end{bmatrix} \right. \\
&\quad \times \left[h_0(\mathbf{X}) + \sum_{k=1}^K A_{(k)} [\mathbf{Z}^\top \boldsymbol{\theta}_k + g_k(\mathbf{X}^\top \boldsymbol{\beta}_k)] - \phi(\mathbf{X}, \mathbf{Z}; \gamma) \right. \\
&\quad \left. \left. - \sum_{k=1}^k (A_{(k)} - \pi_k(\mathbf{X}, \mathbf{Z})) [\mathbf{Z}^\top \boldsymbol{\theta}_k + g_k(\mathbf{X}^\top \boldsymbol{\beta}_k)] \right] \right] \\
&= 2E \left[E \left[(A_{(k)} - \pi_k(\mathbf{X}, \mathbf{Z})) \middle| \mathbf{X}, \mathbf{Z} \right] \begin{bmatrix} g'_k(\mathbf{X}^\top \boldsymbol{\beta}_k) \mathbf{X} \\ Z \end{bmatrix} \left[h_0(\mathbf{X}) - \phi(\mathbf{X}, \mathbf{Z}; \gamma) \right. \right. \\
&\quad \left. \left. + \sum_{k=1}^k \pi_k(\mathbf{X}) [\mathbf{Z}^\top \boldsymbol{\theta}_k + g_k(\mathbf{X}^\top \boldsymbol{\beta}_k)] \right] \right] = 0
\end{aligned}$$

where the first two qualities are trivial, the third equality follows from that $E \left[\mathbf{1}\{T < C\} / G(T) \middle| T \right] = E \left[\mathbf{1}\{T < C\} \middle| T \right] / G(T) = G(T) / G(T) = 1$, the fourth equality follows from (4.2), and the last equality follows from that $E[A = k | \mathbf{X}, \mathbf{Z}] = \pi_k(\mathbf{X}, \mathbf{Z})$.

CURRICULUM VITAE

NAME: Sudaraka Tholkage

ADDRESS: Department of Biostatistics and Bioinformatics
University of Louisville
Louisville, KY 40292

EDUCATION: Bachelor of Science (Honours) in Statistics
University of Kelaniya
2011-2016

Masters in Statistics
Sam Houston State University
2016-2018

PUBLICATIONS: Kulasekera, K. B., Tholkage, S., Kong, M. (2022).
Personalized treatment selection using observational data.
Journal of Applied Statistics, 1-13.

Tholkage, S., Zheng, Q., & Kulasekera, K. B. (2022).
Conditional Kaplan-Meier Estimator with Functional Covariates
for Survival Data. (Submitted)

Tholkage, S., Kulasekera, K. B., Kong, M., & Zheng, Q. (2022).
Identifying the optimal treatment regime using single index models
for survival data. (In preparation)

PRESENTATIONS:

ORAL

Personalized Treatment Selection with Censored Observations,
ASA-KY Chapter Meeting, April, 2022.

Conditional Kaplan-Meier Estimator with Functional Covariates
for Survival Data,
Eastern North American Region (ENAR), March, 2022.

Personalized treatment selection using observational data,
Joint Statistical Meeting (JSM) August, 2021.

Personalized treatment selection using observational data,
ASA-KY Chapter Meeting, April, 2021.

POSTER

Conditional Kaplan-Meier Estimator with Functional Covariates
for Survival Data,
Southern Regional Council on Statistics (SRCOS), October, 2021.

Analyzing the Career Lengths of the Major League Baseball
Players Using Survival Analysis Models,
Conference of Texas Statisticians, April, 2018.

HONORS AND
AWARDS

SRCOS Summer Research Conference Graduate Travel
Award 2021

Best Student Presentation Award, ASA-KY Chapter
Meeting. April 2021

Graduate Fellowship, University of Louisville. August 2018
-May 2020

Pi Mu Epsilon (National Mathematics Honor Society),
inducted 2018

Cecil Hallum Award – Sam Houston State University, 2017-2018

Special Graduate Scholarship program,
Sam Houston State University, 2016-2018

Graduate Studies Scholarship
Sam Houston State University, 2016-2018